GENETIC AND HORMONAL REGULATION OF MERISTEM INITIATION AND MAINTENANCE PATHWAYS DURING MAIZE VEGETATIVE AND REPRODUCTIVE DEVELOPMENT

A Dissertation

presented to

the Faculty of the Graduate School

at the University of Missouri-Columbia

In Partial Fulfillment

of the Requirements for the Degree

Doctor of Philosophy

---

by

KATHERINE L. GUTHRIE

Dr. Paula McSteen, Dissertation Supervisor

July 2021

The undersigned, appointed by the dean of the Graduate School, have examined the thesis entitled

GENETIC AND HORMONAL REGULATION OF MERISTEM INITIATION AND MAINTENANCE PATHWAYS DURING MAIZE VEGETATIVE AND REPRODUCTIVE DEVELOPMENT

presented by Katherine L. Guthrie,

a candidate for the degree of doctor of philosophy,

and hereby certify that, in their opinion, it is worthy of acceptance.

_____

Professor Paula McSteen

_____

Professor David Braun

_____

Professor Kathy Newton

_____

Professor Antje Heese

To the three days that almost defeated me,

and Pippin for getting me through them.

ACKNOWLEDGEMENTS

I would first like to acknowledge the previous rotation students and lab members of the McSteen Lab who were vital in support of this project. This includes those who helped with initial mapping: Drs. Chris Gardner, Ronnie LaCombe, Ben Julius, and undergraduate researcher Zach Rhodes. Previous lab members that aided in bulking and backcrossing seed stocks include Drs. Andrea Skirpan and Diana Roberts-Coats, lab technician Hong Yoa, and undergraduate researchers Jackson Marsch and Austin Morgan. Additional aid was received by fellow graduate students Janlo Robil, who created the *Sos2* cartoon depictions, Eden Johnson, and Prameela Awale.

Special thanks to the support staff at the University of Missouri including the University of Missouri Genetics field manager Chris Browne and the field crews, and MU greenhouse manager Michelle Brooks, and her staff for their aid in plant growth and care. Additional MU Biological Sciences Support staff including Melody Kroll, Nina Emerich, Rebecca Ballew, and members of the Graduate Executive Council (GEC). Also thanks to the Bond Life Sciences Center support staff including: Dean Bergstrom (building manager), Benji Bockting (event coordinator), Patience Okiring (grant support), Victoria Bence (financial/HR), Jeremy Matteson (LSC IT), Walter Gassmann (director), and the custodians that work within the building. Additional thanks to the EM, Confocal, and DNA core facilities and their support staff. Outside of MU, I would like to extend gratitude to the Friendly Isle Growing LLC field manager Nate Oswald and his field staff for hosting my winter nurseries.

Additional Chapter 3 acknowledgements include: Amanda Durbak for help with tissue dissection, Johanna Morrow for help with RNA extraction, Shelbie Wooten and all previous members of the McSteen Lab for help in the field, Nathan Bivens (MU DNA core) for library construction and sequencing, Qingyu Wang and Naomi Altman (Penn State University) and Christopher Bottoms and Diana Coats (MU) for statistical and bioinformatic analysis of the transcriptome data mapped to an earlier version of the Maize Genome.

To my mentors – thank you for being a part of my village. Debbie Allen, your support, especially early in my career, helped me overcome my imposter syndrome and anxiety around graduate school. To Drs. Bethany Stone and Brit Moss thank you for pushing me to think creatively about what it means to be an educator, as well as the time you took from your busy schedules to foster my passion. Dr. Terrell Morton – you have been instrumental in my decision to jump between fields after my PhD. Thank you for always asking the tough questions, that make me critically analyze my actions in the classroom, as well as in my day-to-day life. And finally, my PI Dr. Paula McSteen. You taught me resilience, showed me the realities of being a woman in an academic setting, and how to extend kindness to myself when I fall short of my own set expectations. You are our chief cheerleader, and I am so fortunate to have had you as my PI.

The post-doctoral researchers that have come through the lab have been vital in my journey to become a scientist. To Dr. Diana Roberts-Coats, Micha Matthes, and Norman Best – thank you for your patience and persistence in working with me. The lessons I learned from each of you are invaluable, from lab

techniques to navigating the professional academic world. I promise to pay this forward in the future. To Janlo and Prameela, you are the best co-graduate students and lab mates in the world. Thank you for helping me keep lab work going while I was writing and filling in the holes necessary to keep the lab running.

A huge thanks to my family for this constant support through this journey, especially my father, Jack Guthrie, who helped with green house plantings, summer pollinations, and for taking vacation time to travel to our winter field site to help with tissue collection, pollinations, weeding and overall nursery support. My mom and four sister's encouragement was instrumental in my success. To my many friends that extended grace when plans got canceled last minute, who constantly showered me with support and strength when I needed it – you are appreciated more than you know. Naturally, this also includes my three emotional-support fur babies: Pippin, Bug, and Lemon. And finally, to the Remmington's and Faulkner's – thank you for being my home away from home and providing me with a second family that I could lean on for support.

Chapters 1 to 3 were initially funded by NSF-IOS grant #1256373 to awarded to Dr. Paula McSteen, and subsequently funded via USDA-NIFA predoctoral fellowship #2018-07736. Chapter 3 was funded by National Science Foundation Plant Genome Research Program IOS-0820729/1114484 to Dr. McSteen and IOS-1546873 to Dr. McSteen and Dr. Trupti Joshi. I was additionally supported by the MU Life Sciences Fellowship, the MU Interdisciplinary Plant Group (IPG), and the Douglas Randall Scholarship.

TABLE OF CONTENTS

LIST OF FIGURES

LIST OF TABLES

LIST OF SUPPLEMENTAL MATERIAL

SUPPLEMENTAL TABLES

SUPPLEMENTAL FIGURES

NOTE ON NOMENCLATURE

This document contained references to *Arabidopsis* and maize genes, proteins and genetic loci. Subtle differences in genetic nomenclature exist between these two organisms, which are outlined online at the *Arabidopsis* genetics and genomic database, TAIR (https://www.arabidopsis.org/portals/nomenclature/guidelines.jsp) and the maize genetics and genomic database, MaizeGDB (https://www.maizegdb.org/nomenclature). These differences are summarized in the table below:

	Arabidopsis	Maize
Gene Example:	All capitalized and italicized *CLAVATA1, CLV1*	All lowercase and italicized *thick tassel dwarf1, td1*
Protein Example:	All capitalized CLAVATA1, CLV1	All capitalized THICK TASSEL DWARF 1, TD1
Mutant phenotype Example:	All phenotypes: All lowercase and italicized *clavata1, clv1*	Dominant phenotype: First letter capitalized, italicized *Rolled leaf 1, Rld1* Recessive phenotype: All lowercase and italicized *thick tassel dwarf1, td1*

In cases where genes/proteins/mutant phenotypes names are shared between species, the species initials are prefixed to the beginning of the genes/proteins/mutant phenotype that was found secondary in the literature (e.g: WUSCHEL versus *Zm*WUSCHEL, where *Zm* is abbreviated for *Zea mays*).

LIST OF ABBREVIATIONS

General Developmental/Molecular Biology Terms		Selected Gene/Protien name abbreviations	
ABA	Abscisic Acid	ARF	Auxin Response Factors
AM	Axiallary Meristem	BA	Barren stalk
BC	Backcross	BAM	Barely Any Meristem
BM	Branch Meristem	BIF	Barren Inflorescence
CK	Cytokinin	CLE	Clavata3/Endosperm Surrounding Region
co-IP	co-Immunoprecipitation	CLV	Clavata
CZ	Central Zone	CR4	Crinkly4
cZR	cisZeatin-Riboside	CRN	Coryne
DE	Differentially Expressed	CT2	Compact plant2
DEG	Differentially Expressed Genes	FAS1	Fascicled ear1
FDR	False Discovery Rate	FEA	Fasciated
FM	Floral Meristem	GB1	G-beta subunit1
GA	Gibberillic Acid	HSF	Heat Shock Factor
GO	Gene Ontology	HSP	Heat Shock Protein
HD	Homeodomain	IPT	Isopentenyl Transferases
HPE	Holoprosencephaly	KN1	Knotted1
IAA	Indole Acetic Acid	LG1	Liguless1
IM	Inflorescence Meristem	LOG	Lonely guy
INDEL	Insertion/Deletion	PHB	Phabulosa
JA	Jasmonic Acid	PIN	Pinformed
KRN	Kernel Row Number	RB/RBR	Retinoblastoma-related
OC	Organizing Center	RD1	Rolled leaf1
PZ	Peripheral Zone	REV	Revoluta
RAM	Root Apical Meristem	SHH	Sonic Hedge-Hog
RZ	Rib Zone	SOS	Suppressor of Sessile Spikelets
SA	Salicylic Acid	STM	Shootmeristemless
SAM	Shoot Apical Meristem	TD1	Thick Tassel Dwarf1
SB	Supressed Bract	VT2	Vanishing Tassel2
SEM	Scanning Electron Microscopy	WOX	Wuschel-related homeobox
SM	Spikelet Meristem	WUS	Wuschel
SNP	Single Nucleotide Polymorphisim	ZPR	Little Zipper
SPM	Spikelet Pair Meristem		
TF	Transcription Factor		
tZR	transZeatin-Riboside		

ABSTRACT

Plant development is driven by pools of undifferentiated stem cells called meristems. Meristems have two functions, to divide producing cells that will replenish the stem-cell niche, and cells that will differentiate into new organs. Together, the fine regulation of these divisions is referred to as meristem maintenance. Over a plant's lifetime, meristems undergo a specific developmental progression that continues to create organs throughout vegetative and reproductive development. Defects in the pathways that regulate meristem maintenance result in altered meristem size or number of organs typically produced by a specific meristem type, resulting in altered mature plant morphology. While many meristem maintenance pathways are shared between species, and thus information learned from one developmental time can be used to form another, specificity of these pathways between species can also be seen. Thus, by first chapter focuses on the similarities and differences in meristem maintenance pathways between the model species *Arabidopsis* and maize and touches on lessons researchers can glean from studying general patterns of development.

The semi-dominant *Suppressor of sessile spikelets2* (*Sos2*) gene in maize displays developmental defects in meristem maintenance throughout maize development. The *Sos2* heterozygous mutants display a large variation of phenotypes while the *Sos2* homozygous mutants and seedling lethal. The goal of Chapter 2 was to summarize the role of the *Sos2* gene in known meristem maintenance pathways, as well as understand the genetic and environmental

factors that influence the penetrance and expressivity of the *Sos2* phenotype. In addition, an RNA-seq anlaysis uncovered additional pathways in which the *Sos2* gene may directly or indirectly function, as well as identified a candidate gene for the *Sos2* mutation, one that that has not yet been published to function in maize meristem maintenance pathways.

Links within the literature of genes orthologous to the *Sos2* candidate gene, taken alongside RNA-seq results, indicated *Sos2* might act on phytohormone pathways. To further explore this link, Chapter 3 analysis results from hormone level assays and confocal analysis, which found significant differences in the cytokinin and auxin pathways. *Sos2* is a member of the *Sos* class of mutants, along with *Sos1* and *Sos3.* All three *Sos* mutants have similar mutant phenotypes, in that the structures on the ends of short branches that contain the flowers called spikelets, which are usually produced in pairs, develop singly in the heterozygote. In order to compare the meristem maintenance pathways effected by each *Sos* mutants, as well as determine their individual effects on phytohormone pathways during development, RNA-seq analysis was performed. This study found that *Sos2* and *Sos3* are more likely to share similar functions in meristem maintenance pathways than either when compared to *Sos1.*

Chapter 4 sought to further unravel how phytohormone pathways regulate meristems, specifically at the point of axillary meristem initiation from the inflorescence meristem during reproductive development. To the end, transcriptomes of three auxin mutants *barren stalk 1, barren inflroescnece2,* and *barren stalk 2* were performed and compared using a Weighted Gene Co-

Expression Analysis (WGCNA). This study found less shared elements between these three auxin mutants, as was hypothesized, and highlighted the individual and unique targets of *ba1, bif2,* and *ba2.* These targets provide additional avenues of research that will lead to a better understanding of axillary meristem initiation during reproductive development.

In summary, this study identified a possible gene involved in meristem maintenance not previously described in maize or any other monocot species, and provide insight into how that gene functions in known meristem maintenance and phytohormone pathways. In addition, research in understanding how axillary meristems develop within the context of auxin regulation uncovered unique targets of known auxin development mutants. Taken together, the results outlined in this thesis provide a more comprehensive understanding of meristem maintenance throughout maize development.

CHAPTER 1:

Reiteration of meristem maintenance pathways throughout development: What we know and what we still need to learn.

Katy Guthrie

ABSTRACT

Patterns in development between plant and animal kingdoms exist that can be used to inform research in both kingdoms. A major difference between development in plants and animals is that plants can create organs throughout their lifetime via pools of undifferentiated stem-cells called meristems, while animal organogenesis occurs mainly in the embryo. Plant meristems have to undergo cell division both to replenish the stem-cell pool and produce cells that will differentiate into organs, referred to as meristem maintenance. This review focuses on the molecular pathways that regulate meristem maintenance throughout *Arabidopsis* and maize development, including the *CLV-WUS, STM/KN1* and phytohormone pathways. We compare these pathways between organisms, as well as between meristems as the plant progresses through development. Finally, a case study is presented to illustrate how studies of a human developmental disorder can be used to inform plant development research questions.

INTRODUCTION

Patterns in development

Patterns of development occur between the animal and plant kingdoms, even though the last common ancestor shared between them is predicted to have existed over 1.6 billion years ago (Meyerowitz, 2002). In general, the major difference in development between the plant and animal kingdoms is that in animals, most of the development occurs in the embryo during gestation, whereas in plants, most of the organs are produced after germination and throughout development. In both cases, however, a plane of development is established followed by molecular changes that allow for development of secondary structures. Signaling pathways produce a gradient of molecules that specify the axes eg: top/down, inside/outside. The position of the first few cells that divide along this gradient determine the identify of the organ that subsequent divisions will produce. The reproducibility of this system is also important as it allows for the production of secondary and post-secondary structures from the primary plane of growth.

While patterns of development are maintained, very few developmental genes are found across kingdoms. One of these genes, originally discovered in human eye tumors (Fung et al., 1987; Lee et al., 1987), is *retinoblastoma protein 1* (*rb1*), which controls cell proliferation through regulation of E2F transcription factors in human tumors (Weinberg, 1995). The first retinoblastoma-related protein (RBR) found in plants was isolated from maize (Grafi et al., 1996), and relatively conserved RB genes have subsequently been found in both single and multicellular organisms across Eukaryotes (Desvoyes et al., 2014; Desvoyes &

Gutierrez, 2020). In plants, RB also functions in regulating the cell cycle by interacting with TCP transcription factors, during various stages of development, as recently reviewed by (Desvoyes & Gutierrez, 2020). While this is a great example of how a conserved gene can have a similar function in both plant and animal development, there are not many genes conserved in function across kingdoms. Studying patterns of development instead, is more likely to be used to inform developmental research questions across kingdoms.

Patterns in plant development

Meristems, or small, undifferentiated pools of stem cells, are unique to plants and allow them to produce organs throughout a plant's lifetime. Meristems have two functions: divide to produce cells that differentiate into different tissues and organs, and to sustain a pool of undifferentiated stem cells that will continue this process throughout a plant's lifetime (Steeves & Sussex, 1989). This is controlled, in part, by a fine balance of meristem maintenance pathways. Meristem maintenance, defined as balance between stem cell proliferation and differentiation, includes regulating meristem size, growth, and proper timing of termination.

If the meristem is correctly regulated, then plant growth can be observed as re-iterations of basic developmental units, or phytomers, through both vegetative and reproductive development. In plants, vegetative development is controlled by the shoot apical meristem (SAM). The SAM is composed of an organizing center (OC) in the center of the meristem. Above the OC is a group of cells called the central zone (CZ), that divides slowly but remain undifferentiated. The OC and CZ

regulate each other to control the number of new cells produced and overall meristem size. On either side of the CZ is the peripheral zone (PZ) which gives rise to organ primordia as cells begin to differentiate (Evert et al., 2006; Somssich et al., 2016). The newest organ primordia are often referred to as "P_0," and initiated organs are labeled P1-PX, from newest to oldest (Evert et al., 2006). The rib zone (RZ) is located directly beneath the OC, and cells in this zone are responsible for producing stem tissue. These groups of cells that compose the SAM create phytomeres that consist of stem tissue, referred to as the internode, a leaf, and an axillary meristem (AM) between the leaf and stem, attached at a node (Gray, 1879).

Upon the switch to reproductive development, these units are modified to create the inflorescences. In many dicot plants, the SAM is converted to an apical inflorescence meristem (IM) and the phytomers are comprised of a suppressed bract (SB), a modified leaf-like structure that does not mature, the floral meristem (FM), which is an axillary meristem made by the IM and very short internodes (Long & Barton, 2000). FM are generally determinate, producing a fixed number of floral organs.

Patterns in maize development

In maize, the SAM also produces phytomers with node, internode, leaf and axillary meristem (Fig. 1) and upon the switch to reproductive development, these units are modified to create the male and female inflorescences – the tassel and ear respectively. Grass inflorescences are highly branched and are characterized by the production of spikelets (little branches bearing the flowers) which in maize,

are produced in pairs. After the transition from SAM to IM, the first phytomer is comprised of a suppressed bract, and the spikelet pair meristem (SPM), which is an axillary meristem made by the IM (Galinat, 1959). The SPM produces two spikelet meristems (SM) which are subtended by modified leaf-like structures called glumes (Galinat, 1959). Following this, each SM transitions into two floral meristems (FM) that produce a palea and lemma, modified leaves that protect the floral organs, either the stamens in the tassel or the carpels in the ear (Galinat, 1959). An additional type of AM, the branch meristem (BM) produces long branches at the base of the tassel before the IM transitions to producing SPM (Fig. 1). Therefore, while model systems such as *Arabidopsis* produce only one type of AM (the FM) in the inflorescence, maize produces multiple types of AM (BM, SPM and SM) before producing FM.

SIGNALLING PATHWAYS IN MERISTEM DEVELOPMENT

Meristems across plant species follow phytomeric patterns of development, and have analogous regulatory networks that direct this patterning, so, research from meristem development in one species can generally be used to inform another. However, slight differences in conserved signaling pathways within meristem types on a single plant (SAM, IM, AM, etc.) or between the same meristem type of two different plant species (such as *Arabidopsis* SAMs versus *Zea Mays* SAMs), define unique outcomes and the overall final plant structure.

Lessons from Arabidopsis

The most well-known signaling pathway in meristem maintenance is the CLAVATA pathway (CLV), named based on research in the model species *Arabidopsis*. In *this pathway,* a homeodomain transcription factor *WUSCHEL* (*WUS*) is expressed in the OC, starting in the SAM during embryo development and persisting through to reproductive development, and confers stem cell fate on the cells surrounding this region (Laux et al., 1996; Mayer et al., 1998). When *WUS* is absent in plants, the SAM flattens and produces organs at a slower and decreased rate, ultimately terminating growth early compared to normal siblings (Laux et al., 1996), supporting the central role of *WUS* in meristem maintenance.

WUS negatively regulates its own expression by inducing expression of a small signaling peptide, *CLAVATA3* (*CLV3), in the cells surrounding the OC* (Schoof et al., 2000; Yadav et al., 2011). The *CLV3* ligand is perceived through at least two parallel pathways: *CLV1 and CLV2/CORYNE (CRN).* CLV1 perceives the *CLV3* ligand at the plasma membrane and communicates the signal to repress *WUS* expression in the nucleus (Clark et al., 1997; Fletcher et al., 1999). *CLV3* is also perceived by *CLV2*, which forms a complex with *CRN*, a membrane associated protein, to inhibit the expression of *WUS* in the nucleus (Bleckmann et al., 2010; Müller et al., 2008). Biochemical evidence suggests that CRN proteins may also function to mediate the binding between *CLV1* homodimer and the *CLV2/CRN* complex forming a hexamer, implicating a third *CLV* signal transduction pathway that regulates *WUS* expression (Bleckmann et al., 2010; Müller et al., 2008). Mutations in *CLV1, CLV2*, *CLV3 and CRN genes all* lead to meristem enlargement (Fletcher et al., 1999; Kayes & Clark, 1998), indicating the

significant role of this signaling pathway in restricting WUS expression to maintain meristem size.

The class I knotted-like homeobox (KNOX) transcription factor, *SHOOTMERISTEMLESS* (*STM*) regulates meristems in a parallel pathway to *WUS* (Barton & Poething, 1994; Lenhard et al., 2002; Long et al., 1996). *STM* mutants have a rapid loss of the pool of stem cells within the SAM during embryogenesis, resulting in seedlings with terminated meristems and few, if any, leaves (Endrizzi et al., 1996). This phenotype highlights the necessity of *STM* expression for maintaining meristem identity, upstream of *WUS* (Endrizzi et al., 1996; Hake et al., 2004). This is supported, in part, by the up-regulation of cytokinin biosynthesis by *STM,* a gene that promotes *WUS* expression in the OC (Jasinski et al., 2005; Yanai et al., 2005). In *Arabidopsis*, the induction of cytokinin in the OC, along with the binding of cytokinin-regulated Type B ARR transcription factors (TF) in the promoter of the *ZmWUS1* locus, have been shown to activate *WUS* expression providing a link between STM and WUS meristem maintenance pathways (Chen et al., 2021; Meng et al., 2017).

Expression of *STM* is upregulated by the HD-ZIP III transcription factor, *REVOLUTA* (*REV*) to initiate AM formation in the periphery of the SAM (Shi et al., 2016). HD-ZIP III transcription factors are, in return, regulated by LITTLE ZIPPER (ZPR) proteins, which competitively bind HD-ZIP III transcription factors, ultimately inhibiting *STM* expression (Kim et al., 2008; Wenkel et al., 2007). Furthermore, the expression of HD-ZIP III genes, such as *PHABULOSA* (*PHB*) and *PHAVOLUTA*

(*PHV*), and ZPR proteins also act to define the *WUS* domain in the OC (Wenkel et al., 2007; Williams et al., 2005; Xu et al., 2019).

Additional genes involved in meristem maintenance includes the *BARLEY ANY MERISTEM* (*BAM*) family of receptor-kinases. Genetic studies of *BAM1* and *BAM2* indicate overlapping functions with CLV1 receptors to regulate meristematic cells (DeYoung & Clark, 2008; Nimchuk et al., 2015a). Quadruple mutants between *BAM1, BAM2, BAM3,* and *CLV1* display phenotypes that are stronger than *clv3* mutants, indicating that additional signaling ligands must be present to regulate meristems through these pathways (Nimchuk et al., 2015a). A difference between the two is that the *CLV* genes are expressed in the central zone of the meristem, while the BAM receptors are expressed broadly throughout the plant, with a higher concentration in the peripheral zones (DeYoung & Clark, 2008). In *clv1* mutants, BAM receptors can compensate by turning on expression in the *CLV1* domain (Nimchuk et al., 2015b). This regulation helps to ensure meristems are maintained when there are perturbations on the system.

While this review will not go into detail on the regulation of the OC in the root apical meristem (RAM), it is important to point out that similar patterns of signaling regulate this meristematic region as well. In this region, a receptor kinase, CRINKLY4 (ACR4), forms homo and heterodimers with CLV1 to perceive a ligand, CLE40 to regulate stemness (Gifford et al., 2003; Stahl et al., 2013). In addition, ACR4 may regulate WOX5, a protein with closely related function to the WUS protein in vegetative and reproductive development (Meyer et al., 2015). While most of the work on ACR4 has focused on root development, expression of ACR4

has also been seen in the developing embryo, inflorescence and floral meristems (Gifford et al., 2003), and should not be discounted from function in these tissues without further research.

Meristem maintenance in maize: similarities and differences

In maize, two *WUS* orthologs exist, *ZmWUS1* and *ZmWUS2*, but in different expression patterns. *ZmWUS1* transcripts, shown via RNA *in situ* hybridization (Nardmann & Werr, 2006), and proteins, by confocal microscopy (Je et al., 2016), are expressed in the organizing center of SAMs (Table 1, 2). *ZmWUS1* is similarly regulated by orthologous players of the *CLAVATA* pathway. The *CLV1* ortholog, *thick tassel dwarf (td1)* has been shown to act in a parallel pathway to the *CLV2* ortholog *fasciated ear2 (fea2)* to repress *ZmWUS1* (Bommert et al., 2005b; Je et al., 2018). Although *td1* has been shown to function in both SAM and reproductive development (Lunde & Hake, 2009), *td1* transcripts are present in young, developing leaves and are absent from SAMs (Bommert et al., 2005a), deviating from the pattern of expression of *CLV1* in *Arabidopsis.* FEA2 proteins are localized to the plasma membrane and expressed in the SAM and subsequent reproductive meristems, highlighting its orthologous role to *CLV2* as a regulator of meristem maintenance (Taguchi-Shiobara et al., 2001). Genetic and biochemical interaction studies indicate that FEA2 proteins physically interact with a G-alpha subunit, COMPACT PLANT2 (CT2) or an additional membrane kinase, ZmCRN to control meristem size (Bommert et al., 2013; Je et al., 2018). A co-IP assay independently showed that FEA2-CT2 and FEA2-ZMCRN physically interact; CT2 and ZmCRN

do not physically interact and therefore receive signals through additional pathways to maintain SAM development (Je et al., 2018).

The ortholog to *CLV3*, *ZmCLAVATA3/ESR7* (*ZmCLE7*), also functions as a signaling peptide for the maize *CLAVATA* pathway (Goad et al., 2017; Je et al., 2018). In addition to *ZmCLE7*, another *CLE* peptide named after the orthologous gene in rice, *ZmFON2-LIKE CLE PROTEIN1* (*ZmFCP1*), is expressed in young leaf primordia and regulates *ZmWUS1* expression (Je et al., 2018). Genetic interaction studies and peptide assays found that ZmCLE7 peptides likely signal through FEA2;CT2 complexes, while ZmFCP1 peptides signal through FEA2;ZmCRN complexes (Je et al., 2016, 2018). ZmFCP1 also signals through an LRR kinase, FASCIATED EAR3 *(*FEA3*),* which is expressed in the periphery of the SAM and functions to repress the *ZmWUS1* domain from extending into the RZ (Je et al., 2016). In contrast to these studies, genetic evidence from an independent study suggests that the ZmCLE7 peptide does not signal through a complex with CT2*,* in the inflorescence but rather through the FEA2 and TD1 receptors (Johnson, 2017)*.* As maize has 48 CLE signaling peptides (Goad et al., 2017), it is possible that CT2 interacts with multiple CLE peptides, or that additional signaling pathways exist to perceive CLE ligands that regulate IM size.

The expression of *ZmWUS1* overlaps with another homeobox transcription factor, *knotted1* (*kn1*), orthologous to *STM* in *Arabidopsis* (Jackson et al., 1994) that also can be used as a meristematic marker. Dominant *Kn1* mutants cause ectopic expression of the gene, creating abnormal pools of stem cells, or “knots,” on the leaves (Greene et al., 1994; Smith et al., 1992). Recessive phenotypes of

kn1 included decreased spikelet production in tassels and limited or lack of development in the ear (Kerstetter et al., 1997). Many experiments, including double mutant, biochemical, and RNA-seq analysis highlight the role of KN1 in regulating the expression of over 600 other genes in meristem tissues, including TFs that modulate various phytohormonal pathways instrumental for development (Bolduc et al., 2012; Bolduc & Hake, 2009). Taken together, these studies highlight the importance of this gene in meristematic cell identity in maize.

There are other notable genes involved in regulating meristem size in maize. One is a bZIP transcription factor, *fasciated ear4* (*fea4)*, orthologous to *PERIANTHIA* in *Arabidopsis*, which has increased FM size (Running & Meyerowitz, 1996). Expressed in the SAM periphery, *fea4* acts parallel to the *CLV-WUS* pathway by modulating auxin response in the PZ (Pautler et al., 2015). Another heterotrimeric G protein, G-beta subunit, *ZmGB1*, was found to have enlarged SAMs and fasciated inflorescences, indicating that it too plays a role regulating meristem size during SAM development (Wu et al., 2020). Most recently, a dominant mutant in maize, *Fascicled ear1* (*Fas1*) was found to be caused by expression of two genes, a MADS-box transcription factor *zmm8*, and a YABBY gene *dropping leaf2* (*drl2*), earlier in development than normal (Du et al., 2021). This leads to a change in identity of PZ cells to become more meristematic creating enlarged reproductive organs. Studies of *fea4, ZmGB1,* and *Fas1* demonstrate that multiple additional meristem maintenance pathways, that work in parallel to the CLV-WUS pathway, are still being uncovered in maize.

Phytohormones and meristem maintenance

Meristem maintenance also requires the interplay of phytohormone pathways with developmental genes, particularly the plant growth hormones auxin and cytokinin which function in the PZ and CZ respectively. As mentioned above, FEA4 interacts with auxin in the PZ, as, AUXIN RESPONSE FACTORS (ARFs) and AUX-IAA genes were found to be differentially expressed in *fea4* mutants (Pautler et al., 2015). In addition, FEA4 was shown to physically interact with a glutaredoxin (GRX) protein *MALE STERILE CONVERTED ANTHER1* (*MSCA1*) in a yeast two-hybrid assay, phenotypically named *Aberrant phyllotaxy2* (*Abph2*) (Yang et al., 2015). GRX genes have also been shown to interact with the auxin response pathway, specifically by modulating how plants respond to higher temperatures during development (Cheng et al., 2011). Additionally, *abph2* and *fea4* function additively to regulate meristem maintenance and leaf organogenesis within SAMs (Yang et al., 2015).

Phenotypically similar to *Abph2*, the *aberrant phylotaxy1 (abph1)* gene, which encodes a cytokinin-inducible, type-A response regulator, regulates leaf phyllotaxy from the meristem periphery (Giullni et al., 2004). *abph1* mutants were found to have reduced auxin levels and decreased expression of auxin markers which likely causes a delay in incipient leaf development (Giullni et al., 2004; Lee et al., 2009). Normally, *abph1* functions to limit cytokinin signaling to the OC, which allows auxin signaling to occur at the periphery to signal organ formation (Giullni et al., 2004; Lee et al., 2009). Both *fea4* and *abph2* are also expressed in the periphery of SAMs and overlap with expression of the auxin transporter

ZmPINFORMED1a (*ZmPIN1a*) (Pautler et al., 2015; Yang et al., 2015) supporting the intersection of cytokinin-auxin cross talk in meristem maintenance pathways.

Similarly, *kn1* also connects the auxin and cytokinin pathways. A cytokinin biosynthesis gene, *lonely guy7* (*log7*), which controls the conversion between cytokinin intermediaries and bioactive cytokinins, has previously been shown to regulate meristem size – indicating cytokinin biosynthesis plays a role in meristem maintenance in rice (Tokunaga et al., 2012). Another set of cytokinin biosynthesis genes, *isopentenyl transferases* (*ipt*), are direct targets of *kn1*, again linking cytokinin synthesis and meristem maintenance (Yanai et al., 2005). Conversely, *kn1* also directly regulates the expression of *vanishing tassel2* (*vt2*), an auxin biosynthesis gene, and has been shown to bind the promoters of most of the AUX-IAA proteins and ARF TFs in meristems (Bolduc et al., 2012), highlighting the influence of *kn1* on multiple levels of auxin pathway.

Specificity of meristem maintenance pathways in maize

The studies described in this review are generally used to inform meristem maintenance pathways, but it is important to note that physical evidence of RNA and/or protein expression has yet to be specifically confirmed across all meristem types throughout development. The first line of evidence for a gene's function in a specific meristem type comes from phenotypic analysis. For example, the *TD1, FEA2,* and *CT2* proteins were originally assumed to function in the IM as *td1, fea2,* and *ct2* mutants had enlarged and fasciated IMs, indicative of a meristem maintenance pathway perturbation (Bommert et al., 2005b, 2013; Taguchi-Shiobara et al., 2001). Similarly, meristem size can be implied by the additional or

decreased number of organs that meristem is responsible for making. For example, *td1* mutants have an increased number of floral organs per spikelet (Bommert et al., 2005b), implying *td1* also functions to regulate floral meristems (Table 2).

To determine if a gene is expressed at the transcript level, and the subsequent expression domain within a specific tissue, RNA *in situ* hybridizations have traditionally be used. RNA-seq analysis and RT/qRT-PCR are also acceptable to show gene expression in tissues, although they do not provide specific information on expression domains (eg: *fea2*, Table 2).

In addition to highlighting the expression of key meristem maintenance genes, Table 2 also highlights protein expression studies that confirm the assumed role of these genes determined by phenotypic analysis. For example, Je et al, 2013 analyzed FEA3 protein expression using a *fea3* promotor driven, FEA3 protein fused to RFP, however expression of this construct was not published in every meristem type. It is possible that FEA3 does not function in all meristem types throughout development, and therefore expression provides meristem specificity, but it is also possible that additional studies need to be performed confirm these results.

Thresholding theories argue that specific levels of gene expression need to be meet for different development objectives to occur, for example: cell division for OC stem cell maintenance, meristem identify transitions or axillary meristem development from the SAM or IM (He et al., 2018; Perales et al., 2016; Shi et al., 2016). It is important to confirm the expression of these genes in all meristem types

throughout development to better understand how their levels or expression might impact both function and final developmental outcome. Furthermore, specificity between species needs to be considered. As recently reviewed in (Fletcher, 2018) there is evidence that some genes have different functions in different meristems across species type. This is supported in studies on CLE signaling peptides, which highlighted evolutionary differences in family number between species, indicating these signaling ligands may have sub and neofunctionalizations in different species (Goad et al., 2017)

CONCLUSIONS AND FUTURE DIRECTIONS

Lessons from animal development

Several reviews have discussed the overarching developmental similarities shared in plant and animal kingdoms, including a recent review which called for increased sharing of knowledge between scientific fields (Hamant & Saunders, 2020). The authors argued that while genes may be different for organ development, the shared patterns of development can be used to inform all fields of developmental biology (Hamant & Saunders, 2020).

A case study into how principles can be shared is the research on a human developmental disorder, Holoprosencephaly (HPE), which results in birth defects due to the embryo not being able to fully divide into two hemispheres (Petryk et al., 2015). This disease is caused by a heterozygous, loss-of-function predisposing mutation in the *sonic hedgehog* (*shh*) gene, which encodes a small signaling ligand (Marigo et al., 1995). However, the HPE phenotype is highly variable, ranging from

infant mortality to seemingly normal development (Maryam et al., 2008; Petryk et al., 2015). When the penetrance and expressivity of HPE was studied, it was found that mutations at least nine other genes in the SHH pathway, which regulates patterning, could affect the final expression of the HPE phenotype (Choudhry et al., 2014). Moreover, the exposure to different environmental factors during gestation, such as alcohol, also influenced the final expression of the phenotype (Ahlgren et al., 2002; Kietzman et al., 2014; Petryk et al., 2015). In all, the HPE phenotype is the result of a predisposing mutation (dominant, loss-of function mutation in *shh*) in a developmental regulatory pathway (*SHH* pathway) and the penetrance and expressivity of the phenotype is influenced by both genetic modifiers (mutations in other *SHH* pathway genes) and environmental conditions (such as alcohol) at different stages of embryo development. Furthermore, the severity of the phenotype was proposed to be due to thresholds of function being reached at specific developmental transitions.

Semi-dominant mutants are inherently dose-dependent, so variation is expected between heterozygous and homozygous mutants (Howell, 1999). However, there are cases where semi dominant developmental mutants have a range of variability, like the range seen in HPE. The research presented in this thesis, specifically in Chapters 2 and 3 is an example of a highly-variable, semi-dominant mutant that functions generally in maize development, specifically in meristem maintenance. Utilizing the overarching ideas presented in HPE research informed a lot of the research questions presented in the next few chapters.

Future directions

Moving forward, building meristem-specific networks of regulation will provide the field with more clarity on how plants correctly direct their growth throughout development. Pairing this information with the growing literature of micronutrient and environmental impacts on developmental pathways, will provide the most comprehensive understanding of meristem development in maize and other plants. Understanding common themes in development can also help researchers extrapolate and identify future research questions and current holes in the literature.

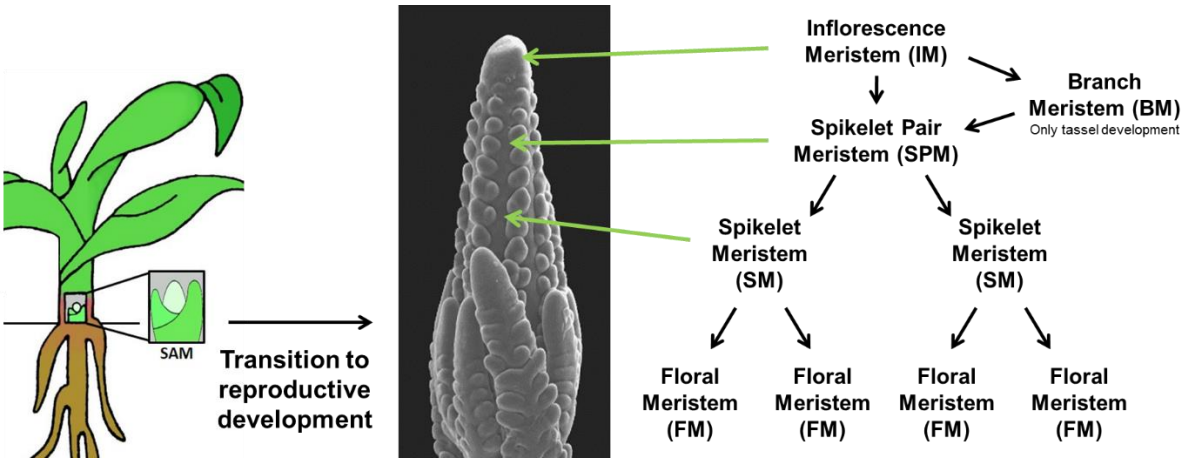

Figure 1: Schematic of normal meristem transitions throughout maize development. SAMs direct all above ground vegetative growth before elongating into the IM to transition to reproductive development. The IM first produces BMs (in tassel development) followed by SPMs. SPM will produce two SM, which will subsequently produce two FM each. Green arrows highlight each meristem type on an immature tassel SEM. Immature tassel SEM performed by Kim Phillips (Phillips et al., 2011).

Table 1: Meristem maintenance genes and orthologs in *Arabidopsis* and maize

Arabidopsis	**Maize**	**Protein**
SHOOTMERISTEMLESS (STM)	*knotted1 (kn1)*	Homeobox transciption factor
REVOLUTA (REV)	*Rolled Leaf 1 (Rld1)*	HD-Zip lll transcription factor
LITTLE ZIPPER3/4 (ZPR3/4)	*Zmlittle zipper4 (ZmZPR4)*	HD-ZIP lll competitive inhibitor
WUSCHEL (*WUS)*	*Zmwuschel1 (ZmWUS1)*	Homeodomain transcription factor
CLAVATA1 (*CLV1*)	*thick-tassel dwarf1 (td1)*	LRR receptor kinase
CLAVATA2 (CLV*2*)	*fasciated ear2 (fea2)*	LRR receptor, no kinase activity
CLAVATA3 (CLV3)	*CLV3/Embryo-surrounding region7* (cle7)	Small signalling ligand
-	*ZmFON2-like cle Protein2 (ZmFCP1)*	Small signalling ligand
CORYNE (CRN)	*Zmcoryne (ZmCRN)*	Ser/Thr membrane associated kinase
GPA1	*compact plant2 (ct2)*	Heteromeric G protein alpha subunit
Gβ SUBUNIT (*AtGB1*)	*ZmGβ subunit (ZmGB1)*	G-beta subunit Protein
-	*fasciated ear3 (fea3)*	LRR recepter
PERIANTHIA (*PAN*)	*fasciated ear4 (fea4)*	bZIP transcription factor
BARELY ANY MERISTEM (BAM)	*Zmbarely any meristem (ZmBAM)*	Receptor-like kinases

Table 1: Select meristem maintenance genes and orthologs in *Arabidopsis* and maize.

Table 2: Evidence for the RNA and Protein expression of select meristem maintenance genes throughout development

		SAM	IM	SPM	SM	FM
wus1	**Transcript**	Yes	Yes	Yes	-	-
	Evidence	RNA *in situ* hybridzation	RNA *in situ* hybridization	RNA *in situ* hybridization		
	Citation	Nardmann and Werr, 2006	Chen et al, 2021	Chen et al, 2021		
	Protein	Yes, at transition	Yes	-	-	-
	Evidence	pZmWUS1-RFP expression	pZmWUS1-RFP expression			
	Citation	Je et al, 2016	Je et al, 2016			
kn1	**Transcript**	Yes	Yes	Yes	Yes	Yes
	Evidence	RNA *in situ* hybridzation	RNA *in situ* hybridzation	RNA *in situ* hybridzation	RNA *in situ* hybridzation	RNA *in situ* hybridzation
	Citation	Jackson et al, 1994	Jackson et al, 1994	Jackson et al, 1994	Jackson et al, 1994	Jackson et al, 1994
	Protein	Yes	Yes	Yes	Yes	Yes, weak
	Evidence	Polyclonal antibody expression	Polyclonal antibody expression	Polyclonal antibody expression	Polyclonal antibody expression	Polyclonal antibody expression
	Citation	Smith et al, 1992	Smith et al, 1992	Smith et al, 1992	Smith et al, 1992	Smith et al, 1992
td1	**Transcript**	Yes, PZ	Yes	Yes	Yes	Yes
	Evidence	RNA *in situ* hybridzation	RNA *in situ* hybridzation	RNA *in situ* hybridzation	RNA *in situ* hybridzation	RNA *in situ* hybridzation
	Citation	Bommert et al, 2015	Bommert et al, 2015	Bommert et al, 2015	Bommert et al, 2015	Bommert et al, 2015
	Protein	Assumed	Assumed	-	Assumed	Assumed
	Evidence	Decreased SAM size	Fasciation of ear IMs		Increased glume number	Increased floral organs
	Citation	Lunde and Hake 2009	Bommert et al, 2005		Bommert et al, 2005	Bommert et al, 2005
fea2	**Transcript**	Yes	-	-	-	-
	Evidence	RT-PCR, SAMs				
	Citation	Je et al, 2016				
	Protein	Assumed	Assumed	Assumed	-	Assumed
	Evidence	Increased SAM size	Fasciation of ear IMs	Fasciation of SPM		Increased floral organs
	Citation	Je et al, 2018	Taguchi-Shiobara et al, 2001	Taguchi-Shiobara et al, 2001		Taguchi-Shiobara et al, 2001
ct2	**Transcript**	Yes	-	-	-	-
	Evidence	SAM RNA-seq Atlas				
	Citation	Knauer et al, 2019				
	Protein	Yes	Yes	Yes	Yes	Yes
	Evidence	CT2-YFP expression	CT2-YFP expression	CT2-YFP expression	CT2-YFP expression	CT2-YFP expression
	Citation	Bommert et al, 2016	Bommert et al, 2016	Bommert et al, 2016	Bommert et al, 2016	Bommert et al, 2016
fea3	**Transcript**	Yes	Yes, weak	-	Yes, ears	-
	Evidence	RNA *in situ* hybridzation	RNA *in situ* hybridzation		RNA *in situ* hybridiztion	
	Citation	Je et al, 2016	Je et al, 2016		Je et al, 2016	
	Protein	Yes	Yes	-	Yes	-
	Evidence	pFEA3::FEA3-RFP expression	pFEA3::FEA3-RFP expression		pFEA3::FEA3-RFP expression	
	Citation	Je et al, 2016	Je et al, 2016		Je et al, 2016	
crn	**Transcript**	Yes, PZ	-	-	-	-
	Evidence	RNA in situ hybridzation				
	Citation	Je et al, 2018				
	Protein	Assumed	Assumed	-	-	-
	Evidence	Increased SAM size	Fasciation of ear IMs			
	Citation	Je et al, 2018	Je et al, 2018			
Zmcle7	**Transcript**	-	Yes	-		
	Evidence		RNA-seq (ear IM)			
	Citation		Liu et al, 2021			
	Protein	Assumed	Assumed	-	-	-
	Evidence	Increased SAM size	Fasciation of ear IMs			
	Citation	Je et al, 2018	Liu et al, 2021			
Zmfcp1	**Transcript**	Yes, in PZ	Yes	-	-	-
	Evidence	RNA *in situ* hybridzation	RNA-seq			
	Citation	Je et al, 2016	Liu et al, 2021			
	Protein	Assumed	Assumed	-	-	-
	Evidence	Increased SAM size	Fasciation of ear IMs			
	Citation	Je et al, 2016	Je et al, 2016			

Table 2: Evidence for the RNA and protein expression of select meristem maintenance genes in maize. For each gene he published evidence for expression in each meristem type described in this review is provided. Dashes indicate published evidence (phenotypic, transcriptomic, proteomic, etc.) is not yet available.

WORKS CITED

Ahlgren, S. C., Thakur, V., & Bronner-Fraser, M. (2002). Sonic hedgehog rescues cranial neural crest from cell death induced by ethanol exposure. *Proceedings of the National Academy of Sciences of the United States of America*, *99*(16), 10476–10481. https://doi.org/10.1073/pnas.162356199

Barton, M. K., & Poething, R. S. (1994). Formation of the shoot apical meristem in Arabidopsis thaliana: an analysis of development in the wild type and in the shoot meristemless mutant. *Development*, *119*(2), 823–831. https://doi.org/10.1016/0168-9525(94)90143-0

Bleckmann, A., Weidtkamp-Peters, S., Seidel, C. A. M., & Simon, R. (2010). Stem cell signaling in Arabidopsis requires CRN to localize CLV2 to the plasma membrane. *Plant Physiology*, *152*(1), 166–176. https://doi.org/10.1104/pp.109.149930

Bolduc, N., & Hake, S. (2009). The maize transcription factor KNOTTED1 directly regulates the gibberellin catabolism gene ga2ox1. *Plant Cell*, *21*(6), 1647–1658. https://doi.org/10.1105/tpc.109.068221

Bolduc, N., Yilmaz, A., Mejia-Guerra, M. K., Morohashi, K., O'Connor, D., Grotewold, E., & Hake, S. (2012). Unraveling the KNOTTED1 regulatory network in maize meristems. *Genes and Development*, *26*(15), 1685–1690. https://doi.org/10.1101/gad.193433.112

Bommert, P., Je, B. il, Goldshmidt, A., & Jackson, D. (2013). The maize Gα gene COMPACT PLANT2 functions in CLAVATA signalling to control shoot meristem size. *Nature*, *502*(7472), 555–558. https://doi.org/10.1038/nature12583

Bommert, P., Lunde, C., Nardmann, J., Vollbrecht, E., Running, M., Jackson, D., Hake, S., & Werr, W. (2005a). Thick tassel dwarf1 encodes a putative maize ortholog of the Arabidopsis CLAVATA1 leucine-rich repeat receptor-like kinase. *Development*, *132*(6), 1235–1245. https://doi.org/10.1242/dev.01671

Bommert, P., Lunde, C., Nardmann, J., Vollbrecht, E., Running, M., Jackson, D., Hake, S., & Werr, W. (2005b). Thick tassel dwarf1 encodes a putative maize ortholog of the Arabidopsis CLAVATA1 leucine-rich repeat receptor-like kinase. *Development*, *132*(6), 1235–1245. https://doi.org/10.1242/dev.01671

Chen, Z., Li, W., Gaines, C., Buck, A., Galli, M., & Gallavotti, A. (2021). Structural variation at the maize WUSCHEL1 locus alters stem cell organization in inflorescences. *Nature Communications*, *12*(1), 1–12. https://doi.org/10.1038/s41467-021-22699-8

Cheng, N. H., Liu, J. Z., Liu, X., Wu, Q., Thompson, S. M., Lin, J., Chang, J., Whitham, S. A., Park, S., Cohen, J. D., & Hirschi, K. D. (2011). Arabidopsis monothiol glutaredoxin, AtGRXS17, is critical for temperature-dependent postembryonic growth and development via modulating auxin response. *Journal of Biological Chemistry*, *286*(23), 20398–20406. https://doi.org/10.1074/jbc.M110.201707

Choudhry, Z., Rikani, A. A., Choudhry, A. M., Tariq, S., Zakaria, F., Asghar, M. W., Sarfraz, M. K., Haider, K., Shafiq, A. A., & Mobassarah, N. J. (2014). Sonic hedgehog signalling pathway: A complex network. *Annals of Neurosciences*, *21*(1), 28–31. https://doi.org/10.5214/ans.0972.7531.210109

Clark, S. E., Williams, R. W., & Meyerowitz, E. M. (1997). The CLAVATA1 gene encodes a putative receptor kinase that controls shoot and floral meristem size in arabidopsis. *Cell*, *89*(4), 575–585. https://doi.org/10.1016/S0092-8674(00)80239-1

Desvoyes, B., de Mendoza, A., Ruiz-Trillo, I., & Gutierrez, C. (2014). Novel roles of plant RETINOBLASTOMA-RELATED (RBR) protein in cell proliferation and asymmetric cell division. *Journal of Experimental Botany*, *65*(10), 2657–2666. https://doi.org/10.1093/jxb/ert411

Desvoyes, B., & Gutierrez, C. (2020). Roles of plant retinoblastoma protein: cell cycle and beyond. *The EMBO Journal*, *39*(19). https://doi.org/10.15252/embj.2020105802

DeYoung, B. J., & Clark, S. E. (2008). BAM receptors regulate stem cell specification and organ development through complex interactions with CLAVATA signaling. *Genetics*, *180*(2), 895–904. https://doi.org/10.1534/genetics.108.091108

Du, Y., Lunde, C., Li, Y., Jackson, D., Hake, S., & Zhang, Z. (2021). Gene duplication at the Fascicled ear1 locus controls the fate of inflorescence meristem cells in maize. *Proceedings of the National Academy of Sciences of the United States of America*, *118*(7). https://doi.org/10.1073/pnas.2019218118

Endrizzi, K., Moussian, B., Haecker, A., Levin, J. Z., & Laux, T. (1996). The SHOOT MERISTEMLESS gene is required for maintenance of undifferentiated cells in Arabidopsis shoot and floral meristems and acts at a different regulatory level than the meristem genes WUSCHEL and ZWILLE. *Plant Journal*, *10*(6), 967–979. https://doi.org/10.1046/j.1365-313X.1996.10060967.x

Evert, R. F., Eichhorn, S. E., & Edition, T. (2006). Esau ' s Plant Anatomy ESAU ' S PLANT ANATOMY. In *Development*. http://doi.wiley.com/10.1002/0470047380

Fletcher, J. C. (2018). The CLV-WUS stem cell signaling pathway: A roadmap to crop yield optimization. In *Plants* (Vol. 7, Issue 4). MDPI AG. https://doi.org/10.3390/plants7040087

Fletcher, J. C., Brand, U., Running, M. P., Simon, R., & Meyerowitz, E. M. (1999). Signaling of cell fate decisions by CLAVATA3 in Arabidopsis shoot meristems. *Science*, *283*(5409), 1911–1914. https://doi.org/10.1126/science.283.5409.1911

Fung, Y. K. T., Linn Murphree, A., T'Ang, A., Qian, J., Hinrichs, S. H., & Benedict, W. F. (1987). Structural evidence for the authenticity of the human retinoblastoma gene. *Science*, *236*(4809), 1657–1661. https://doi.org/10.1126/science.2885916

Galinat, W. C. (1959). *THE PHYTOMER IN RELATION TO FLORAL HOMOLOGIES IN THE AMERICAN MAYDEAE* (Vol. 19, Issue 1).

Gifford, M. L., Dean, S., & Ingram, G. C. (2003). The Arabidopsis ACR4 gene plays a role in cell layer organisation during ovule integument and sepal margin development. *Development*, *130*(18), 4249–4258. https://doi.org/10.1242/dev.00634

Giullni, A., Wang, J., & Jackson, D. (2004). Control of phyllotaxy by the cytokinin-inducible response regulator homologue ABPHYL1. *Nature*, *430*(7003), 1031–1034. https://doi.org/10.1038/nature02778

Goad, D. M., Zhu, C., & Kellogg, E. A. (2017). Comprehensive identification and clustering of CLV3/ESR-related (CLE) genes in plants finds groups with potentially shared function. *New Phytologist*, *216*(2), 605–616. https://doi.org/10.1111/nph.14348

Grafi, G., Burnett, R. J., Helentjaris, T., Larkins, B. A., Decaprio, J. A., Sellers, W. R., & Kaelin, W. G. (1996). A maize cDNA encoding a member of the retinoblastoma protein family: Involvement in endoreduplication. *Proceedings of the National Academy of Sciences of the United States of America*, *93*(17), 8962–8967. https://doi.org/10.1073/pnas.93.17.8962

Gray, A. (1879). *Structural Botany*. Cambridge University Press.

Greene, B., Walko, R., & Hake, S. (1994). Mutator insertions in an intron of the maize knotted1 gene result in dominant suppressible mutations. *Genetics*, *138*(4), 1275–1285. https://doi.org/10.1093/genetics/138.4.1275

Hake, S., Smith, H. M. S., Holtan, H., Magnani, E., Mele, G., & Ramirez, J. (2004). The role of Knox genes in plant development. In *Annual Review of Cell and Developmental Biology* (Vol. 20, pp. 125–151). Annu Rev Cell Dev Biol. https://doi.org/10.1146/annurev.cellbio.20.031803.093824

Hamant, O., & Saunders, T. E. (2020). Shaping Organs: Shared Structural Principles across Kingdoms. In *Annual Review of Cell and Developmental Biology* (Vol. 36, pp. 385–410). Annual Reviews Inc. https://doi.org/10.1146/annurev-cellbio-012820-103850

He, J., Xu, M., Willmann, M. R., McCormick, K., Hu, T., Yang, L., Starker, C. G., Voytas, D. F., Meyers, B. C., & Poethig, R. S. (2018). Threshold-dependent repression of SPL gene expression by miR156/miR157 controls vegetative phase change in Arabidopsis thaliana. *PLoS Genetics*, *14*(4). https://doi.org/10.1371/journal.pgen.1007337

Howell, S. H. (1999). Molecular genetics of plant development. In *Choice Reviews Online* (Vol. 36, Issue 05). Cambridge University Press. https://doi.org/10.5860/choice.36-2743

Jackson, D., Veit, B., & Hake, S. (1994). Expression of maize KNOTTED1 related homeobox genes in the shoot apical meristem predicts patterns of morphogenesis in the vegetative shoot. *Development*, *120*(2), 405–413. https://doi.org/10.1242/dev.120.2.405

Jasinski, S., Piazza, P., Craft, J., Hay, A., Woolley, L., Rieu, I., Phillips, A., Hedden, P., & Tsiantis, M. (2005). KNOX action in Arabidopsis is mediated by coordinate regulation of cytokinin and gibberellin activities. *Current Biology*, *15*(17), 1560–1565. https://doi.org/10.1016/j.cub.2005.07.023

Je, B. il, Gruel, J., Lee, Y. K., Bommert, P., Arevalo, E. D., Eveland, A. L., Wu, Q., Goldshmidt, A., Meeley, R., Bartlett, M., Komatsu, M., Sakai, H., Jönsson, H., Jackson, D., & Danforth, D. (2016). Signaling from maize organ primordia via FASCIATED EAR3 regulates stem cell proliferation and yield traits. *Nature Publishing Group*, *48*(7), 785–791. https://doi.org/10.1038/ng.3567

Je, B. il, Xu, F., Wu, Q., Liu, L., Meeley, R., Gallagher, J. P., Corcilius, L., Payne, R. J., Bartlett, M. E., & Jackson, D. (2018). The clavata receptor fasciated ear2 responds to distinct cle peptides by signaling through two downstream effectors. *ELife*, *7*. https://doi.org/10.7554/eLife.35673

Kayes, J. M., & Clark, S. E. (1998). CLAVATA2, a regulator of meristem and organ development in Arabidopsis. *Development*, *125*(19), 3843–3851. https://doi.org/10.1242/dev.125.19.3843

Kerstetter, R. A., Laudencia-Chingcuanco, O., Smith, L. G., & Hake, S. (1997). Loss-of-function mutations in the maize homeobox gene, knotted1, are defective in shoot meristem maintenance. *Development*, *124*(16), 3045–3054. https://doi.org/10.1242/dev.124.16.3045

Kietzman, H. W., Everson, J. L., Sulik, K. K., & Lipinski, R. J. (2014). The teratogenic effects of prenatal ethanol exposure are exacerbated by sonic Hedgehog or Gli2 haploinsufficiency in the mouse. *PLoS ONE*, *9*(2). https://doi.org/10.1371/journal.pone.0089448

Kim, Y. S., Kim, S. G., Lee, M., Lee, I., Park, H. Y., Pil, J. S., Jung, J. H., Kwon, E. J., Se, W. S., Paek, K. H., & Park, C. M. (2008). HD-ZIP III activity is modulated by competitive inhibitors via a feedback loop in Arabidopsis shoot apical meristem development. *Plant Cell*, *20*(4), 920–933. https://doi.org/10.1105/tpc.107.057448

Laux, T., Mayer, K. F. X., Berger, J., & Jürgens, G. (1996). The WUSCHEL gene is required for shoot and floral meristem integrity in Arabidopsis. *Development*, *122*(1), 87–96. https://doi.org/10.1242/dev.122.1.87

Lee, B. H., Johnston, R., Yang, Y., Gallavotti, A., Kojima, M., Travençolo, B. A. N., Costa, L. D. F., Sakakibara, H., & Jackson, D. (2009). Studies of aberrant phyllotaxy1 mutants of maize indicate complex interactions between auxin and cytokinin signaling in the shoot apical meristem 1. *Plant Physiology*, *150*(1), 205–216. https://doi.org/10.1104/pp.109.137034

Lee, W.-H., Bookstein, R., Hong, F., Young, L.-J., Shew, J.-Y., & Y-H Lee, E. P. (1987). Human Retinoblastoma Susceptibility Gene: Cloning, Identification, and Sequence. In *New Series* (Vol. 235, Issue 4794).

Lenhard, M., Jürgens, G., & Laux, T. (2002). The WUSCHEL and SHOOTMERISTEMLESS genes fulfil complementary roles in Arabidopsis shoot meristem regulation. *Development*, *129*(13), 3195–3206. https://doi.org/10.1242/dev.129.13.3195

Long, J. A., Moan, E. I., Medford, J. I., & Barton, M. K. (1996). A member of the KNOTTED class of homeodomain proteins encoded by the STM gene of Arabidopsis. *Nature*, *379*(6560), 66–69. https://doi.org/10.1038/379066a0

Long, J., & Kathryn Barton, M. (2000). *Initiation of Axillary and Floral Meristems in Arabidopsis*. https://doi.org/10.1006/dbio.1999.9572

Lunde, C., & Hake, S. (2009). The interaction of knotted1 and thick tassel dwarf1 in vegetative and reproductive meristems of maize. *Genetics*, *181*(4), 1693–1697. https://doi.org/10.1534/genetics.108.098350

Marigo, V., Roberts, D. J., Lee, S. M. K., Tsukurov, O., Levi, T., Gastier, J. M., Epstein, D. J., Gilbert, D. J., Copeland, N. G., Seidman, C. E., Jenkins, N. A., Seidman, J. G., McMahon, A. P., & Tabin, C. (1995). Cloning, Expression, and Chromosomal Location of SHH and IHH: Two Human Homologues of the Drosophila Segment Polarity Gene Hedgehog. *Genomics*, *28*(1), 44–51. https://doi.org/10.1006/GENO.1995.1104

Maryam, N., Firouzeh, A., & Irani, S. (2008). Holoprosencephaly: A Case Report and Review of Prenatal Sonographic Findings. *Undefined*.

Mayer, K. F. X., Schoof, H., Haecker, A., Lenhard, M., Jürgens, G., & Laux, T. (1998). Role of WUSCHEL in regulating stem cell fate in the Arabidopsis shoot meristem. *Cell*, *95*(6), 805–815. https://doi.org/10.1016/S0092-8674(00)81703-1

Meng, W. J., Cheng, Z. J., Sang, Y. L., Zhang, M. M., Rong, X. F., Wang, Z. W., Tang, Y. Y., & Zhang, X. S. (2017). Type-B ARABIDOPSIS RESPONSE REGULATORs specify the shoot stem cell niche by dual regulation of WUSCHEL. *Plant Cell*, *29*(6), 1357–1372. https://doi.org/10.1105/tpc.16.00640

Meyer, M. R., Shah, S., Zhang, J., Rohrs, H., & Rao, A. G. (2015). Evidence for intermolecular interactions between the intracellular domains of the arabidopsis receptor-like kinase ACR4, its homologs and the Wox5 transcription factor. *PLoS ONE*, *10*(3). https://doi.org/10.1371/journal.pone.0118861

Meyerowitz, E. M. (2002). Comparative genomics. Plants compared to animals: The broadest comparative study of development. *Science*, *295*(5559), 1482–1485. https://doi.org/10.1126/science.1066609

Müller, R., Bleckmann, A., & Simon, R. (2008). The receptor kinase CORYNE of Arabidopsis transmits the stem cell-limiting signal CLAVATA3 independently of CLAVATA1. *Plant Cell*, *20*(4), 934–946. https://doi.org/10.1105/tpc.107.057547

Nardmann, J., & Werr, W. (2006). The shoot stem cell niche in angiosperms: Expression patterns of WUS orthologues in rice and maize imply major modifications in the course of mono- and dicot evolution. *Molecular Biology and Evolution*, *23*(12), 2492–2504. https://doi.org/10.1093/molbev/msl125

Nimchuk, Z. L., Zhou, Y., Tarr, P. T., Peterson, B. A., & Meyerowitz, E. M. (2015a). Plant stem cell maintenance by transcriptional cross-regulation of related receptor kinases. *Development (Cambridge)*, *142*(6), 1043–1049. https://doi.org/10.1242/dev.119677

Nimchuk, Z. L., Zhou, Y., Tarr, P. T., Peterson, B. A., & Meyerowitz, E. M. (2015b). Plant stem cell maintenance by transcriptional cross-regulation of related receptor kinases. *Development (Cambridge)*, *142*(6), 1043–1049. https://doi.org/10.1242/dev.119677

Pautler, M., Eveland, A. L., Larue, T., Yang, F., Weeks, R., Lunde, C., il Je, B., Meeley, R., Komatsu, M., Vollbrecht, E., Sakai, H., & Jackson, D. (2015). FASCIATED EAR4 encodes a bZIP transcription factor that regulates shoot

meristem size in maize. *Plant Cell*, *27*(1), 104–120. https://doi.org/10.1105/tpc.114.132506

Perales, M., Rodriguez, K., Snipes, S., Yadav, R. K., Diaz-Mendoza, M., & Reddy, G. V. (2016). Threshold-dependent transcriptional discrimination underlies stem cell homeostasis. *Proceedings of the National Academy of Sciences of the United States of America*, *113*(41), E6298–E6306. https://doi.org/10.1073/pnas.1607669113

Petryk, A., Graf, D., & Marcucio, R. (2015). Holoprosencephaly: Signaling interactions between the brain and the face, the environment and the genes, and the phenotypic variability in animal models and humans. In *Wiley Interdisciplinary Reviews: Developmental Biology* (Vol. 4, Issue 1, pp. 17–32). John Wiley and Sons Inc. https://doi.org/10.1002/wdev.161

Phillips, K., Skirpan, A. L., Liu, X., Christensen, A., Slewinski, T. L., Hudson, C., Barazesh, S., Cohen, J. D., Malcomber, S., & McSteen, P. (2011). vanishing tassel2 encodes a grass-specific tryptophan aminotransferase required for vegetative and reproductive development in maize. *The Plant Cell*, *23*(2), 550–566. https://doi.org/10.1105/TPC.110.075267

Running, M. P., & Meyerowitz, E. M. (1996). Mutations in the PERIANTHIA gene of Arabidopsis specifically alter floral organ number and initiation pattern. *Development*, *122*(4), 1261–1269. https://pubmed.ncbi.nlm.nih.gov/8620853/

Schoof, H., Lenhard, M., Haecker, A., Mayer, K. F. X., Jürgens, G., & Laux, T. (2000). The stem cell population of Arabidopsis shoot meristems is maintained by a regulatory loop between the CLAVATA and WUSCHEL genes. *Cell*, *100*(6), 635–644. https://doi.org/10.1016/S0092-8674(00)80700-X

Shi, B., Zhang, C., Tian, C., Wang, J., Wang, Q., Xu, T., Xu, Y., Ohno, C., Sablowski, R., Heisler, M. G., Theres, K., Wang, Y., & Jiao, Y. (2016). Two-Step Regulation of a Meristematic Cell Population Acting in Shoot Branching in Arabidopsis. *PLoS Genetics*, *12*(7), e1006168. https://doi.org/10.1371/journal.pgen.1006168

Smith, L. G., Greene, B., Veit, B., & Hake, S. (1992). A dominant mutation in the maize homeobox gene, Knotted-1, causes its ectopic expression in leaf cells with altered fates. *Development*, *116*(1), 21–30. https://doi.org/10.1242/DEV.116.1.21

Somssich, M., il Je, B., Simon, diger, & Jackson, D. (2016). *CLAVATA-WUSCHEL signaling in the shoot meristem*. https://doi.org/10.1242/dev.133645

Stahl, Y., Grabowski, S., Bleckmann, A., Kühnemuth, R., Weidtkamp-Peters, S., Pinto, K. G., Kirschner, G. K., Schmid, J. B., Wink, R. H., Hülsewede, A., Felekyan, S., Seidel, C. A. M., & Simon, R. (2013). Moderation of arabidopsis root stemness by CLAVATA1 and ARABIDOPSIS CRINKLY4 receptor kinase complexes. *Current Biology*, *23*(5), 362–371. https://doi.org/10.1016/j.cub.2013.01.045

Steeves, Taylor A; Sussex, I. M. (1989). *Patterns in Plant Development*.

Taguchi-Shiobara, F., Yuan, Z., Hake, S., & Jackson, D. (2001). *The fasciated ear2 gene encodes a leucine-rich repeat receptor-like protein that regulates shoot meristem proliferation in maize*. https://doi.org/10.1101/gad.208501

Tokunaga, H., Kojima, M., Kuroha, T., Ishida, T., Sugimoto, K., Kiba, T., & Sakakibara, H. (2012). Arabidopsis lonely guy (LOG) multiple mutants reveal a central role of the LOG-dependent pathway in cytokinin activation. *Plant Journal*, *69*(2), 355–365. https://doi.org/10.1111/j.1365-313X.2011.04795.x

Weinberg, R. A. (1995). The retinoblastoma protein and cell cycle control. In *Cell* (Vol. 81, Issue 3, pp. 323–330). Cell Press. https://doi.org/10.1016/0092-8674(95)90385-2

Wenkel, S., Emery, J., Hou, B. H., Evans, M. M. S., & Barton, M. K. (2007). A feedback regulatory module formed by Little Zipper and HD-ZIPIII genes. *Plant Cell*, *19*(11), 3379–3390. https://doi.org/10.1105/tpc.107.055772

Williams, L., Grigg, S. P., Xie, M., Christensen, S., & Fletcher, J. C. (2005). Regulation of Arabidopsis shoot apical meristem and lateral organ formation by microRNA miR166g and its AtHD-ZIP target genes. *Development*, *132*(16), 3657–3668. https://doi.org/10.1242/dev.01942

Wu, Q., Xu, F., Liu, L., Char, S. N., Ding, Y., Je, B. il, Schmelz, E., Yang, B., & Jackson, D. (2020). The maize heterotrimeric G protein β subunit controls shoot meristem development and immune responses. *Proceedings of the National Academy of Sciences of the United States of America*, *117*(3), 1799–1805. https://doi.org/10.1073/pnas.1917577116

Xu, Q., Li, R., Weng, L., Sun, Y., Li, M., & Xiao, H. (2019). Domain-specific expression of meristematic genes is defined by the LITTLE ZIPPER protein DTM in tomato. *Communications Biology*, *2*(1), 1–14. https://doi.org/10.1038/s42003-019-0368-8

Yadav, R. K., Perales, M., Gruel, J., Girke, T., Jönsson, H., & Venugopala Reddy, G. (2011). WUSCHEL protein movement mediates stem cell homeostasis in the Arabidopsis shoot apex. *Genes and Development*, *25*(19), 2025–2030. https://doi.org/10.1101/gad.17258511

Yanai, O., Shani, E., Dolezal, K., Tarkowski, P., Sablowski, R., Sandberg, G., Samach, A., & Ori, N. (2005). Arabidopsis KNOXI proteins activate cytokinin biosynthesis. *Current Biology*, *15*(17), 1566–1571. https://doi.org/10.1016/j.cub.2005.07.060

Yang, F., Bui, H. T., Pautler, M., Llaca, V., Johnston, R., Lee, B. H., Kolbe, A., Sakai, H., & Jackson, D. (2015). A maize glutaredoxin gene, Abphyl2, regulates shoot meristem size and phyllotaxy. *Plant Cell*, *27*(1), 121–131. https://doi.org/10.1105/tpc.114.130393

CHAPTER 2:

The Suppressor of sessile spikelets (Sos2) gene regulates meristem maintenance throughout maize development.

Katy Guthrie, Connor Nordwald, Norman Best, Hannah Seberg, Micha Matthes, Paula McSteen

ABSTRACT

Grasses are classified by the production of florets in small branches called “spikelets”, which maize produces in pairs, one pedicellate and one sessile. The semi-dominant mutant, *Suppressor of sessile spikelets2* (*Sos2*), displays meristem maintenance defects throughout maize development. When homozygous, *Sos2* mutants fail to germinate or are seedling lethal, indicating meristem maintenance defects during embryonic development. When heterozygous, *Sos2* mutants have defects in reproductive development, in both the tassel (which produces the male florets) and the ear (which produces the female florets). Typical phenotypes include single and aborted spikelets in the tassel and a failure to develop paired kernel rows in the ear. In severe cases, plants will develop a tassel without a main spike, or no tassel at all, and small rudimentary ears with only a few kernels. These phenotypes indicate defects in meristem maintenance, as each meristem transitions from one meristem type to the next, during reproductive development. The variation in phenotype suggests that the underlying mutation is influenced by both genetic and environmental modifiers. Genetic analysis of field grown plants indicated that this variation is a result of a semi-dominant mutation together with a recessive epistatic enhancer. Moreover, growth chamber experiments, shows that higher temperatures suppress the mutant phenotype.

As phenotypic analysis indicated meristem maintenance defects in *Sos2* mutants during reproductive development, double mutants were made with *Sos2* and known meristem maintenance mutants in the maize *CLAVATA* pathway, *fasciated ear2* (*fea2*), *thick tassel dwarf1* (*td1*), and *compact plant2* (*ct2*). This

analysis provided genetic evidence that *Sos2* functions in a different pathway from *Sos1*. This study was complimented by RNA-seq analysis, which showed a significant decrease in the expression of the homeodomain transcription factor, *ZmWUSCHEL1*, which functions in stem cells. Furthermore, other differentially expressed genes (DEGs) in this data set allow for the hypothesis that additional pathways play a role in maize meristem maintenance. In addition, DEGs were enriched for GO terms “response to heat/temperature stimulus”, supporting findings from the growth chamber experiments. Fine mapping and whole genome re-sequencing placed the *Sos2* mutation in a roughly 223kb region on the short arm of chromosome 10 (bin 10.01). This mapping, coupled with transcriptomic studies, identified a strong candidate gene, which is significantly increased in expression in *Sos2* mutants. Therefore, this study paints a comprehensive picture of how *Sos2* functions in maize development and provides a novel player in the canonical meristem maintenance pathway.

INTRODUCTION

Meristems, undifferentiated pools of stem cells, are unique to plants and allow them to produce organs throughout their lifetime. In general, meristems have two functions: to divide and produce cells that differentiate into different tissues and organs, and to sustain a pool of undifferentiated stem cells that maintain growth throughout the plants' lifetime (Steeves & Sussex, 1989). As plants grow, meristems will either transition from one type to another, or lead to the production of additional meristems to produce different types of organs.

In maize, meristems produce leaves throughout vegetative development, and the male and female reproductive structures, the tassel and ear respectively, during reproductive development. Both the tassel and the ear are comprised of short branches called spikelets which house the florets. Unlike other important cereal crops like rice, wheat, and barley, maize produces spikelets in pairs, a phenomenon that leads to an even numbers of kernel rows on ears. All of these structures are produced by the correct developmental progression of meristem types (See Chapter 1, Fig. 1). During vegetative development, the shoot apical meristem (SAM) functions to produce leaves (Evert et al., 2006; Steeves & Sussex, 1989). Upon the switch to reproductive development, however, the SAM will elongate and transition into the inflorescence meristem (IM) (Evert et al., 2006). The IM will then produce spikelet pair meristems (SPM) along the periphery that will branch to produce two spikelet meristems (SM), which mature into spikelet pairs. In these pairs, one spikelet will develop a short pedicle and the other, which will subtend the first attaching close to the tassel rachis, are known as the

pedicellate and sessile spikelet, respectively (Kiesselbach, 1949). Each SM gives rise to two floral meristems (FM) which produce the floral organs (Evert et al., 2006; Kiesselbach, 1949).While the organs produced by the meristems are specified by meristem identity genes, the function of all meristems are controlled by meristem maintenance genes.

Meristem maintenance is the balance between stem cell proliferation and differentiation vital for correct plant development. The most well-known molecular pathway that controls meristem maintenance in plants is the CLAVATA-WUSCHEL pathway, named after the canonical CALVATA genes described in *Arabidopsis* (reviewed in (Fletcher, 2018). At the center of this pathways is *WUSCHEL* (*WUS*), a homeodomain transcription factor (TF) that marks stem cell-ness (Mayer et al., 1998). *WUS* is negatively regulated by signaling from *CLAVATA3* (*CLV3*), a small, secreted CLE peptide, through *CLAVATA1* (*CLV1*) and *CLAVATA2* (*CLV2*), a LRR-receptor kinase and LRR-protein with no kinase activity, respectively (Brand et al., 2000; Clark et al., 1995; Fletcher, 1999). In maize, the orthologous homeodomain TF, *ZmWUSCHEL1* (*ZmWUS1*), paralog *ZmWUS2*, and other WUSCHEL-LIKE HOMEOBOX (WOX) TFs mark stem cell-ness within the meristem organizing center (OC) during SAM and early IM development (Je et al., 2016; Nardmann & Werr, 2006). It is important to note that while the CLAVATA pathway is widely conserved across plants and meristem types, there are differences, such as which TF defines stem cells, which CLE protein acts as the regulatory signal, and which CLV protein that receives that signal, that are specific to each meristem type (Fletcher, 2020; Goad et al., 2017).

The maize *CLV1* ortholog, *thick tassel dwarf 1 (td1)* encodes a LRR receptor-like kinase that signals independently of the *CLV2* ortholog, *fasciated ear2 (fea2)* in IMs (Bommert et al., 2005b). In *Arabidopsis,* CLV1 perceives the CLV3 ligand to repress *WUS* and maintain meristem size (Clark et al., 1995), however, there is still no functional evidence that the *CLV3* ortholog, ZmCLE7, signals through TD1 in maize (reviewed in (Fletcher, 2018). While *td1* does function in vegetative development, as evidenced by its decreased plant height (Bommert et al., 2005b; Lunde & Hake, 2009), RNA *in situ* hybridization shows that *td1* is not expressed in the same pattern in SAMs as it is in IMs, SPMs, SMs, and FMs, providing another of meristem specificity in the CLAVATA pathway (Bommert et al., 2005b). In *Arabidopsis, CLV1* acts antagonistically to *SHOOT MERISTEMLESS* (*STM*), a KNOX1-like transcription factor, to regulate the SAM and IM (Endrizzi et al., 1996; Lenhard et al., 2002; Long et al., 1996). In contrast, the maize homolog to *STM*, *knotted1* (*kn1*) (Vollbrecht et al., 2000) is epistatic to *td1* in maize indicating the KN1 and TD1 act in the same pathway to regulate IM size (Lunde & Hake, 2009).

The *fea2* gene encodes an LRR-receptor kinase that can form homodimers (Taguchi-Shiobara et al., 2001) as well as complexes with co-receptors, such as the pseudokinase, ZmCORYNE (ZmCRN) or the G-alpha protein, COMPACT PLANT 2 (CT2) (Bommert, Nagasawa, et al., 2013; Je et al., 2018). Evidence from peptide applications to SAMs indicates that ZmFCP1 signals through the FEA2/ZmCRN complex, while ZmCLE7 signals through the FEA2/CT2 complexes to restrict ZmWUS1 (Je et al., 2018). An additional receptor, FASCIATED EAR 3

(FEA3) was also found to be able to perceive the ZmFCP1 ligand to restrict ZmWUS1 expression from the bottom of the OC domain in IMs (Je et al., 2016). Absence of the *td1, fea2, ct2, Zmcrn, fea3, Zmfcp1,* or *Zmcle7* genes all result in fasciation of the ear and increased spikelet density in the tassel (Bommert et al., 2005b; Bommert, Nagasawa, et al., 2013; Je et al., 2016, 2018; Liu et al., 2021; Taguchi-Shiobara et al., 2001), highlighting their importance in restricting the size of the IM during reproductive development.

Meristems are also maintained through additional signaling pathways that act in parallel with the CLAVATA pathway in ways that are yet to be clearly defined in maize. In *Arabidopsis*, Class III homeodomain-leucine zipper (HD-ZIP IIII) TFs, such as *REVOLUTA* interact with the cytokinin pathway via Type B response regulators to induce *WUS* expression, allowing for the establishment and maintenance of the SAM (Zhang et al., 2017). Additionally, *REV* has been shown to up-regulate *STM* in leaf axillary meristem (AM) cells, which is important to reach the threshold of expression of *STM* needed for AM initiation to occur (Shi et al., 2016). These TFs are negatively regulated by small inhibitory proteins called LITTLE ZIPPER proteins (ZPRs) via competitive dimerization to a similar domain in the HD-ZIP III proteins (Kim et al., 2008; Wenkel et al., 2007). In the most severe cases, overexpression of *ZPR* genes in *Arabidopsis* leads to premature termination of the SAM (Wenkel et al., 2007) similar to the *stm* phenotype (Endrizzi et al, 1996). Taken together, these phenotypes support roles of *ZPR* genes in meristem maintenance and regulation of HD-ZIP III (Wenkel et al., 2007). In support of findings in *Arabidopsis*, ZPR proteins in tomato have also been shown

to play a role in meristem maintenance by restricting the expression domains of *SlCLV3* and *SlWUS* (Xu et al., 2019). While a HD-ZIPIII protein, ROLLED LEAF 1 (RD1), has been characterized in maize (Juarez et al., 2004), additional studies are needed to demonstrate how ZPR proteins interact specifically with the HD-ZIPIII/KN1 pathway in meristem maintenance in maize and other monocots.

This study focuses on *Sos2,* a member of the *Suppressor of sessile spikelet* (*Sos*) class of semi-dominant maize reproductive mutants. The *Sos* mutants were named for the phenotype of *Sos1,* the founding member of this class, which is caused by suppression of one of the two spikelets in the pair, the sessile spikelet, during tassel and ear development (Doebley et al., 1995; Wu et al., 2009). Unlike *Sos1,* the semi-dominant *Sos2* mutant affects plant development more broadly, including the regulation of the shoot apical meristem (SAM) in addition to the inflorescence meristems (IM) and all subsequent meristems that produce the reproductive organs. The *Sos2* phenotypes range from seedling lethality to abortion of the FM. Characterization of the *Sos2* phenotype indicates that *sos2* functions during the transition from each meristem type to the next and variation in the phenotype is due to naturally occurring genetic modifiers as well as temperature-sensitive environmental modifiers that effect the penetrance and expressivity of the *Sos2* phenotype. We demonstrate the interaction of the *Sos2* mutation with the maize *CLAVATA* pathway and show reduced expression of the *ZmWUS1* gene in *Sos2* mutants indicating that *sos2* functions to regulate meristem maintenance through a different pathway from *sos1.* Additional pathways affected by *Sos2* were uncovered using RNA-seq analysis of immature

tassels. By fine mapping and expression analysis, we identify a potential candidate gene that could underlie the *Sos2* phenotype, a *ZmSPR4-like* gene, located on the short arm of Chromosome 10, that is increased in expression in *Sos2* tassels, indicating that *sos2* functions in a previously uncharacterized meristem maintenance pathway in maize.

RESULTS

Sos2 *mutants display a variety of phenotypes*

In normal maize development, 4-5 leaves will have developed in the embryo before germination (Freeling & Walbot, 1994), and seedling lethality that occurs before emergence of these leaves indicates a defect in the SAM during embryo development. Normally, plants will produce 18-22 leaves from the SAM (Freeling & Walbot, 1994) before transitioning to reproductive development. Mature tassels will include numerous branches at the base of the main rachis and characteristic paired spikelets along the branches and the main spike (Fig. 1C). Mature ears will have characteristic even-paired rows of kernels due to the production of paired spikelets with single florets (Fig. 1A).

The *Sos2/+* mutant phenotypes vary in expressivity. We performed most of our analysis in the W22-acr, non-reference, genetic background (which has mutations in the A, C and R pigmentation genes producing yellow kernels (Brink et al., 1968), where the *Sos2* phenotype was expressed. The most common *Sos2/+* phenotype in ears in W22-acr is the break-down of the paired row phenotype producing an ear with mostly single-kernel rows, or rows with irregular

spacing and distribution of paired and single-row kernels (Fig. 1A). This phenotype can be seen early in ear development by SEM, where SPM produce either one or two SM (Fig. 1B). The most severe expression of this phenotype is a short, rounded, club-shaped ear with as few as a single kernel to 25 kernels produced in no apparent row-order (Fig. 1A). When these ears are analyzed early in development, it is hard to deduce where the IM is established, or if the IM is being maintained (Fig. 1B). These phenotypes indicate that the *sos2* gene is involved in the SPM to SM transition as well as the establishment of the IM in more severe cases (Chapter 1, Fig. 1).

These phenotypes are mirrored in tassel development (Fig. 1C), with the additional effect of decreased tassel branching, due to a failure of the IM to produce BM (data not shown). Along the length of the main rachis, there is an increase in the number of single spikelets and decrease in the number of paired spikelets (quantified later in manuscript). In addition, SEM analysis of *Sos2*/+ immature tassels also showed production of single or paired SM from the SPM (Fig. 1D). The failure to consistently produce paired spikelets in *Sos2*/+ tassels again highlights a failure of the SPM to transition into two SM, during reproductive development in these mutants.

In addition to the paired-spikelet phenotype, *Sos2*/+ mutants also have disrupted floral development. In ears, *Sos2*/+ plants will have rudimentary kernels (hardened by empty glumes) in place of viable ones which can be seen early in ear development via SEM analysis (Fig. 1B). In tassels, spikelets that lack floral organs can be seen throughout the length of the main spike. Mature spikelet

phenotyping uncovered five different mature spikelet phenotypes: paired spikelets (both viable), paired spikelets with either one or both spikelets in the pair aborted, single spikelets (viable), and single spikelets (aborted) (Fig. 1E). SEM analysis showed the production of empty glumes similar to the phenotype in ears (Fig. 1D). The more severe *Sos2/+* phenotypes in the tassel include the failure to produce a main rachis, or the inability to produce a tassel at all (Fig. 1C). Together, these phenotypes indicate that *Sos2* not only affects the SPM to SM transition, but also FM development, as reproductive structures are formed but not viable, and IM maintenance, as can be seen when tassels form without a main rachis, or fail to form at all (Chapter 1, Fig 1).

To uncover the homozygous phenotype from the variation of phenotypes seen, outcrossed (*Sos2* crossed to W22-acr) and selfed (*Sos2* plants crossed by themselves) segregating family phenotypes were compared (Fig. 1F, G). Based on segregation ratios of seedling lethality in outcrossed versus selfed segregating families, we found a significant increase in the number of seed that did not germinate (15% in outcrossed lines compared to 36% in selfed lines, respectively) and the appearance of seedling lethal phenotypes where plants died after leaf three (Fig. 1H). In general, a certain percentage of maize plants will not germinate due to environmental factors, such as animal destruction or soil pathogens. However, taking this into account, the increased number of plants that did not germinate in selfed lines was above normal and above outcrossed lines and is likely the result of *Sos2/Sos2* homozygosity (Fig. 1H). Furthermore, outcrosses of *Sos2* plants that made it to maturity, always segregated normal and *Sos2* mutant

plants, indicating that *Sos2* reproductive phenotypes, weak or severe, are due to *Sos2* heterozygosity. The lack of germination and seedling lethal phenotype is indicative of *sos2* gene function in SAM maintenance during vegetative development, in addition to the previously described functions in reproductive development (Chapter 1, Fig. 1).

It is important to note that one phenotype might occur in the ear, and another phenotype in the tassel; similarity in ear and tassel phenotypes does not necessarily appear in the same plant. For instance, a plant could have a very typical tassel phenotype (i.e. decreased branches, increase in single and reduced number of paired-spikelets) and a severe ear phenotype (i.e. failure to produce an ear within the husk leaves). This implies that the expressivity of the *Sos2* phenotype can vary over developmental time, and/or is influenced by environmental factors throughout growth and development.

Sos2 ***segregating lines indicate possible genetic and environmental modifiers***

The variation in the *Sos2* phenotype led us to hypothesize that a multiple-gene interaction might be at play. To test for this, *Sos2* was backcrossed three times into the W22-acr inbred background, selfed and phenotyped (Fig. 2A). Mature tassels were categorized on a scale of 1-8 in increasing severity: 1 = normal siblings, 2(N))= modified normal; plants that look like normal tassels with slightly fewer branches, 2(S) = modified *Sos2*, sparse tassel with single spikelets on the main spike, fewer branches than normal, some long and some short, 3 =

Sos2 typical, single spikelets throughout the main spike, few, short branches, 4 = *Sos2* tassels with no branches, 5 = *Sos2* club tassel, no main spike present, 6 = *Sos2*-tasselless, or no tassel present, 7 = seedling lethal at leaf three, 8 = did not germinate (Fig. 2A). Originally, class 2 was a single category to group tassels that were phenotypically between normal and *Sos2*-typical phenotypes. However, this category could be further broken down to normal-modified and *Sos2*-modified subcategories, both of which phenotypically fall between normal and *Sos2*-typical tassels, during the analysis.

A total of 866 plants were phenotyped in the Missouri 2020 season, and both Mendelian and epistatic ratios were analyzed using chi squared testing, in various iterations of phenotypic groupings (Fig. 2B). Of all the ratios tested, only the “dominant and recessive interaction” had a chi-squared value (0.145) that was lower than the critical value (3.841) (Fig. 2B). This indicates that the difference between the observed and expected ratios were likely due to chance, and that the variation in the *Sos2* phenotype is due to a dominant and recessive gene interaction – with *Sos2* being the causative dominant gene, and a recessive modifier influencing the expressivity of the phenotype. Results from the Missouri 2019 field season mirrored the results reported in the MO2020 field seasons (data not shown).

To determine if the *Sos2* phenotype had any naturally occurring modifiers in other genetic backgrounds, the *Sos2* mutation was backcrossed into the B73, A188, A632, A619, Mo17, and Oh43 genetic backgrounds, for three generations, and then selfed for phenotypic analysis. The *Sos2*:B73 lines did not have good

germination, and no conclusive results can be reported, however, *Sos2* introgressions into A188, A632, Oh43, and A632 lines all had a decrease in the number of *Sos2* phenotypes indicating a possible genetic modifier that masks the *Sos2* phenotype. *Sos2*:Mo17 segregating families were the only genetic background that maintained a mendelian ratio of 1:3 (N:*Sos2*) segregation ratio for a dominant mutant, and segregating families had no apparent increased in the number of plants that did not germinate (Fig. 2C). This result creates an additional hypothesis for future studies: that the 1:3 Mendelian segregation in *Sos2*:Mo17 is due to the absence of the recessive genetic modifiers predicted to be present in the *Sos2*:W22 segregating lines. In contrast, *Sos2*:A619 and Sos2:A632 had a ratio of 3:1 (N:*Sos2*) while *Sos2*:Oh43 had a ratio of 9:1 indicating the possible presence of a suppressor that masks the *Sos2/+* phenotype in these genetic backgrounds, which should be followed up on. Therefore, multiple types of genetic modifiers of the *Sos2* phenotype are present in diverse maize inbred lines.

To test if there was an environmental impact on the phenotypic variation seen in *Sos2* mutants, *Sos2*/+ mutants outcrossed to the W22-acr background were grown to maturity in growth chambers to control environmental factors influencing phenotype and tassel phenotypes classified according to the scheme in Fig. 2A. It was discovered over three replicates that the hotter growth chambers displayed fewer *Sos2* phenotypes, and more modified and normal phenotypes (Fig. 2D). In contrast, the cooler growth chambers displayed more *Sos2* phenotypes than would be expected from an outcrossed family, and very few modified phenotypes (Fig. 2D). This indicates that cooler temperature increases

both the penetrance (number of plants that show the *Sos2* phenotype) of the mutation, as well as the expressivity (how the mutation is displayed (i.e. class of mutation) of the mutation involved in the *Sos2* phenotype.

Sos2 *may function in the meristem maintenance developmental pathway*

Previous work on the founding member of the *Sos* class of mutants, *Sos1,* which has similar phenotypes to *Sos2* determined that *Sos1* functioned in the *CLAVATA* pathway (Johnson, 2017). This data, along with the *Sos2* mutant phenotypes described above, led to the hypothesis that *Sos2* also functioned in the maize *CLAVATA* meristem maintenance pathway. To assess this function, *Sos2/+* mutants were crossed to members of the maize *CLAVATA* pathway: *td1, fea2,* and*, ct2* and backcrossed three times to the W22-acr line inbred line and selfed for analysis. Vegetative traits measured were leaf number and overall plant height (Table 1) and reproductive characteristics measured included tassel composition (number of single, single-aborted, double, and double-aborted spikelets) and kernel row number (KRN) in the ear (Table 2). Both are described for each double mutant combination below.

Plant height measures the ability of the SAM to produce phytomeric units: a node, where a leaf with a subtending axillary meristem are attached, and an internode consisting of elongated stem tissue (Gray, 1879). Leaf number measures the number of lateral primordia produced from the SAM (Evert et al., 2006; Gray, 1879). The first double mutant cross analyzed was *Sos2* and *td1*. Previous studies had shown the role of *td1* in regulating the SAM during vegetative

development (Bommert et al., 2005a; Lunde & Hake, 2009), due to the decrease in plant height and leaf number (Bommert et al., 2005a). In W22-acr, *td1* mutants had reduced leaf number similar to the phenotype published in B73 (Bommert et al., 2005a), though the plant height was not statistically significantly different from normal siblings (Table 1). *Sos2; td1* double mutants as well as *Sos2/+* single mutants did not have a statistically significant difference in plant height compared to normal siblings in the W22-acr background (Table 1). However, the *Sos2/+;td1/td1* double mutant leaf number was increased compared to *td1* and was not statistically significantly different from *Sos2/+* single mutants (Table 1), showing that *Sos2* can compensate for the decreased leaf phenotype of *td1* mutants. This provides additional evidence that the *sos2* gene functions in the SAM during the leaf initiation process.

Previous studies found that the *sos1* gene functions in the *td1* pathway during reproductive development, as evidenced by a fasciated phenotype in *Sos1/Sos1;td1/td1* double mutant ears and rescued phenotype in double mutant tassels (Johnson, 2017). To test if this same interaction was seen in *Sos2/+; td1/td1* double mutants, ears and tassels were analyzed (Fig. 3A,B, Table 2). In tassel development, *td1/td1* single mutants in W22-acr had an increased number of single spikelets compared to normal siblings, similar to what was reported in *td1/td1* single mutants back-crossed to W22-ACR in previous studies (Table 2) (Bommert et al., 2005a). However, *td1/td1* mutants have a larger IM (Bommert et al., 2005a), and therefore have more initiation events (BM + SPM) than *Sos2/+* single mutants or normal siblings. Taking this into account, percentages were used

to compare the changes in spikelet composition between all mutant categories in this analysis (Supplemental Table 1). Similar to *td1/td1* mutants, *Sos2/+* single mutants had an increased number of single spikelets (55% of total composition) and decreased number of paired spikelets (45% of total spikelet composition) compared to normal siblings (35% and 65%, respectively) (Table 2; Supplemental Table 1). The *Sos2/+; td1/td1* double mutants were not significantly different from *Sos2/+* single mutants and normal siblings in terms of single spikelets (Table 2), however, when looking at spikelet composition, *Sos2/+;td1/td1* double mutants had more single spikelets (71%) than *Sos2/+* (55%) and *td1/td1* (59%) single mutants or normal siblings (35%) (Supplemental Table 1). This indicates that *Sos2/+;td1/td1* double mutant single spikelet phenotype is enhanced compared to either single mutant, and that both *Sos2* and *td1* genes function in regulating the SPM to SM branching events.

When phenotyping tassels, it was discovered that *Sos2* mutants regularly produced aborted spikelets, indicating the transition between SM to FM development was occasionally impaired in these mutants. Looking within the *Sos2/+;td1/td1* segregating families, 21% of *Sos2/+* single mutant tassels were composed of aborted single spikelets (6%) or spikelet pairs (15%) compared to the 2% of total spikelets in *td1/td1* single mutants or 1% of spikelets in normal siblings (Supplemental Table 1). *Sos2/+;td1/td1* single mutants also had a statistically significant increase in percentage of aborted spikelets compared to *td1/td1* single mutants and normal siblings (Table 2). Previous studies showed *td1* expression in FM through RNA *in situ* hybridization, as well as increased floral number within

spikelets, indicating the *td1* gene does function in FMs (Bommert et al., 2005a). Similar to the conclusion from SPM to SM branching events, the enhancement of aborted spikelets seen in *Sos2/+;td1/td1* double mutants indicates that both *Sos2* and *td1* genes function to regulate FMs.

In the ear, kernel row number (KRN) is due to a combination of the production of SPM from the IM and the production of two SM from the SPM. *Sos2/+* and *td1* had contrasting effects on KRN compared to normal siblings; *Sos2/+* plants made statistically fewer (due to production of single spikelets) while *td1/td1* plants made statistically more kernel rows compared to normal siblings (due to an enlarged IM producing more SPM) (Fig. 3B, Table 2). *Sos2/+;td1/td1* DMs had significantly fewer kernel rows than *td1/td1* plants, however, which was not statistically different from either *Sos2/+* or normal siblings (Table 2). Therefore, unlike the *Sos1;td1* interaction, *td1* was unable to suppress the phenotype of the *Sos2* mutant indicating that *Sos1* and *Sos2* function in different pathways. Whether the *Sos2; td1* double mutant phenotype is caused by having the Sos2 IM phenotype and the *td1* SPM phenotype or the *td1* IM phenotype and the *Sos2* SPM phenotype requires further SEM analysis.

To test is *Sos2* signaled through the *fea2* pathway instead, double mutants were constructed in the W22-acr background. During vegetative development, *Sos2/+;fea2/fea2* double mutants show no statistical difference in plant height or leaf number (Table 1), similar to what was seen in *fea2* mutants in the B73 background (Taguchi-Shiobara et al., 2001). These results imply that *Sos2* does not interact with *fea2* in the SAM during vegetative development, aligning with

previous studies that show *fea2* has no functional significance during this stage of development (Taguchi-Shiobara et al., 2001).

In the W22-acr background, *fea2* has a less fasciated phenotype than the same allele previously published in the B73 background (Taguchi-Shiobara et al., 2001); however, *fea2/fea2* mutants in W22-acr are still slightly fasciated compared to normal siblings (Fig. 2 D). In contrast to the interaction with *td1, fea2/fea2* rescued *the Sos2*/+ KRN phenotype in *Sos2/+;fea2/fea2* double mutants (Table 1, Fig. 3D); *Sos2/*+ plants had significantly fewer kernel rows than normal siblings, whereas double mutants had a KRN which was not statistically different from normal or *fea2/fea2* siblings (Table 1). These results provide evidence that *fea2/fea2* acts epistatically *to Sos2/*+ during the production of kernels from the IM during ear development. As *fea2* and *Sos2* have opposite phenotypes, this would be interpreted as *fea2* acting downstream of *Sos2* (Avery & Wasserman, 1992).

Similar to the *Sos2/+;td1/td1* analysis, variation in spikelet composition was seen in *Sos2/+;fea2/fea2* mutants (Fig. 3C). There was an increase in the number of single spikelets in *Sos2/*+ and *Sos2/+;fea2/fea2* mutants compared to normal siblings (Fig. 3C, Table 2). Looking at the SPM to SM branching events via single and double spikelet composition, *Sos2/*+ and *fea2/fea2* single mutants and *Sos2/+;fea2/fea2* double mutants all had significantly more single spikelets than normal siblings (Table 2). Due to variability, there were no statistical differences in any mutant category compared to normal siblings for the number of paired spikelets, although *Sos2/*+ single mutants had statistically fewer paired spikelets compared to *fea2/fea2* single and *Sos2+;fea2/fea2* double mutants (Table 2).

When comparing percentages of spikelet composition in these mutant categories, the same trend emerged – *Sos2/+;fea2/fea2* double mutants seemed to have intermediate levels of single (42%) and paired (58%) spikelets compared to *Sos2/+* (58% single, 42% double spikelets) and *fea2/fea2* (36% single, 64% double spikelets) single mutants. This indicates that *fea2* can partially rescue the *Sos2/+* single and paired spikelet phenotypes, making the double mutant look more normal compared to *Sos2/+* single mutants and that this interaction occurs in the SPM, indicating an interaction between these two genes at the developmental stage. Interestingly, the *Sos2/+;fea2/fea2* segregating family did not have many aborted spikelets, even in *Sos2/+* single mutants (Table 2). Because of these low numbers, and lack of statistical significance between categories, no conclusive interaction can be determined about *sos2* and *fea2* gene interaction in FMs.

As *fea2* and *ct2* are known to physically interact with each other (Bommert, Je, et al., 2013; Je et al., 2018), we also tested the genetic interaction between *Sos2* and *ct2*. *ct2/ct2* plants have a very strong vegetative phenotype, whereas *Sos2/+* do not, so it is surprising that *Sos2/+;ct2/ct2* double mutants vegetatively were not statistically different from *Sos2/+* single mutants rather than *ct2;ct2* single mutants (Table 1). Therefore, similar to the interaction with *td1*, *Sos2* suppressed the plant height and leaf number phenotype of *ct2* (but not the leaf shape phenotype) providing further evidence that *Sos2* functions in vegetative development.

In terms of KRN, *ct2/ct2* mutants were not significantly different from normal siblings, however, *ct2/ct2* mutants are clearly fasciated at the tip of developed ears.

This inconsistency is due to the location used for KRN quantification: to reduce bias in KRN quantification, KRN was measured one inch down from the tip of the ear in all double mutant analysis. In the case of *ct2/ct2* ears, fasciation appeared above this measurement threshold, so KRN was unable to accurately represent the *ct2/ct2* ear phenotype. *Sos2+* and *Sos2/+ct2/ct2* double mutants did have a significantly lower KRN than normal (Fig. 3F; Table 1) due to an effect on the SPM. Regardless of the difficulty in KRN quantification in *ct2/ct2* segregating single mutants, the obvious *Sos2*-severe ball shaped phenotype in *Sos2/+;ct2/ct2* double mutants implies that *ct2* fails to suppress the *Sos2* phenotype during ear development. Interestingly, the opposite seemed to hold true for initiation events during tassel development; *Sos2/+ct2/ct2* double mutants and *ct2/ct2* single mutants had significantly more initiation events (number of SPM and BM produced from IM) when compared to *Sos2/+* and normal siblings (Table 1). Therefore, *Sos2* and *ct2* interaction during IM initiation in tassel development may be different than their interaction during ear development.

Interestingly, *Sos2+;ct2/ct2* double mutants had a significant increase in the number of single spikelets compare to both single mutants and normal siblings, and the number of double spikelets was greatly decreased in *Sos2/+;ct2/ct2* double mutants (Fig. 3E, Table 2b). This indicates that *ct2* enhances the *Sos2* SPM/SM mutant phenotype. The same pattern can be seen in FM development for *Sos2/+;ct2/ct2* double mutants. The *ct2/ct2* single mutants had no statistical difference in aborted spikelets, either single or double, compared to normal siblings, however *Sos2/+* single mutants did have the expected statistical increase

in both aborted single and double spikelets (Table 2b). This means that whatever small role *ct2* might play in FM initiation, not typically displayed by *ct2* single mutants, is heightened by the presence of the *Sos2* mutation, causing a phenotype that exceeds what would be expected from an epistatic or additive interaction. The differing results with *Sos2* double mutants with *fea2* and *ct2* indicate that *sos2* may act in the *fea2/ZmCRN* pathway rather than the *fea2/ct2* pathway which can be further

tested by double mutant interactions between *Sos2* in double mutant interactions with *ZmCRN*.

The Sos2 mutation maps to the short arm of chromosome 10

To determine the identity of the gene underlying the *Sos2* mutation, fine mapping was performed with two different mapping populations. The first was planted in Missouri in 2012; the *Sos2* mutation that had been introgressed into the W22-acr (non-reference) background was crossed to A632, back-crossed three times to A632 and 235 plants were phenotyped and genotyped, narrowing the location to a 220,896 bp region between markers bnlg1451 and umc1582 on chromosome 10s (Fig. 4A), based on the W22-ACR reference genome. A second mapping population was planted in Missouri in 2019, in which the *Sos2* mutation was backcrossed into the W22-acr (non-reference) background for over three generations and then selfed. A total of 765 plants were phenotyped and genotyped for a polymorphic INDEL marker designed in an uncharacterized gene, GRMZM2G165695, which further narrowed the region to 216,662 bp (Fig. 4A).

Linkage analysis indicated that GRMZM2G165695, was 0.33 cM from the Sos2 locus.

In parallel with fine mapping efforts, whole genome sequencing was performed on *Sos2*/+ mutants and normal siblings. This was first done in the *Sos2*, W22-acr (non-reference) line, and five *Sos2*-tasselless (phenotypic class 5, Fig. 2B) plants were pooled, sequenced, and aligned to the W22-ACR reference genome. When this was done, seven peaks were seen that differentiated the *Sos2* mutants from W22-ACR (Supplemental Fig. 1). At first, it was thought that these peaks were indicative that the *Sos2* mutation was not originally in the W22 inbred background, and that we had mapped the causative loci as well as genetic modifiers. Upon further investigation, it was found that at least two peaks were in known regions of difference between W22-acr (non-reference) and W22-ACR reference lines. To ensure that the rest of the peaks were not a result of inherited differences between W22-acr and W22-ACR, *Sos2* was introgressed from the W22-acr background into the W22-ACR (reference) background, backcrossed twice, selfed and re-sequenced.

Plants from four segregating families in the W22-ACR background, were categorized by mature tassel phenotype (Normal, *Sos2*-Typical Class 3, and *Sos2*-no tassel Class 6) and leaf tissue was collected (n=24,24,3 respectively). Because of the heterozygous state of the *Sos2* mature phenotype, we expected the allele frequency close to the *Sos2* locus to be around 0.5. Again, multiple peaks were uncovered, however all of these peaks were also seen in Normal siblings, including one that matched the fine mapping location on Chromosome 10 (Fig. 4B).

However, when chromosome 10 INDELs were mapped, this candidate gene region overlapped with a valley; a region with fewer reads aligning than normal siblings and therefore decreased coverage (Fig. 4C). This valley with decreased coverage indicates INDELs within this region could not map to the W22-ACR reference genome. Therefore, it is likely that the reads in this region are of the original mutant background, supporting fine mapping placement of the *Sos2* mutation in this region.

To further support the map location of the *Sos2* mutation, an RNA-seq analysis was performed on *Sos2*-typical (Class 3), heterozygous plants introgressed into the W22-acr (non-reference) background. RNA-seq has been used to aid in identification of other maize mutants, including dominant mutants, such as *Ts5* (Lunde et al., 2019). DEGs were determined via EdgeR and filtered based on an FDR of 0.05 (Robinson et al., 2009). Of the 2,789 DEG that were filtered out, only two significant DEG fell within the mapping window (Fig. 4A,B): a LITTLE ZIPPER4-like gene, Zm000014b037901 (W22 gene ID)/Zm00001d023405 (B73_V4 gene ID), and PEBP3/ZCN3-like gene Zm00004b037909 (W22 gene ID)/Zm00001d023419 (B73_V4 gene ID). ZmZPR4-like was upregulated by over three-fold, and the ZCN3 was down regulated one-fold compared to normal siblings (Fig. 4D). As the *Sos2* is a dominant mutation, the most likely cause is over-expression of the candidate gene, as seen in other dominant maize mutants like *Sos1*, *Bif3*, and *Fas1,* among others (Chen et al., 2021; Du et al., 2021; Lunde et al., 2019; Wu et al., 2009). Of the genes in the region between *blng1451* and *umc1582*, there were 47 B73_v3 gene IDs, 24

B73_v4 gene IDs, and 23 W22 gene IDs. Of these, only ten W22 predicted genes had an average read count value of ten or more in either *Sos2* replicates or normal sibling replicates. When the average read count values of these ten genes within the mapping window were graphed, *ZmZPR4-like* was the only gene in the window that saw an increase in expression in *Sos2* mutants compared to normal siblings (Fig. 4D). Due to the location of the *ZmZPR4-like* gene within the mapping region, the significant expression change of the *ZmZPR4-like* gene in the RNA-seq analysis, the function of *ZPR* like genes in meristem maintenance in other species (Wenkel et al., 2007; Xu et al., 2019) and in comparison to the other expressed genes in the region, ZmZPR4-like is the most likely candidate gene for the *Sos2* phenotype.

***Sos2* RNA-seq analysis indicates Sos2 acts in heat shock and meristem maintenance pathways**

To better understand which pathways the *Sos2* mutations might play a role in, further bioinformatic analysis was performed on the RNA-seq of *Sos2*/+ immature tassels compared to normal (W22-acr) siblings. A total of 2,789 genes were differentially expressed with an FDR of < 0.05 in this data set, with 1,392 genes differentially up-regulated and 1,395 genes differentially down regulated.

DEGs were analyzed via AgriGO for significant Gene Ontology (GO) terms (Z. Du et al., 2010), and up-regulated genes were enriched for categories relating to general development, including ones expected such as regulation of meristem development (GO:0048509), reproductive structure development (GO:0048608),

and flower development (GO:0009908). GO also was enriched for terms unexpected like root development (GO:0048364), leaf development (GO:0048366) and response to temperature stimulus (GO:0009266) (Fig. 5A). Similar GO terms were enriched in down-regulated genes from this data set as well, including reproductive structure development (GO:0048608) and temperature response related GO terms like response to heat (GO:0009408) and protein folding (GO:006457) (Fig. 5A).

The appearance of temperature related GO terms supports findings from our environmental analysis that temperature acts as an environmental modifier of the *Sos2* phenotype. When known heat shock proteins (HSP) were mined from the RNA-seq analysis, all but one, *hsp70*, were differentially expressed (Fig. 5B). Of these, 12 were significantly differentially down regulated, and one was differentially up regulated (Fig. 5B). In an opposing pattern, heat shock factor transcription factors (HSFTF) were mostly up regulated, with the exception of four: *hsftf11*, *hsftf17*, *hsftf24, hsftf8* (Fig. 5B). However, only five of those were significantly differentially expressed: *hsftf11, hsft24 and hsft8* were all significantly down regulated, while *hsftf27* and *hsftf9* were differentially up regulated (Fig. 5B). This indicates that *Sos2* may also function in regulating the HSP pathway in addition to meristem maintenance pathways.

To determine which developmental pathways, *Sos2* functioned in, expression of known genes was examined (Fig. 5C). Of the three *CLAVATA* genes that were tested by double mutant analysis, only *ct2* was significantly differentially expressed, being slightly up regulated in *Sos2/+* immature tassels. In addition,

ZmWUS1 was significantly down regulated by over 2-fold, and *kn1* was significantly up regulated by over 1-fold in *Sos2*/+ compared to normal supporting the double mutant analysis of a role of *sos2* in regulating meristem maintenance. To follow up on this finding, *Sos2*/+ was crossed to the pWUS:WUS::NLS-RFP transgenic protein (Q. Wu et al., 2013), and are currently growing in the field for confocal analysis. To further verify the RNA-seq results with *kn1*, RNA *in situ* hybridization was performed on normal and *Sos2*/+ tassel meristems with a *kn1* antisense probe (Jackson et al., 1994). This analysis showed a possible increase in the expression domain of *kn1* in *Sos2*/+ immature tassels compared to normal siblings, but the for the most part *kn1* expression was consistent between *Sos2*/+ and normal tassel SM (data not shown).

In addition to seeing a significant decrease in *ZmWUS1* expression, 12 additional homeobox-containing proteins were also differentially expressed, along with *zmm8*, one of the genes responsible for the *Fas1* mutation (Du et al., 2021), which was significantly down regulated (Fig. 5C). Additional genes of developmental interest and their subsequent expression are highlighted in Fig. 5C, genes that are differentially expressed are denoted with a single or double asterisk.

To follow-up on the candidate genes that map in the *Sos2* region, *HD-ZIPIII* TF and additional *little zipper* genes were mined from the data. In support of the candidate gene, HD-ZIPIII *hb25* and *ZmZPR4-like* were the only genes that were significantly DEG (Fig. 5C). To validate the expression of *ZmZPR4-like*, I have created a *ZmZPR4-like* RNA *in situ* hybridization probe which subsequent studies will be able to use to analyze *ZmZPR4-like* expression in immature tassels.

DISCUSSION

The *Sos2* phenotype is due to multiple different factors that act in coordination to direct overall maize development, specifically at meristem transition time points. While the *Sos2* phenotype is largely due to a predisposing mutation on the short arm of chromosome 10, the penetrance and expressivity of the *Sos2* phenotype is dependent on the environment in which it is grown as well as other genetic modifiers, depending on the genetic inbred line that the *Sos2* mutation is introgressed into. All of these factors affect development at specific times, multiple times throughout maize development, resulting in different mature reproductive phenotypes. The fact that *Sos2* mutants display higher levels of seedling lethality in selfed lines indicates that the normal function of this gene is necessary for the maintenance of SAMs, stunted, ball-shaped ears and tassel indicate *Sos2* functions to maintain IMs, the inability of SPMs to branch into to SMs indicates *Sos2* function in SPM maintenance, and aborted spikelets implies the function of *Sos2* in regulating SMs and FMs as well.

Dominant mutants are inherently dose dependent, and fall under four different categories: Neomorph, anitmorph, hypermorphic, and hypomorphic (Muller, 1932). Hypomorphs and antimorphs are loss-of-function mutations, where hypomorphs are unable to produce enough wild-type function when only one copy of the gene is present, and antimorph, or dominant negative mutations, interfere with wild-type function (Muller, 1932). Since *Sos2* is a semi-dominant mutation, and the increase in mutant copy number leads to more severe phenotypes (embryo lethal), it is unlikely that *Sos2* is a hypomorph. Antimorphs, or dominant

negative mutations, lead to the production of mutated proteins that interfere with the wild-type protein function (Muller, 1932; Veitia, 2007) however we did not detect any strong effect SNPs in the coding region of any candidate genes in the region using SNPeff. For antimorphs, we might not see differences between wild-type and mutants at the transcriptional level, unless the gene auto-regulates its own expression. Neomorphs and hypermorphs are gain-of-function mutations; neomorphic mutations happen when a gene gains a new function, usually by being expressed in tissue that it normally is not expressed. Hypermorphic mutations are when there is increased expression of the wild-type gene (Muller, 1932).

Most of the dominant mutants in maize are either neomorphs, and the result of ectopic expression of a gene, or a hypermorph caused by the overexpression of a gene due to a chromosome rearrangement such as a tandem duplication or a promotor region mutation. Dominant neomorphs include the *Kn1-O* mutation which is the result of the mis-expression of the *kn1* gene in leaf tissue where it is not normally expressed, which results in the production of ectopic growth (Smith et al., 1992). The same holds true for other semi-dominant mutations such as *Liguleless3* (*Lg3*), which is caused by the mis-expression of another homeodomain protein (Muehlbauer et al., 1999), and *Rolled-leaf1 (Rld1),* where a gene that is usually expressing in shoot apices becomes mis-expressed in older leaf primordia (Juarezet al., 2004). Dominant hypermorphic maize mutants include *Fascicled ear 1 (Fas1),* is the result of two duplicated transcription factors *ZMM8* and *drooping-leaf2* (*drl2*) leading to the increased expression of these genes in inflorescence

meristems (Du et al., 2021). *Bif3* is caused by a tandem duplication of the *ZmWUS1* locus, also causing an over-expression of the gene (Chen et al., 2021).

Based on the nature of dominant mutations in maize, as discussed above, it is reasonable to hypothesize that the *Sos2* phenotype is likely caused by the over-expression of a gene in meristematic regions. Of the genes found within the mapping window on chromosome 10s, only two genes were differentially expressed: *ZmZPR4*, which is over-expressed by three-fold, and *ZmPEBP3,* which is just over one-fold decreased in expression. Based on the molecular defects of previously published dominant maize mutations, it can be hypothesized that the over expression of *ZmZPR4* is the predisposing mutation that causes the *Sos2* phenotype and that it is a hypermorphic mutation. As *ZmZPR4* is increased in expression in tassels compared to normal we predict that it is a hypermorphic mutation, but RNA *in situ* hybridization and qRT-PR is required to test if it's a neomorph.

To further support *ZmZPR4-like* as the causative *Sos2* mutation, the results of this study were compared with studies of orthologous genes in *Arabidopsis* and tomato. Phenotypic studies of *ZPR4* in *Arabidopsis* uncovered a premature termination of the SAM when the gene was over-expressed (Wenkel et al., 2007). This is reminiscent of the early termination of meristems throughout maize development seen in *Sos2* mutants: seedling lethality is a premature termination of the SAM, the ball ear and tassel are premature terminations of the IM, the presence of single spikelets indicates premature termination of the SPM, and aborted spikelets are a result of premature termination of the FM. A paper on the

orthologous gene in tomato, *defective tomato meristem 1* (*dtm1*), connected *ZPR* function to the CLV-WUS pathway – showing that decreased *dtm1* expression expanded the *SlWUS1* and *SlCLV3* domains (Xu et al., 2019). Therefore, the increase of *ZmZPR4-like* expression in *Sos2/+* tassels correlates with the significantly decreased expression of *ZmWUS1* and is supported by the results of the orthologous *dtm* gene function in tomato.

It is important to point out that *ZmZCN3-like/PEBP3* was also significantly differentially expressed within the *Sos2* map window. *CENTRORADIALIS*, the cornerstone *PEBP*-gene that acts as the flowering signal in Antirrhinum has also shown variability in phenotype when temperature has been altered between growth conditions, similar to what we see in *Sos2* (Cremer et al., 2001). The orthologous gene to *Antirrhinum CEN* in *Arabidopsis* is *TERMINAL FLOWER1* (*TFL1*) which functions in both vegetative and reproductive phases, where *CEN* is only expressed in the inflorescence meristem (Hanano & Goto, 2011). Mutants in *tfl1* produce an IM that prematurely terminates in a single flower(Hanano & Goto, 2011), which could correspond to the single spikelet phenotype in *Sos2*. As there is also a case to be made for the *ZmZCN3-like/PEBP3* gene as the causative gene underlying the Sos2 phenotype, additional studies on this gene would also have to be preferred in tandem to studies on the *ZmZPR4-like* gene.

As *Sos2* is similar in phenotype to *Sos1,* which has been shown to interact in the maize *CLAVATA* pathway (Johnson, 2017), *Sos2* was also crossed to maize *CALVATA* mutants *fea2, td1,* and *ct2* to analyze interactions within this pathway. When the *Sos2* and *Sos1* double mutant analysis were compared, it was found

that these two genes function in separate, but overlapping, pathways. *Sos1* for instance, was found to signal through the *td1* and *td1;fea2* receptors/receptor complexes, as *Sos1;td1* double mutants resemble *td1* single mutants and *Sos1;fea2* mutants have an intermediate phenotype indicating receptor compensation, such as the presence of *fea2-td1* receptor complexes, might be occurring (Johnson, 2017)In contrast, *Sos2;td1* double mutants look like *Sos2* indicating that *sos2* likely does not function through this signaling cascade like *Sos1* (Fig. 7). However, *Sos2* may function through the *fea2* pathway, as evidenced by the double mutants resembling *fea2* phenotypes. As *Sos2;ct2* double mutants enhanced the *Sos2* phenotype, it is likely that these genes overlap in function, although opposite to the interaction of *Sos2* with *fea2* (Fig. 7). The differing results with *Sos2* double mutants with *fea2* and *ct2* indicate that *sos2* may act the *fea2/ZmCRN* pathway rather than the *fea2/ct2* pathway which can be further tested by double mutant interactions between *Sos2* in double mutant interactions with *ZmCRN*. As the overlap between *Sos1* and *Sos2* function appears to occur through *fea2*, where *Sos1* signals through *fea2;td1* signaling complexes and *Sos2* signals through *fea2;ZmCRN* signaling complexes. Additional double mutant analysis with *Sos2;ZmCRN* will be needed to support this theory, and these double mutant segregating lines are currently being backcrossed and bulked for this end.

The function of *Sos2* is also influenced by both genetic and environmental modifiers. Evidence from an *Sos2-W22-acr* population showed statistical likelihood that the variation seen in the *sos2* phenotype was due to the presence of a

recessive modifier – one that enhanced the phenotype of *Sos2* in selfed lines and increased the number of *Sos2* phenotypes present in outcrossed lines. In other inbred lines, such as A632, A619, and Oh43, the increase in the number of normal phenotypes compared to what was expected, indicates the presence of a recessive modifier that is a suppressor. Therefore, the diversity in maize provides natural enhancement and compensation for the *Sos2* mutation, in a dose dependent matter – something that should be followed up in subsequent studies. In addition, the growing conditions in which *Sos2* plants are subject to also influenced the penetrance and expressivity of the phenotype, supported by the response of heat-related gene expression in the *Sos2* RNA-seq analysis.

Understanding the role of the *Sos2* gene will provide insight on genes that underlie meristem maintenance throughout development. This research provides further evidence of the complexity and interconnectivity of molecular systems that have to act synchronously throughout development in order for a maize plant to be reproductively normal. The *Sos2* mutant gives insight to the importance of regulating meristem maintenance throughout maize meristem transitions – and that the balance can be thrown off at multiple stages of development if the correct gene thresholds and environmental conditions are not met.

METHODS

Plant material for phenotyping, mapping populations and double mutant analysis

Sos2 originated in a Mutator Transposon (MU) active background over a decade ago. Since the line was obtained by the McSteen lab, the mutation has been introgressed into the W22-acr genetic background for over 3 generations. For fine mapping, the *Sos2*-W22-acr line was also backcrossed to the A632 genetic background for three generations and selfed. For sequencing, *Sos2*-W22-acr was also introgressed into the W22-ACR background which is the reference line for W22 (Brink et al., 1968; Springer et al., 2018).

Seed stocks of *fea2, ct2,* and *td1* reference alleles were all obtained from the Jackson lab at Cold Spring Harbor Laboratories in the B73 genetic background. Plants were crossed to *Sos2* mutants in the W22 genetic background between three to five generations. Families were genotyped for *fea2, ct2,* and *td1* mutations using the (Leach et al., 2016) protocol each season and phenotyped for the *Sos2* tassel phenotype at the time of pollination. Summer growing seasons are held at the MU Genetics Farm run by the Missouri Maize Center at the University of Missouri – Columbia and winter seasons are run by Friendly Isle Growing Company in Molokai, Hawaii. All lines used for analysis were double heterozygous plants selfed to ensure segregating single mutants, double mutant, and WT siblings but as the *Sos2/Sos2* homozygotes are embryo/seedling lethal, double mutants are with *Sos2*/+ plants.

Plant height was measured from the point of soil emergence to the flag leaf after tassels had shed out for the season to ensure plant growth had terminated. Leaf counts were only performed during summer field seasons as winter season are performed in Hawaii. KRN was counted on all ears an inch from the top of the

cob with the exception of the ball ear phenotype. Spikelets (single, single aborted, double, double aborted, and triple spikelets) were counted along the entire length of the main spike after the branching region. Initiation events = sum of all spikelets types, i.e. number of SPM produced from IM, and include BM initiations as well (data not shown),

Scanning electron microscopy

Sos2/+, W22-*acr* segregating lines were used for SEM analysis. They were grown under standard greenhouse conditions, 16 hours of light, 8 hours of dark, watered every other day with Peter's fertilizer. Plants were grown for 3 to 4 weeks before immature tassels were excised, and plants were grown for 12-13 weeks before immature ears were excised. Tissue was preserved in FAA before undergoing a dehydration sequence and critical point drying was subsequently performed by the MU Electron Microscopy Core. Dried tissue was coated in 0.01um of platinum and imaged on a Hitachi S4700 Field Emission Scanning Electron Microscope.

Environmental analysis

Two side-by-side growth chambers at the East Campus Plant Growth Facility were utilized sharing the following settings: 16-hour light, 8-hour dark, constant light intensity, and 50% humidity. One chamber was set to a daily high temperature of 88 degrees Fahrenheit, which correlates with the average temperature between June-August in Columbia, MO. The other chamber was set to 78 degrees Fahrenheit, which correspond to the average temperature between

December-February in Kaunakakai, HI. In both, the lowest temperature setting was 67 degrees Fahrenheit when the lights are off, which corresponds with the average nightly temperature at both locations. A total of 24 plants were grown from seed in each chamber for each replicate from 1:1 segregating *Sos2* line in the W22-acr inbred background. Plants were grown to maturity and terminated between 72-80 days after germination, at which point plant height and other phenotypic data was collected. Three biological replicates were performed over a 14-month period.

Sos2 *whole genome sequencing*

For the first sequencing analysis, tissue from five *Sos2*-tasselless (Class 6) plants was collected from three *Sos2/+*;W22-acr selfed segregating families. Plants were genotyped for an INDEL marker in the GRMZM165695 gene, which segregates at a higher frequency for *Sos2*-tasselless (Class 6) phenotypes, and phenotyped at reproductive maturity. In the second sequencing analysis, tissue was collected from four 1:1 *Sos2/+*:W22-ACR segregating families. Plants were grouped based on phenotype and tissue was collected from the flag leaf (WT phenotype n=24, *Sos2*-typical phenotype n=23, *Sos2*-tasselless phenotype n=3). DNA was extracted using the urea-phenol extraction method (Leach et al., 2016).

DNA was sent to Macrogen for sequencing on the Illumina HiSeq-X with paired-end 125bp-reads. Raw reads were downloaded as Fastq files and adapters were trimmed using the Trimmomatic software with standard settings: LEAD/TRAIL:3:15, SLIDINGWINOW:4:15, MINLEN:36 (Bolger et al., 2014). Reads were aligned to the Zm-W22-REFERENCE-NRGENE-2.0 genome

downloaded from Maize GDB using hisat2 with standard parameters, resulting in 17x coverage (D. Kim et al., 2015). SNP calling was performed by samtools-1.9 and bcftools-1.8 and were filtered on read and position quality, and for over 2 reads per strand (Danecek et al., 2021). SNPeff was utilized to predict SNF effects, and candidate gene map positions were called using a 100 SNP sliding window.

Sos2 transcriptomic analysis

Plants were grown for four weeks in the Missouri 2019 field season at the MU Genetics Farm. Tassels were excised, phenotyped *Sos2*/+ vs Nsib), measured, and flash frozen in liquid nitrogen. Three replicates of six tassels of each phenotypic class were pooled and RNA was extracted using the Qiagen RNA extraction kit. RNA was then sent to Psomogen for library prep and sequencing (read length 101, TruSeq Stranded mRNA LT Sample Prep) on the Illumina HiSEQ-X sequencer. FastQ files were downloaded for subsequent DE analysis. Reads were first trimmed with Trimmomatic-0.36 software and aligned using hisat2-2.2.0: *Sos2*/+_Nsib to the Zm-W22-REFERENCE-NRGENE-2.0 genome (Bolger et al., 2014; D. Kim et al., 2015). Aligned raw read counts were counted using htseq2, and differential expression was performed using EdgeR with standard parameters (Anders et al., 2015; Robinson et al., 2009). Subsequent GO analysis was performed using the AgriGO online tool (Z. Du et al., 2010).

AUTHOR CONTRIBUTIONS

KG designed and performed experiments, data analysis, and wrote the manuscript, CN and MM helped with data collection, NB provided advice and base

code for sequencing analysis, and HS initially mapped the *Sos2* mutation. PM oversaw the project as the PI.

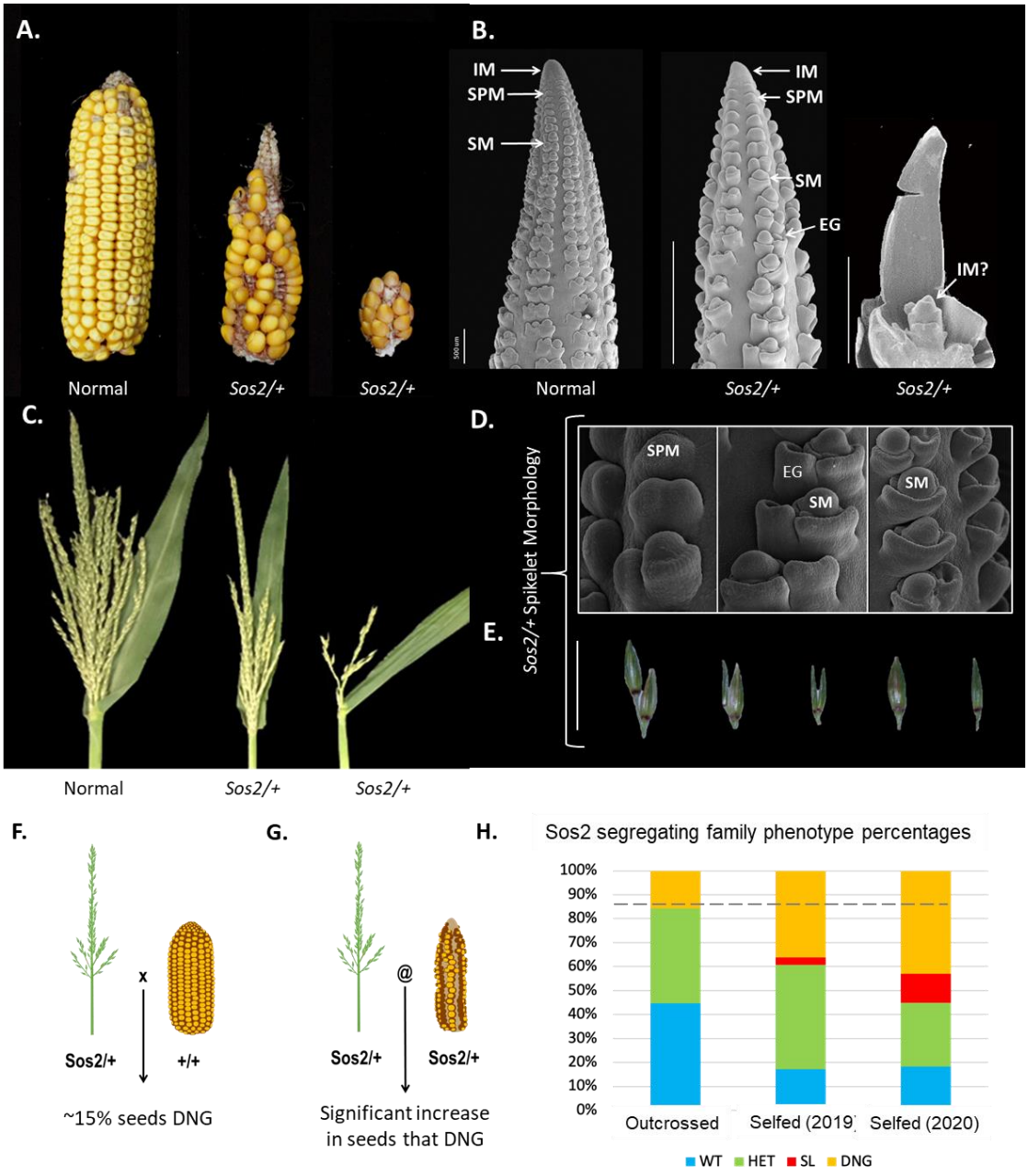

Figure 1: *Sos2* phenotypes. **A.** Mature ear phenotype: normal plants have even-paired rows of kernels, *Sos2*/+ ears have a suppression of spikelets resulting in missing rows or in extreme cases have very small ball shaped ears. **B.** Immature ear SEM phenotypes. Additional phenotypes seen are the development of empty glumes in *Sos2*/+ ears and the absence of a clear IM in severe cases **C.** Mature tassel phenotypes: normal plants have a main spike and many branches

composed of paired-spikelets, *Sos2/+* tassels have decreased branching and single instead of paired-spikelets or fail to produce a main spike. **D.** Close up SEM of immature tassels to highlight spikelet meristem development in normal plants (first panel) and *Sos2/+* plants. Note the presence of empty glumes and single as well as paired spikelet meristems. **E.** Mature spikelet phenotypes seen on *Sos2/+* tassels in order: paired, paired – one aborted (equivalent to the empty glume phenotype visible on SEM), paired – both aborted, single, single – aborted. **B,D.** IM = inflorescence meristem, SPM = spikelet pair meristem, SM = spikelet meristem, EG = empty glume. **E.** Cartoon depictions of mature phenotypes used in an outcross, as a control to identify *Sos2* homozygous phenotypes. **F.** Cartoon depiction of mature phenotypes used in selfed families to identify *Sos2* homozygous phenotypes. **G.** results from the crosses in **F-G** which show selfed lines have an increase in the number of plants that do not germinate, that surpasses the number of plants expected to not germinate due to field conditions and animal damage (dashed line). SL = seedling lethal, DNG = did not germinate.

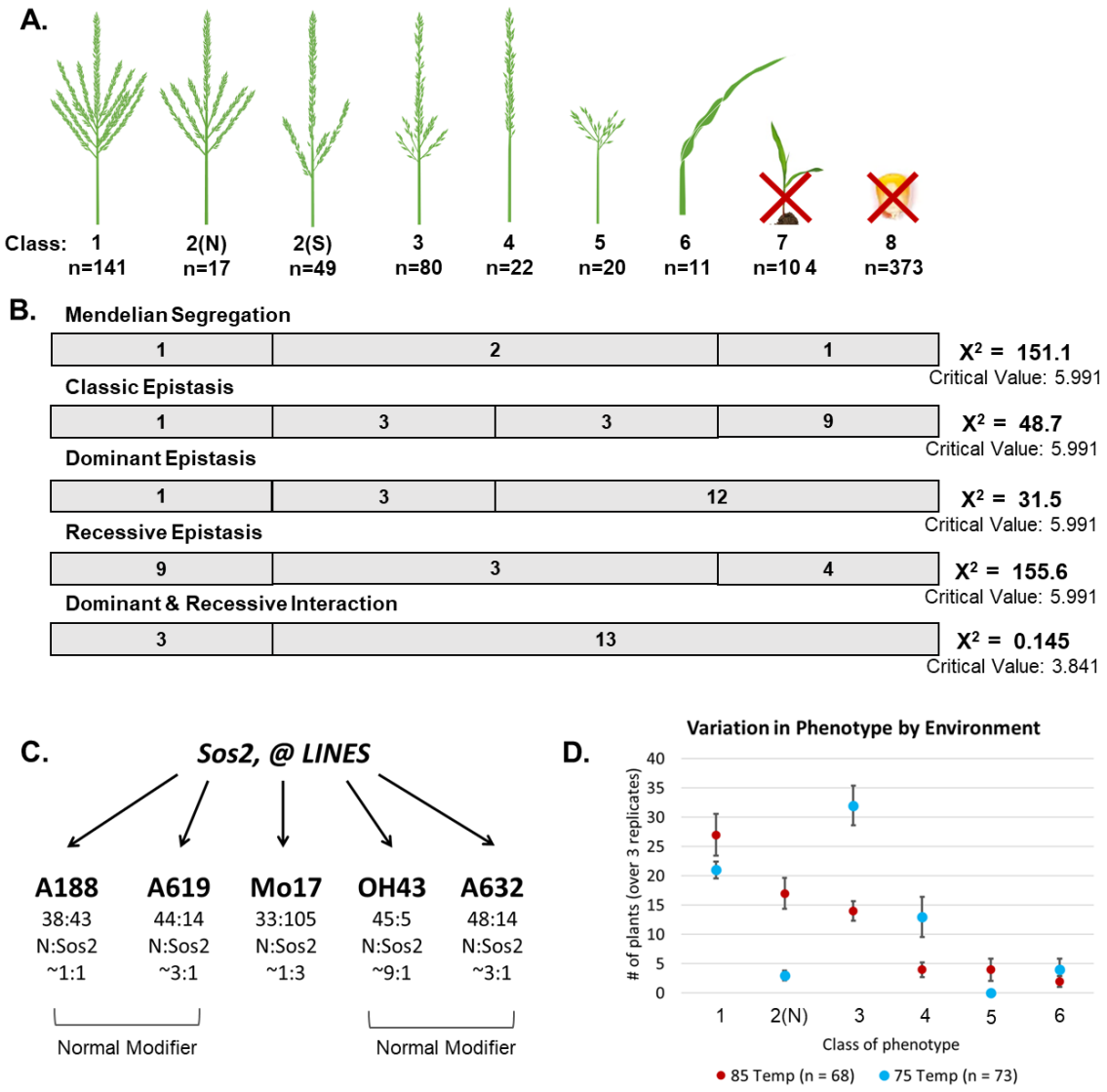

Figure 2: Variation in *Sos2* phenotype due to modifiers. **A.** Cartoon depictions of variations in the mature *Sos2/+* tassel phenotypes broken down as a scale from 1-8, with two categories of class 2 present: 2 – Normal modified and 2 – *Sos2* modified. **B.** Chi-squared analysis of epistatic ratios to determine if variation in phenotype is due to the presence of another gene. Plants included in each category are aligned with the cartoon depictions in A. **C.** Natural variation effects on the *Sos2* phenotype in *Sos2/+* selfed segregating families in different genetic

backgrounds. **D.** Variation in *Sos2* phenotype in different temperatures of *Sos2/+* outcrossed families grow in warm (85F/28C, red dots) and cold (75F/23C, blue dots) growth chambers. Results shown are the mean number of plants per category over three biological replicates.

Table 1. Vegetative characteristics of *Sos2* double mutants and normal siblings

Genotype	n =	Plant Height (cm)	Leaf Number	
+/+; +/+	8	193.25 ± 12.07	18.63 ± 1.18^{a}	
+/+; *Sos2* /+	7	187.57 ± 26.88	19.00 ± 1.14^{a,c}	MO2019
td1/td1; +/+	5	192.80 ± 25.89	16.25 ± 0.95^{b,d}	
td1/td1; Sos2 /+	4	181.75 ± 31.22	17.00 ± 0.00^{a,c}	
+/+; +/+	9	169.00 ± 16.37	17.78 ± 1.71^{a}	
+/+; *Sos2* /+	5	180.60 ± 24.73	17.60 ± 1.14^{a,c}	MO2019
fea2/fea2; +/+	14	170.64 ± 21.69	16.43 ± 1.34^{b,c}	
fea2/fea2; Sos2 /+	6	159.44 ± 22.72	15.50 ± 1.38^{b,d}	
+/+; +/+	3	208.28 ± 8.79^{a}	19.33 ± 0.58^{a}	
+/+; *Sos2* /+	10	133.25 ± 41.48^{bc}	19.03 ± 1.40^{a}	MO2020
ct2/ct2; +/+	3	77.04 ± 13.06^{bde}	12.50 ± 1.80^{b}	
ct2/ct2; Sos2 /+	7	112.32 ± 14.76^{bcf}	19.67 ± 0.89^{a}	

PH not significant in *Sos2;td1* of *Sos2;fea2* segregating families.

Table 1: Vegetative characteristics of *Sos2* double mutants and normal siblings. Plant height is measured from soil level to flag leaf, and shows no significant difference in *Sos2;td1* or *Sos2;fea2* segregating lines. Subscripts denote significance in a one-way ANOVA, ± indicates standard deviation.

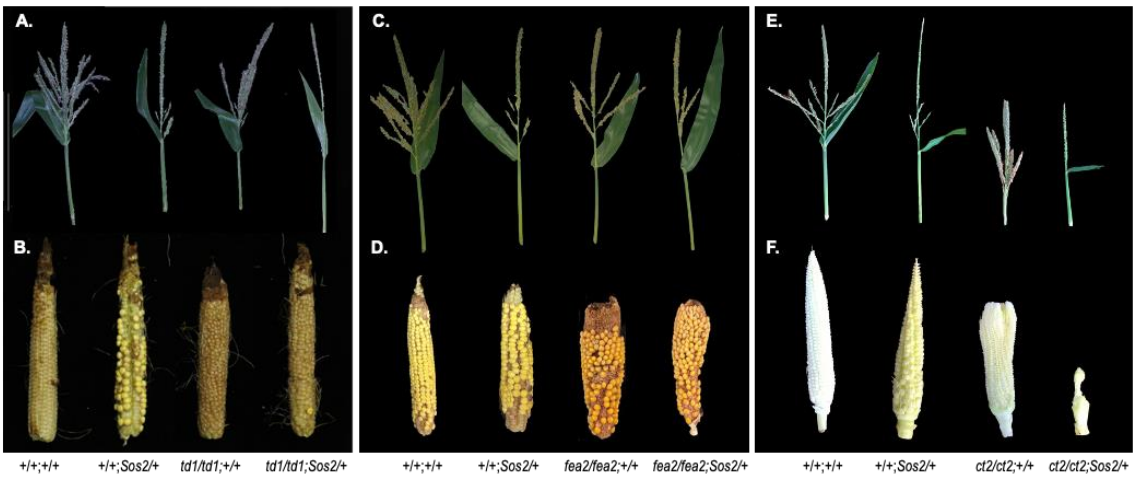

Figure 3: *Sos2* double mutant and normal sibling mature reproductive phenotypes. **A,C,D:** Normal tassels have a main rachis with many branches composed mainly of paired spikelets, *Sos2*/+ mutants have decreased branching, an increase in single spikelets and a decrease in paired spikelets. **B,D,F:** Normal ears have even KRN, *Sos2*/+ ears show uneven row pairing due to sporadic production of single instead of paired spikelets. **A.** *td1/td1* mutants have bushy tassels with many branches and an obvious abundance of spikelets on the main rachis, *Sos2;td1/td1* tassels have decreased branching and are phenotypically similar to *Sos2*. **B.** *td1/td1* ears are slightly fasciated, *Sos2/+;td1/td1* ears look normal with irregular rows. **C.** *fea2/fea2* tassels are slightly fasciated at the top of the main rachis and have fewer branches than normal siblings, *Sos2/+;fea2/fea2* tassels are slightly fasciated at the top, but are otherwise phenotypically similar to *Sos2*/+ single mutants. **D.** *fea2/fea2* ears are fasciated as are *Sos2/+;fea2/fea2* double mutants. **E.** *ct2/ct2* tassels are compact and bushy with many branches, *Sos2/+;ct2/ct2* tassels are also compact but lack branches and produce single spikelets. **F.** Not

fully-mature ear phenotypes – *ct2/ct2* ears are very fasciated and *Sos2/+;ct2/ct2* ears resemble *Sos2/+* severe ball ear phenotypes, or *Sos2/+* typical phenotypes (picture not shown) **A-F:** Genotype on the bottom correlates with the tassel and ear above.

Table 2a. Reproductive traits of *Sos2* double mutants and normal siblings

Genotype	n =	Initation Events	KRN	Single	Double
+/+; +/+	7	137.57 ± 19.21	14.86 ± 1.57[a]	45.43	83.43
+/+; *Sos2* /+	7	125.00 ± 11.58	7.50 ± 2.07[b,c]	65.71	52.57
td1/td1; +/+	8	146.75 ± 42.56	23.38 ± 4.50[b,d,e]	80.63	55.38
td1/td1; Sos2 /+	7	127.57 ± 39.61	12.71 ± 4.03[a,d,f]	87.86	35.43
+/+; +/+	7	142.86 ± 23.75[a]	15.14 ± 2.54[a]	41.00	92.00
+/+; *Sos2* /+	4	155.00 ± 58.18[a]	10.50 ± 3.87[b,c]	86.75	61.75
fea2/fea2; +/+	6	181.33 ± 24.87[b]	18.67 ± 1.75[b,d]	62.33	111.33
fea2/fea2; Sos2 /+	8	171.63 ± 23.57[b]	17.38 ± 3.34[a,d]	70.75	97.13
+/+; +/+	7	134.43 ± 50.58[a]	16.14 ± 2.34[a]	33.71	88.71
+/+; *Sos2* /+	8	136.00 ± 18.44[a,c]	9.7 ± 5.44[b,c]	54.63	76.75
ct2/ct2; +/+	6	188.67 ± 33.28[b,d]	16.00 ± 0.00[a,d,e]	29.33	142.00
ct2/ct2; Sos2 /+	2	184.50 ± 4.95[a,d]	7.5 ± 0.71[b,d,f]	118.50	63.50

Table 2b. Tassel composition of *Sos2* double mutants and normal siblings

Genotype	n =	Single	Single - Aborted*	Double	Double-Aborted*
+/+; +/+	7	45.00 ± 24.11[a]	0.43 ± 0.79[a]	82.14 ± 24.93[a]	1.29 ± 1.60[a]
+/+; *Sos2* /+	7	58.43 ± 19.91[a]	7.29 ± 4.57[b,c]	35.29 ± 20.93[b]	17.29 ± 5.91[b,c]
td1/td1; +/+	8	79.25 ± 32.27[b]	1.38 ± 0.29[a,d,e]	53.38 ± 15.23[b,e]	2.00 ± 2.20[a,d,e]
td1/td1; Sos2 /+	7	72.71 ± 36.71[a]	15.14 ± 16.60[b,c,f]	20.43 ± 17.29[b,f]	15.00 ± 12.14[b,c,f]
+/+; +/+	7	40.71 ± 22.35[a]	0.29 ± 0.76[a]	87.86 ± 24.88	4.14 ± 2.91
+/+; *Sos2* /+	4	81.75 ± 33.95[b]	5.00 ± 4.69[b]	53.50 ± 27.40[c]	8.25 ± 6.95
fea2/fea2; +/+	6	58.67 ± 8.98[b]	3.67 ± 2.06[b]	106.00 ± 17.15[d]	5.33 ± 3.72
fea2/fea2; Sos2 /+	8	66.63 ± 24.53[b]	4.13 ± 3.80[b]	89.38 ± 26.41[d]	7.75 ± 5.73
+/+; +/+	7	33.43 ± 18.79[a]	0.29 ± 0.76[a]	87.14 ± 43.96[a]	1.57 ± 2.07[a]
+/+; *Sos2* /+	8	46.25 ± 27.22[a]	8.38 ± 5.07[b,c]	53.13 ± 31.96[a,c]	23.63 ± 16.47[b,c]
ct2/ct2; +/+	6	29.33 ± 16.44[a,e]	0.00 ± 0.00[a,d,e]	140.33 ± 29.93[b,d,e]	1.67 ± 1.63[a,d,e]
ct2/ct2; Sos2 /+	2	88.00 ± 43.84[b,f]	30.50 ± 14.85[b,d,f]	20.00 ± 24.04[a,c,f]	43.50 ± 3.54[b,c,f]

[a,b,c,d,e,f] Significance determined via 1-Way ANOVA, for each characteristic compared to respective double mutant categoreis (separated by grey bars), $p < 0.05$

* Equal variance cannot be assumed in these categories, with the exception of "Double-Aborted" for Sos2;fea2 double mutants

Table 2: Quantification of reproductive characteristics of *Sos2* double mutants and normal siblings. **2a:** Initiation events counts on all meristems produces by the IM (SPM + BM) in the tassel, KRN counts the number of kernels one inch down from the tip of the ear (a combination of SPM produced from the IM and SM produced from SPM), “Single” is the average number of single spikelets, including single-

aborted spikelets, in the tassel (represents SPM that produce single SM). “Double” is the average number of paired spikelets, including those with one or both of the spikelets aborted in the tassel (represents SPM that produce two SM) **2b:** Tassel composition of *Sos2* double mutants and normal siblings, with aborted spikelets separated out to analyze SM maintenance phenotypes. Subscripts denote significance in a one-way ANOVA, ± indicates standard deviation.

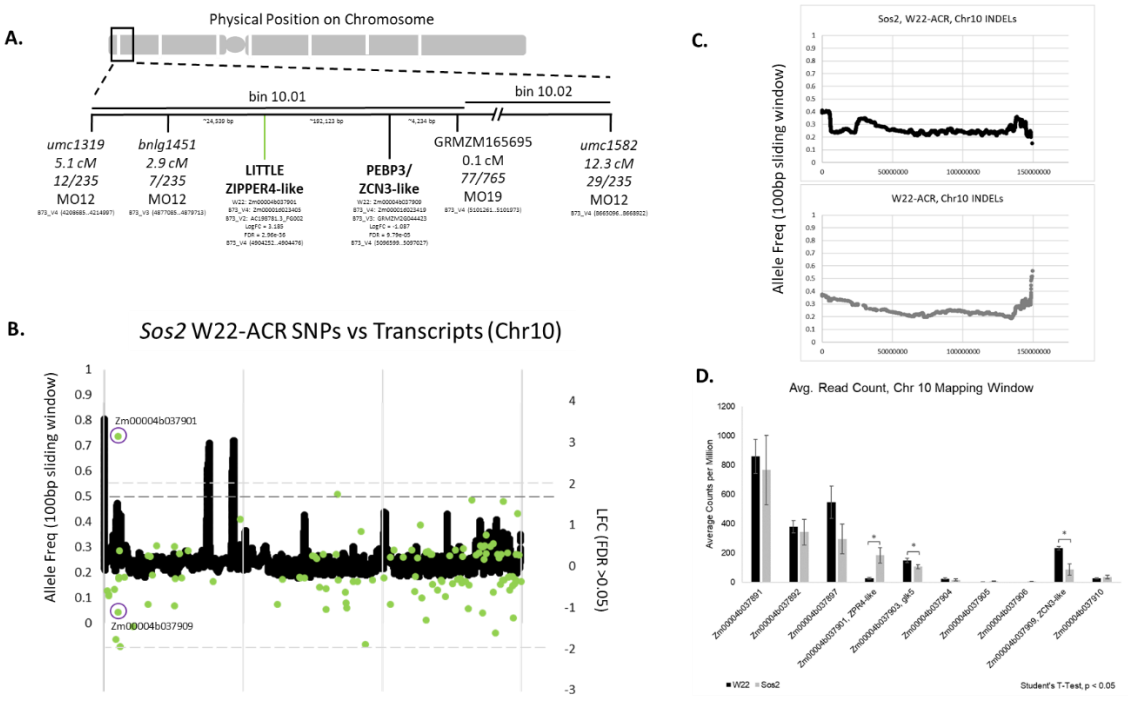

Figure 4: Mapping of the *Sos2* mutation. **A.** Fine-mapping of *Sos2* placed the mutation on the short arm of chromosome 10, the markers used are denoted by a black line and italics, cM = centimorgan distance from the *Sos2* locus. Green bars and bold lettering highlight two genes within the map window that were identified by RNA-seq analysis – logfold change and FDR values are listed below. **B.** Genomic sequencing of chromosome 10 (black line) has a small peak within the map window which is close to the allelic frequency expected peak value of 0.5 (left y-axis) for the *Sos2*/+ mutation (dark grey dotted line). Differentially expressed genes (FCR < 0.05) are super imposed on to genomic sequencing (green dots), light grey bars denote a logfold change value of either 2 or -2 (right y-axis). The x-axis is the physical position on the chromosome. Purple circles highlight the two DEGs within the fine mapping window that are significant by p-value and FDR. **C.** Graph of mapped INDELs on chromosome 10, using the position of the first altered

base pair on a 100 bp sliding window. A valley was found which included the fine mapping position that had lower coverage than the rest of the INDELs mapped on this chromosome. **D.** Graph of average read counts of genes within the fine mapping window that had over 10 read counts total. Only three genes were differentially expressed, two significantly, and only one (*ZmZPR4-like*) had a logfold value greater than 2, and was also the only gene up-regulated in *Sos2* compared to normal in this map window.

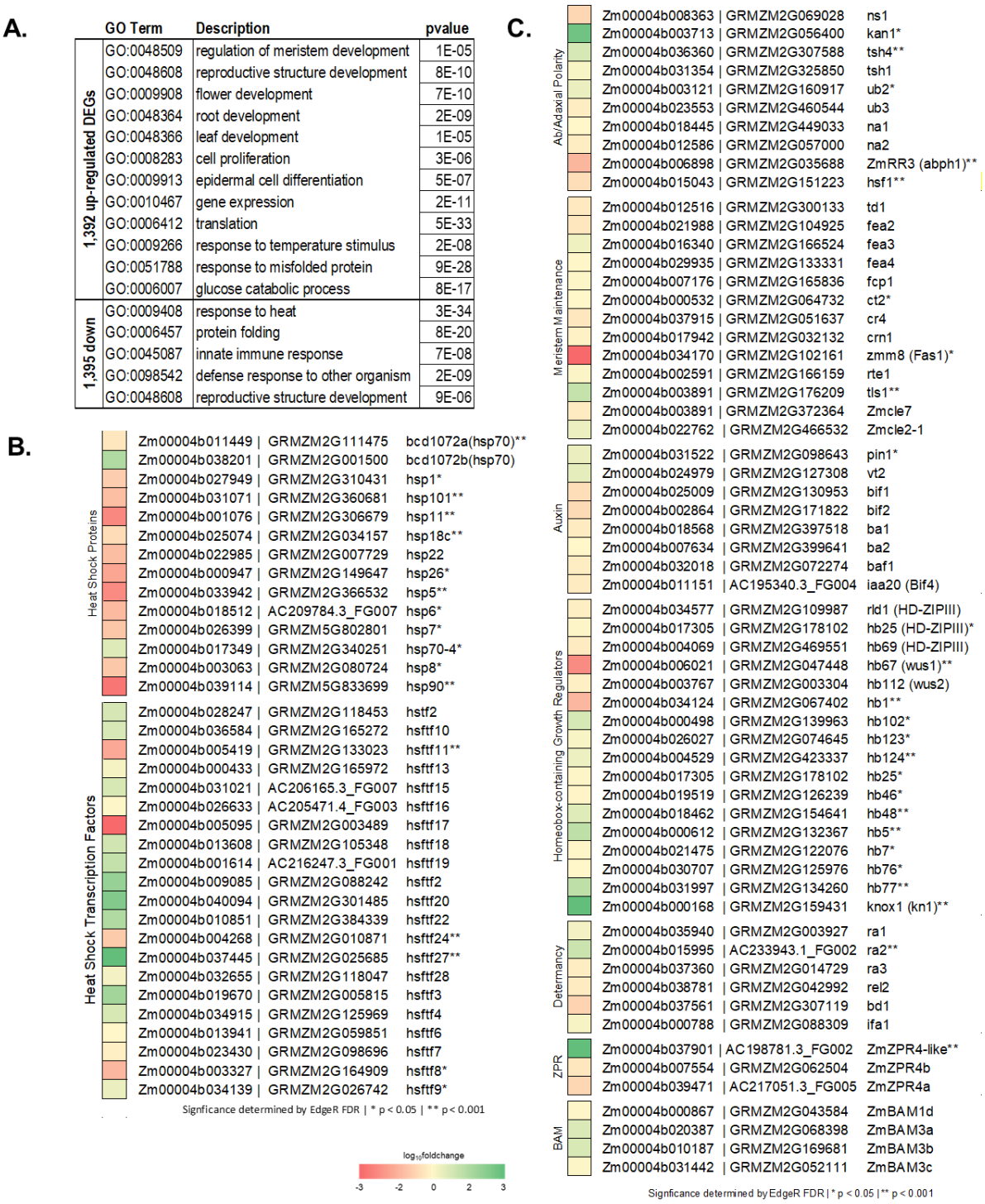

Figure 5: RNA-seq analysis of *Sos2*/+ immature tassels. **A.** Enriched GO terms for up and down regulated genes. **B.** Expression of heat shock proteins and heat shock transcription factors. **C.** Expression of select genes known to be involved in

development, categorized with labels to the left. **B-C:** A single asterisk (*) denotes a differentially expressed gene with an FDR < 0.05, a double asterisk (**) denotes a differentially expressed gene with an FDR < 0.001, no asterisks means that gene was not significantly differentially expressed.

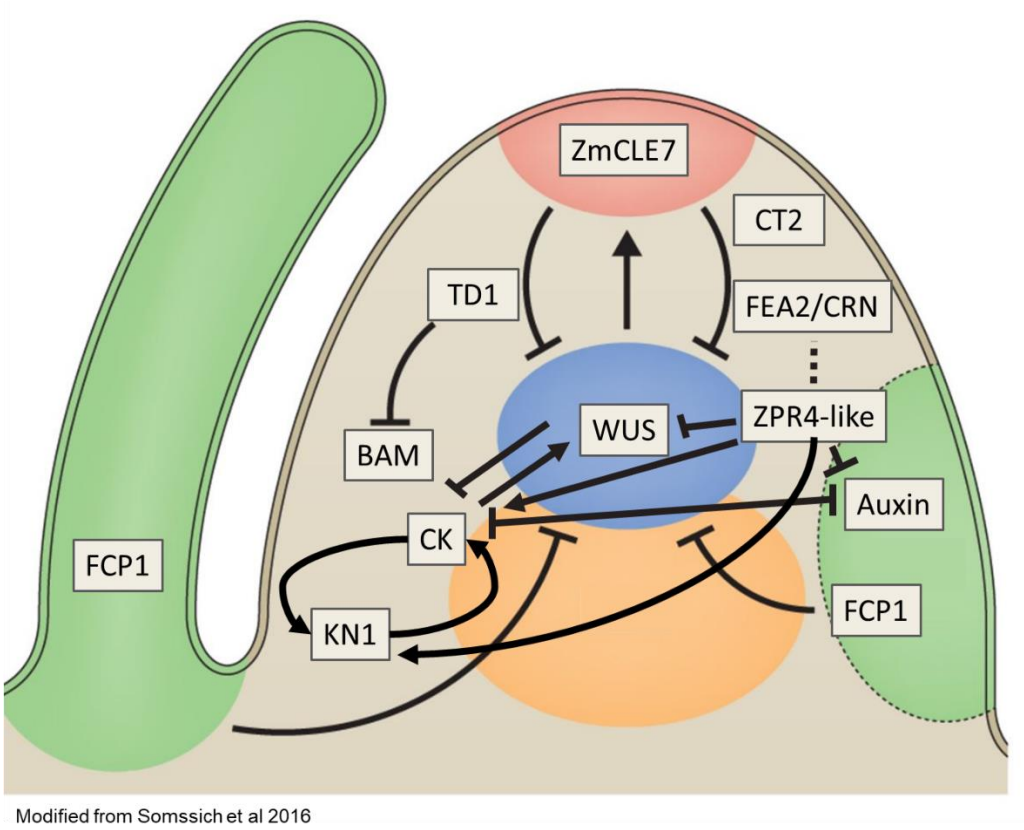

Figure 6: Schematic of meristem maintenance pathway, in IMs rather than the SAM depicted, with *ZmZPR4-like* included. Arrows and caped lines show positive and negative regulation and dotted lines show an interaction that has not yet been determined. Figure was modified from (Somssich et al., 2016).

Supplemental Table 1: Tassel composition as percentages for *Sos2* double mutants and normal siblings

Genotype	n =	Single	Single - Aborted	Double	Double-Aborted
+/+; +/+	7	34.92%	0.33%	63.75%	1.00%
+/+; *Sos2* /+	7	49.40%	6.16%	29.83%	14.61%
td1/td1; +/+	8	58.27%	1.01%	39.25%	1.47%
td1/td1; Sos2 /+	7	58.98%	12.28%	16.57%	12.17%
+/+; +/+	7	30.61%	0.21%	66.06%	3.11%
+/+; *Sos2* /+	4	55.05%	3.37%	36.03%	5.56%
fea2/fea2; +/+	6	33.78%	2.11%	61.04%	3.07%
fea2/fea2; Sos2 /+	8	39.69%	2.46%	53.24%	4.62%
+/+; +/+	7	27.30%	0.23%	71.18%	1.28%
+/+; *Sos2* /+	8	35.20%	6.37%	40.44%	17.98%
ct2/ct2; +/+	6	17.12%	0.00%	81.91%	0.97%
ct2/ct2; Sos2 /+	2	48.35%	16.76%	10.99%	23.90%

Supplemental Table 1: Tassel composition of *Sos2* double mutants and normal siblings as decimal percentages for comparing phenotypes.

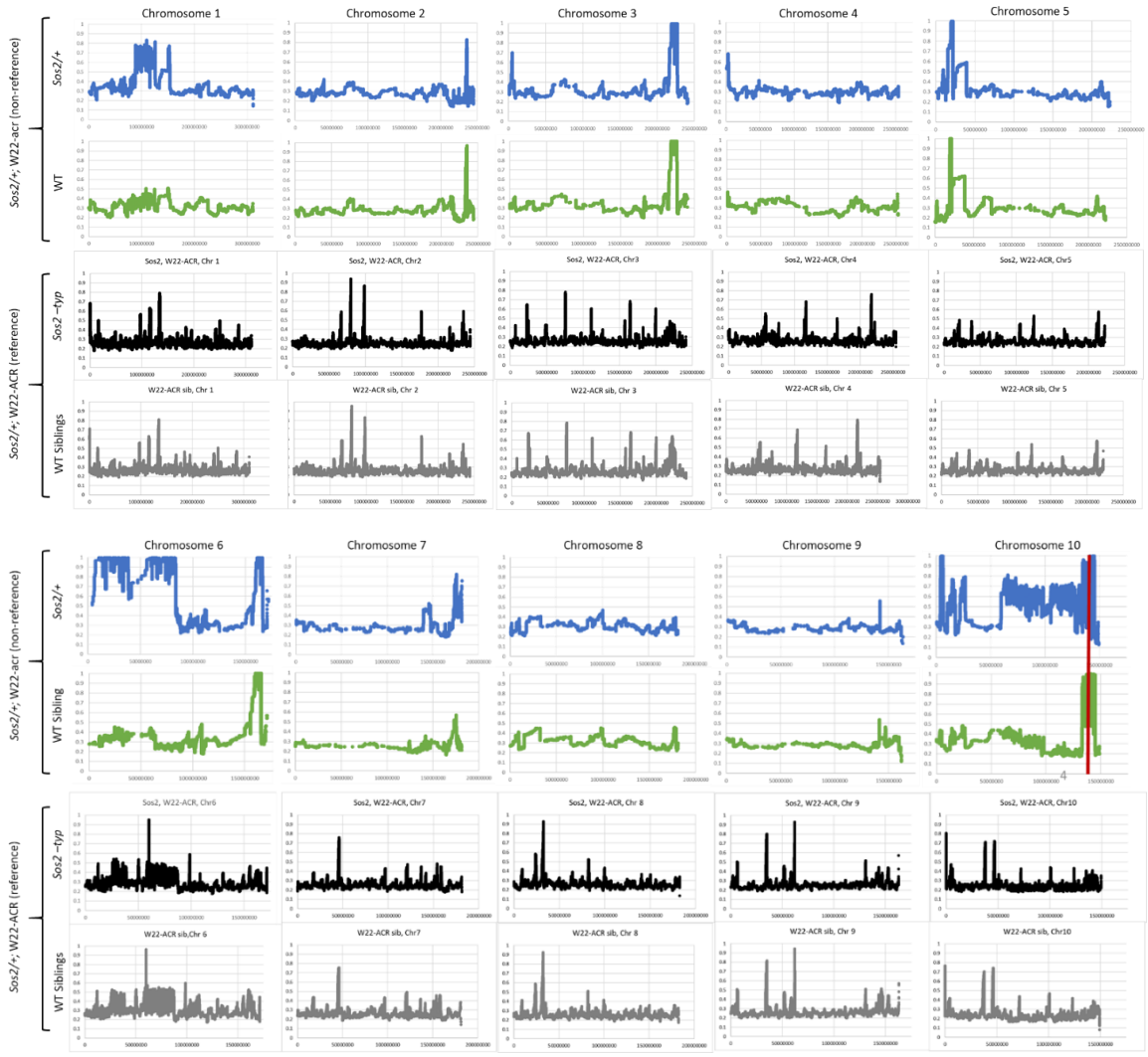

Supplemental Figure 1: Genome-wide sequencing analysis of the *Sos2* mutation in W22-acr and W22-ACR genetic backgrounds.

WORKS CITED

Anders, S., Pyl, P. T., & Huber, W. (2015). HTSeq-A Python framework to work with high-throughput sequencing data. *Bioinformatics*, *31*(2), 166–169. https://doi.org/10.1093/bioinformatics/btu638

Avery, L., & Wasserman, S. (1992). Ordering gene function: the interpretation of epistasis in regulatory hierarchies. In *Trends in Genetics* (Vol. 8, Issue 9, pp. 312–316). Trends Genet. https://doi.org/10.1016/0168-9525(92)90263-4

Bolger, A. M., Lohse, M., & Usadel, B. (2014). Trimmomatic: A flexible trimmer for Illumina sequence data. *Bioinformatics*, *30*(15), 2114–2120. https://doi.org/10.1093/bioinformatics/btu170

Bommert, P., Je, B. il, Goldshmidt, A., & Jackson, D. (2013). The maize Gα gene COMPACT PLANT2 functions in CLAVATA signalling to control shoot meristem size. *Nature*, *502*(7472), 555–558. https://doi.org/10.1038/nature12583

Bommert, P., Lunde, C., Nardmann, J., Vollbrecht, E., Running, M., Jackson, D., Hake, S., & Werr, W. (2005a). Thick tassel dwarf1 encodes a putative maize ortholog of the Arabidopsis CLAVATA1 leucine-rich repeat receptor-like kinase. *Development*, *132*(6), 1235–1245. https://doi.org/10.1242/dev.01671

Bommert, P., Lunde, C., Nardmann, J., Vollbrecht, E., Running, M., Jackson, D., Hake, S., & Werr, W. (2005b). Thick tassel dwarf1 encodes a putative maize ortholog of the Arabidopsis CLAVATA1 leucine-rich repeat receptor-like kinase. *Development*, *132*(6), 1235–1245. https://doi.org/10.1242/dev.01671

Bommert, P., Nagasawa, N. S., & Jackson, D. (2013). Quantitative variation in maize kernel row number is controlled by the FASCIATED EAR2 locus. *Nature Genetics*, *45*(3), 334–337. https://doi.org/10.1038/ng.2534

Brand, U., Fletcher, J. C., Hobe, M., Meyerowitz, E. M., & Simon, R. (2000). Dependence of stem cell fate in Arabidopsis on a feedback loop regulated by CLV3 activity. *Science*, *289*(5479), 617–619. https://doi.org/10.1126/science.289.5479.617

Brink, A., Styles, D., & Axtell, J. (1968). Paramutation: directed genetic change. Paramutation occurs in somatic cells and heritably alters the functional state of a locus. *Science*, *159*, 161–170. https://www.jstor.org/stable/1723264?seq=1

Chen, Z., Li, W., Gaines, C., Buck, A., Galli, M., & Gallavotti, A. (2021). Structural variation at the maize WUSCHEL1 locus alters stem cell organization in inflorescences. *Nature Communications*, *12*(1), 1–12. https://doi.org/10.1038/s41467-021-22699-8

Clark, S. E., Running, M. P., & Meyerowitz, E. M. (1995). CLAVATA3 is a specific regulator of shoot and floral meristem development affecting the same processes as CLAVATA1. *Development*, *121*(7), 2057–2067. https://doi.org/10.1242/dev.121.7.2057

Cremer, F., Lö, W.-E., Saedler, H., & Huijser, P. (2001). *The Delayed Terminal Flower Phenotype Is Caused by a Conditional Mutation in the CENTRORADIALIS Gene of Snapdragon*. https://academic.oup.com/plphys/article/126/3/1031/6103609

Danecek, P., Bonfield, J. K., Liddle, J., Marshall, J., Ohan, V., Pollard, M. O., Whitwham, A., Keane, T., McCarthy, S. A., Davies, R. M., & Li, H. (2021). Twelve years of SAMtools and BCFtools. *GigaScience*, *10*(2). https://doi.org/10.1093/gigascience/giab008

Doebley, J., Stec, A., & Kent, B. (1995). Suppressor of Sessile spikelets 1 (Sos1): A Dominant Mutant Affecting Inflorescence Development in Maize. *American Journal of Botany*, *82*(5), 571. https://doi.org/10.2307/2445415

Du, Y., Lunde, C., Li, Y., Jackson, D., Hake, S., & Zhang, Z. (2021). Gene duplication at the Fascicled ear1 locus controls the fate of inflorescence meristem cells in maize. *Proceedings of the National Academy of Sciences of the United States of America*, *118*(7). https://doi.org/10.1073/pnas.2019218118

Du, Z., Zhou, X., Ling, Y., Zhang, Z., & Su, Z. (2010). agriGO: A GO analysis toolkit for the agricultural community. *Nucleic Acids Research*, *38*(SUPPL. 2), W64. https://doi.org/10.1093/nar/gkq310

Endrizzi, K., Moussian, B., Haecker, A., Levin, J. Z., & Laux, T. (1996). The SHOOT MERISTEMLESS gene is required for maintenance of undifferentiated cells in Arabidopsis shoot and floral meristems and acts at a different regulatory level than the meristem genes WUSCHEL and ZWILLE. *Plant Journal*, *10*(6), 967–979. https://doi.org/10.1046/j.1365-313X.1996.10060967.x

Evert, R. F., Eichhorn, S. E., & Edition, T. (2006). Esau ' s Plant Anatomy ESAU ' S PLANT ANATOMY. In *Development*. http://doi.wiley.com/10.1002/0470047380

Fletcher, J. C. (1999). Signaling of cell fate decisions by CLAVATA3 in Arabidopsis shoot meristems. *Science*, *283*(5409), 1911–1914. https://doi.org/10.1126/science.283.5409.1911

Fletcher, J. C. (2018). The CLV-WUS stem cell signaling pathway: A roadmap to crop yield optimization. In *Plants* (Vol. 7, Issue 4). MDPI AG. https://doi.org/10.3390/plants7040087

Fletcher, J. C. (2020). Recent Advances in Arabidopsis CLE Peptide Signaling. In *Trends in Plant Science* (Vol. 25, Issue 10, pp. 1005–1016). Elsevier Ltd. https://doi.org/10.1016/j.tplants.2020.04.014

Freeling, M., & Walbot, V. (Eds.). (1994). *The Maize Handbook* (1st ed.). Springer-Verlag New York.

Goad, D. M., Zhu, C., & Kellogg, E. A. (2017). Comprehensive identification and clustering of CLV3/ESR-related (CLE) genes in plants finds groups with potentially shared function. *New Phytologist*, *216*(2), 605–616. https://doi.org/10.1111/nph.14348

Gray, A. (1879). *Structural Botany*. Cambridge University Press.

Hanano, S., & Goto, K. (2011). Arabidopsis TERMINAL FLOWER1 Is Involved in the Regulation of Flowering Time and Inflorescence Development through Transcriptional Repression C W OA. *The Plant Cell*, *23*, 3172–3184. https://doi.org/10.1105/tpc.111.088641

Jackson, D., Veit, B., & Hake, S. (1994). Expression of maize KNOTTED1 related homeobox genes in the shoot apical meristem predicts patterns of morphogenesis in the vegetative shoot. *Development*, *120*(2), 405–413. https://doi.org/10.1242/dev.120.2.405

Je, B. il, Gruel, J., Lee, Y. K., Bommert, P., Arevalo, E. D., Eveland, A. L., Wu, Q., Goldshmidt, A., Meeley, R., Bartlett, M., Komatsu, M., Sakai, H., Jönsson, H., Jackson, D., & Danforth, D. (2016). Signaling from maize organ primordia via FASCIATED EAR3 regulates stem cell proliferation and yield traits. *Nature Publishing Group*, *48*(7), 785–791. https://doi.org/10.1038/ng.3567

Je, B. il, Xu, F., Wu, Q., Liu, L., Meeley, R., Gallagher, J. P., Corcilius, L., Payne, R. J., Bartlett, M. E., & Jackson, D. (2018). The clavata receptor fasciated ear2 responds to distinct cle peptides by signaling through two downstream effectors. *ELife*, *7*. https://doi.org/10.7554/eLife.35673

Johnson, E. (2017). *Evolution and development of the paired spikelet trait in maize and other grasses (Poaceae)*.

Juarez, M. T., Kui, J. S., Thomas, J., Heller, B. A., & Timmermans, M. C. P. (2004). microRNA-mediated repression of rolled leaf1 specifies maize leaf polarity. *Nature*, *428*(6978), 84–88. https://doi.org/10.1038/nature02363

Juarez, M. T., Twigg, R. W., & Timmermans, M. C. P. (2004). Specification of adaxial cell fate maize leaf development. *Development*, *131*(18), 4533–4544. https://doi.org/10.1242/dev.01328

Kiesselbach, T. A. (1949). *The Structure and Reproduction of Corn* (2nd ed.). Cold Spring Harbor Laboratory Press.

Kim, D., Langmead, B., & Salzberg, S. L. (2015). HISAT: A fast spliced aligner with low memory requirements. *Nature Methods*, *12*(4), 357–360. https://doi.org/10.1038/nmeth.3317

Kim, Y. S., Kim, S. G., Lee, M., Lee, I., Park, H. Y., Pil, J. S., Jung, J. H., Kwon, E. J., Se, W. S., Paek, K. H., & Park, C. M. (2008). HD-ZIP III activity is modulated by competitive inhibitors via a feedback loop in Arabidopsis shoot apical meristem development. *Plant Cell*, *20*(4), 920–933. https://doi.org/10.1105/tpc.107.057448

Leach, K. A., McSteen, P. C., & Braun, D. M. (2016). Genomic DNA Isolation from Maize (Zea mays) Leaves Using a Simple, High-Throughput Protocol . *Current Protocols in Plant Biology*, *1*(1), 15–27. https://doi.org/10.1002/cppb.20000

Lenhard, M., Jürgens, G., & Laux, T. (2002). The WUSCHEL and SHOOTMERISTEMLESS genes fulfil complementary roles in Arabidopsis shoot meristem regulation. *Development*, *129*(13), 3195–3206. https://doi.org/10.1242/dev.129.13.3195

Liu, L., Gallagher, J., Arevalo, E. D., Chen, R., Skopelitis, T., Wu, Q., Bartlett, M., & Jackson, D. (2021). Enhancing grain-yield-related traits by CRISPR–Cas9 promoter editing of maize CLE genes. *Nature Plants*, *7*(3), 287–294. https://doi.org/10.1038/s41477-021-00858-5

Long, J. A., Moan, E. I., Medford, J. I., & Barton, M. K. (1996). A member of the KNOTTED class of homeodomain proteins encoded by the STM gene of Arabidopsis. *Nature*, *379*(6560), 66–69. https://doi.org/10.1038/379066a0

Lunde, C., & Hake, S. (2009). The interaction of knotted1 and thick tassel dwarf1 in vegetative and reproductive meristems of maize. *Genetics*, *181*(4), 1693–1697. https://doi.org/10.1534/genetics.108.098350

Lunde, C., Kimberlin, A., Leiboff, S., Koo, A. J., & Hake, S. (2019). Tasselseed5 overexpresses a wound-inducible enzyme, ZmCYP94B1, that affects jasmonate catabolism, sex determination, and plant architecture in maize. *Communications Biology*, *2*(1), 1–11. https://doi.org/10.1038/s42003-019-0354-1

Mayer, K. F. X., Schoof, H., Haecker, A., Lenhard, M., Jürgens, G., & Laux, T. (1998). Role of WUSCHEL in regulating stem cell fate in the Arabidopsis shoot meristem. *Cell*, *95*(6), 805–815. https://doi.org/10.1016/S0092-8674(00)81703-1

Muehlbauer, G. J., Fowler, J. E., Girard, L., Tyers, R., Harper, L., & Freeling, M. (1999). Ectopic expression of the maize homeobox gene Liguleless3 alters cell fates in the leaf. *Plant Physiology*, *119*(2), 651–662. https://doi.org/10.1104/pp.119.2.651

Muller, H. J. (1932). Further studies on the nature and causes of gene mutations. *Proceedings of the 6th International Congress of Genetics*, 213–255.

Nardmann, J., & Werr, W. (2006). The shoot stem cell niche in angiosperms: Expression patterns of WUS orthologues in rice and maize imply major modifications in the course of mono- and dicot evolution. *Molecular Biology and Evolution*, *23*(12), 2492–2504. https://doi.org/10.1093/molbev/msl125

Robinson, M. D., McCarthy, D. J., & Smyth, G. K. (2009). edgeR: A Bioconductor package for differential expression analysis of digital gene expression data. *Bioinformatics*, *26*(1), 139–140. https://doi.org/10.1093/bioinformatics/btp616

Shi, B., Zhang, C., Tian, C., Wang, J., Wang, Q., Xu, T., Xu, Y., Ohno, C., Sablowski, R., Heisler, M. G., Theres, K., Wang, Y., & Jiao, Y. (2016). Two-Step Regulation of a Meristematic Cell Population Acting in Shoot Branching in Arabidopsis. *PLoS Genetics*, *12*(7), e1006168. https://doi.org/10.1371/journal.pgen.1006168

Smith, L. G., Greene, B., Veit, B., & Hake, S. (1992). A dominant mutation in the maize homeobox gene, Knotted-1, causes its ectopic expression in leaf cells with altered fates. *Development*, *116*(1), 21–30. https://doi.org/10.1242/DEV.116.1.21

Somssich, M., il Je, B., Simon, diger, & Jackson, D. (2016). *CLAVATA-WUSCHEL signaling in the shoot meristem*. https://doi.org/10.1242/dev.133645

Springer, N. M., Anderson, S. N., Andorf, C. M., Ahern, K. R., Bai, F., Barad, O., Barbazuk, W. B., Bass, H. W., Baruch, K., Ben-Zvi, G., Buckler, E. S., Bukowski, R., Campbell, M. S., Cannon, E. K. S., Chomet, P., Kelly Dawe, R., Davenport, R., Dooner, H. K., Du, L. H., … Brutnell, T. P. (2018). The maize w22 genome provides a foundation for functional genomics and transposon biology. *Nature Genetics*, *50*(9), 1282–1288. https://doi.org/10.1038/s41588-018-0158-0

Steeves, Taylor A; Sussex, I. M. (1989). *Patterns in Plant Development*.

Taguchi-Shiobara, F., Yuan, Z., Hake, S., & Jackson, D. (2001). *The fasciated ear2 gene encodes a leucine-rich repeat receptor-like protein that regulates shoot meristem proliferation in maize*. https://doi.org/10.1101/gad.208501

Veitia, R. A. (2007). Exploring the molecular etiology of dominant-negative mutations. In *Plant Cell* (Vol. 19, Issue 12, pp. 3843–3851). Oxford University Press. https://doi.org/10.1105/tpc.107.055053

Vollbrecht, E., Reiser, L., & Hake, S. (2000). Shoot meristem size is dependent on inbred background and presence of the maize homeobox gene, knotted1. *Development*, *127*(14), 3161–3172. https://doi.org/10.1242/dev.127.14.3161

Wenkel, S., Emery, J., Hou, B. H., Evans, M. M. S., & Barton, M. K. (2007). A feedback regulatory module formed by Little Zipper and HD-ZIPIII genes. *Plant Cell*, *19*(11), 3379–3390. https://doi.org/10.1105/tpc.107.055772

Wu, Q., Luo, A., Zadrozny, T., Sylvester, A., & Jackson, D. (2013). Fluorescent protein marker lines in maize: Generation and applications. *International Journal of Developmental Biology*, *57*(6–8), 535–543. https://doi.org/10.1387/ijdb.130240qw

Wu, X., Skirpan, A., & McSteen, P. (2009). Suppressor of sessile spikelets1 functions in the ramosa pathway controlling meristem determinacy in maize. *Plant Physiology*, *149*(1), 205–219. https://doi.org/10.1104/pp.108.125005

Xu, Q., Li, R., Weng, L., Sun, Y., Li, M., & Xiao, H. (2019). Domain-specific expression of meristematic genes is defined by the LITTLE ZIPPER protein DTM in tomato. *Communications Biology*, *2*(1), 1–14. https://doi.org/10.1038/s42003-019-0368-8

Zhang, F., May, A., & Irish, V. F. (2017). Type-B ARABIDOPSIS RESPONSE REGULATORs Directly Activate WUSCHEL. In *Trends in Plant Science* (Vol. 22, Issue 10, pp. 815–817). Elsevier Ltd. https://doi.org/10.1016/j.tplants.2017.08.007

CHAPTER 3:

Sos2 mutants have defects in auxin and cytokinin cross talk and have similar transcriptomic profiles to *Sos3* mutants.

Katy Guthrie, Connor Nordwald, Amanda Blythe, Paula McSteen

ABSTRACT

The *Suppressor of sessile spikelet* class of semi-dominant mutants, which include *Sos1, Sos2* and *Sos3,* share phenotypic similarities in their mature reproductive phenotypes, primarily in the production of single instead of paired spikelets in the tassel and the ear. Recent studies of *Sos2* found that the mutant phenotype may be caused by increased expression of a *LITTLE-ZIPPER4-like* inhibitory protein involved in meristem maintenance (Chapter 2). A previous study on *ZPR4* in *Arabidopsis* hypothesized a link to phytohormone pathways. Therefore, This study explores the link between *Sos2* mutants and two common developmental phytohormones, auxin and cytokinin. In this study, we found increased levels of cytokinin intermediaries cZR and tZR, and decreased levels of IAA in immature *Sos2* mutant tassels compared to normal. These results were supported by imaging of immature *Sos2* tassels crossed to the TCS-tdTomato (cytokinin response), ZmPIN1a-YFP (auxin transport) and DR5-RFP (auxin response) transgenic marker lines. To assess the impact of the *Sos2* mutation on these pathways at a transcriptomic level, as well as to understand the roles of phenotypically similar *Sos1* and *Sos3* mutants in these phytohormone pathways, a comparative RNAseq experiment was performed. This analysis found that *Sos2* and *Sos3* were more similar in gene expression than either, compared to *Sos1.* In addition, this experiment highlighted three possible avenues of further investigation: 1) the impact of the *Sos2* mutation on the cytokinin pathway, specifically the involvement of cytokinin response genes, 2) the role of the *Sos3*

gene in the auxin pathway, 3) whether *Sos1* mutants affect phytohormone levels at the chemical and/or protein signaling level, as transcriptionally auxin and cytokinin pathways were not significantly impacted in *Sos1* mutations.

INTRODUCTION

Plant hormones are well understood to direct plant growth and development (Coenen & Lomax, 1997; Shimizu-Sato et al., 2009; Su et al., 2011). Specifically, the antagonistic interaction between the auxin and cytokinin pathway define different domains of development, such as the peripheral zone and the stem cells respectively in the shoot apical meristem (SAM) or inflorescence meristem (IM) (Steeves & Sussex, 1989). In addition, the synthesis of these phytohormones is directly regulated by meristem specific genes, such as *knotted1* (*kn1*), a KNOX transcription factor involved in meristem maintenance (Bolduc & Hake, 2009).

The role of cytokinin in regulating shoot apical meristem (SAM) size has been well documented (Skylar & Wu, 2011). In brief, cytokinin regulates meristem maintenance via two types of response regulators (ARRs) Type-A and Type-B. Type-B ARRs are transcriptional activators that induce cytokinin signaling (Xie et al., 2018). Type-A ARRs function in a negative feedback loop to regulate cytokinin signaling; they are induced by and subsequently repress cytokinin signaling (To et al., 2004; Xie et al., 2018). One of these type-A response regulators in maize is *aberrant phyllotaxy1* (*abph1*). By limiting cytokinin signaling within the SAM, *abphl1* decreases cytokinin signaling (Giullni et al., 2004; Lee et al., 2009), and positively regulates the expression of the auxin transporter ZmPINFORMED1a (ZmPIN1a) in the periphery of the meristem (Lee et al., 2009). ZmPIN1 is phosphorylated by the Serine/Threonine protein kinase, BARREN INFLORESCENCE2 (BIF2) (McSteen & Hake, 2001; McSteen et al., 2007; Skirpan et al., 2008). *bif2* mutants display an analogous phenotype in inflorescence

development similar to that of the Arabidopsis *pinoid* mutant, where tassels are unable to initiate axillary meristems (AMs) resulting in a short, sterile main rachis (McSteen & Hake, 2001). In addition to regulating ZmPIN1a, BIF2 phosphorylates a transcription factor, BARREN STALK1 (BA1) which acts downstream of auxin (Skirpan et al., 2008). Like *ZmPIN1a*, *ba1* plays a role in of axillary meristem formation in maize SAMs and IMs (Gallavotti et al., 2004). Another barren stalk transcription factor, BA2, physically interacts with BA1 and is also impaired in production of axillary meristems from the IM (Yao et al., 2019). Therefore, *ZmPIN1a* is involved in auxin transport, whereas *ba1* and *ba2* act downstream of auxin signaling.

The homeobox transcription factor, KNOTTED1 (KN1), orthologous to SHOOTMERISTEMLESS (STM) in *Arabidopsis,* also connects auxin and cytokinin pathways (Kerstetter et al., 1997). KN1 directly up-regulates *vanishing tassel2* (*vt2*), which is a gene involved in auxin biosynthesis, and binds to the promoters of a majority of the AUX-IAAs and ARF genes (Bolduc et al., 2012). Another direct targets of KN1 includes the cytokinin biosynthesis gene, *ipt*. IPT proteins catalyze the rate limiting step in cytokinin biosynthesis (Sun et al., 2003; Takei et al., 2001), and induction of this gene indicates a role of cytokinin in promoting meristematic cell identity (Jasinski et al., 2005). These studies highlight connections in the cytokinin and auxin pathways during meristem establishment and maintenance through KN1 regulation. Furthermore, *ZmWUS1* expression is induced by cytokinin signaling in the organizing center of meristems and ZmWUS1 regulates its own expression by subsequently repressing type-A ARRs, discussed above

(D'Agostino et al., 2000; Gordon et al., 2009). The overlap of cytokinin signaling on the expression domains of these two genes, *Zmwus1* and *kn1*, illustrate its role in regulating meristem maintenance.

Previous work on the *Sos2* mutant in maize has narrowed the causative locus down to two genes, ZmLITTLEZIPPER4a and ZmPEBP3, on the short arm of Chromosome 10 (Chapter 2, Results and Discussion). Both of these genes have previously been shown to interact with phytohormone pathways in other species, therefore, I investigated *Sos2* mutants for defects in hormone pathways. These results show a significant increase of cytokinin intermediaries and decrease of the active auxin, IAA, in *Sos2* mutants – which was supported by fluorescence protein imaging.

The other two *Sos* mutants, *Sos1* and *Sos3* both have phenotypic similarities to *Sos2. Sos1* heterozygote ears also have decreased kernel row pairing, and tassels have decreased number of branches and paired spikelets, and an increase in single spikelets (Johnson, 2017; Wu et al., 2009). Similarly, *Sos3* heterozygotes also have decreased kernel row pairing in ears and decreased branching/paired spikelets along with an increase in single spikelets in tassels (Blythe and Guthrie, unpublished). Due to the similar phenotypic nature of the three *Sos* mutants, a transcriptomic analysis was performed to determine if either of these mutants also effected plant hormone and development pathways. This study demonstrates the relationship of the *Sos2* mutant with the cytokinin and auxin pathways. In agreement with genetic analysis, these results indicate similarity in

gene expression between *Sos2* and *Sos3* mutants and differences from the transcript profiles of *Sos1.*

RESULTS

Sos2 *mutants have altered cytokinin, ABA, and auxin levels*

To determine hormone levels in *Sos2* mutants compared to normal, immature, green-house grown tassels were dissected, frozen and sent for hormone analysis by LC-MS at University of Nebraska, Lincoln. These measurements found a significant increase ($p<0.001$) in the cytokinin intermediates (chemical structures that will be catalyzed to form active cytokinins) trans- and cis- zeatin riboside in *Sos2/+* mutants compared to normal siblings (Fig. 1E). There was no statistically significant difference in the active form of cytokinin, trans-zeatin, between *Sos2/+* or normal siblings. Cis-zeatin was below the level of detection for both *Sos2/+* and normal tassels.

To further investigate this notable difference on a spatial level, a confocal analysis was performed with *Sos2/+* mutant plants crossed to the cytokinin inducible TCSv2:NLS:tdTomato fluorescent tagged marker for cytokinin maxima (Chen et al. 2014). Segregating families were planted in the greenhouse, grown for three weeks and treated with BASTA, a herbicide that plants with the TCSv2:NLS:tdTomato construct are resistant to. BASTA resistant plants were genotyped, and for those that were positive for RFP, tassels were excised and imaged with confocal microscopy. Control plants, those that were Basta susceptible, were also imaged as a negative control. Plants imaged were also

compared to the published response in B73 which showed a cupped domain of TCS at the base of the SPM (Jasinski et al., 2005).

Sos2/+ typical tassels displayed a slight change in expression domain compared to normal siblings; The cytokinin maxima domain was expanded and more oblong in shape in *Sos2/+* mutants (Fig. 1B, D) compared to the more cup-shaped domain expected in normal siblings (Fig. 1A, D). The *Sos2/+* severe mutants fail to maintain an IM (Fig. 1C, blue arrow), and immature severe tassels imaged were mostly composed of SPM, as defined by the lack of glume (Fig. 1C, yellow arrow), and SM, as defined by the presence of a glume (Fig. 1C, white arrow). In *Sos2/+* severe tassels, there was a clear increase in cytokinin response compared to normal, when comparing SPM of the two under the same confocal settings (Fig. 1C). This experiment supported the hormone assay findings; cytokinin response is increased in *Sos2/+* mutants compared to normal siblings.

The same hormone assay described above also showed a significant ($p<0.05$) decrease in ABA and active IAA, the most common form of auxin in plants, compared to normal siblings (Figure. 2A). While not statistically significant, auxin catabolite, IAA-aspartate trended to be higher in normal tassels compared to *Sos2/+* tassels, but Methyl-IAA and IAA-tryptophan were comparable between mutant and normal plants, and IAA-alanine was not detected in either (Figure 2A). Since auxin levels are seen at sites of AM formation, it is possible that the decreased number of SPM produced from the SM (Chapter 2, Results and Discussion), could account for this decrease in IAA seen in *Sos2* mutants.

To determine whether these changes were visible at the spatial level, *Sos2*/+ plants were crossed to PIN1a-YFP/+; DR5-RFP/+ double transgenic auxin reporter segregating lines (Gallavotti et al., 2008; Wu et al., 2013). Basta resistant plants that were positive for both constructs were dissected and tassel imaged with a fluorescent microscope. Control plants, those that were Basta susceptible, were also imaged to ensure the signal seen in positive lines was due to the transgenic construct and not autofluorescence (Figure 2B). PIN1a-YFP expression in normal siblings (Fig. 2C, top panel) was compared to *Sos2/*+ (Fig 2.C, bottom panel), and showed broad PIN1a-YFP expression in both normal and *Sos2* immature tassels. Signal at the base of SPM appears to be slightly increased compared to that of normal siblings, which correlates with *Sos2* RNA-seq data which found *pin1* transcripts to be differentially up-regulated in *Sos2* plants compared to normal siblings (Chapter 2, Results, Figure 5b). It is important to investigate this pattern further using confocal imaging to gain a better spatial understanding of the differences in ZmPIN1a expression in *Sos2/*+ mutants compared to normal siblings.

Another transgenic auxin marker, DR5-RFP, which is a marker for auxin response, was also imaged in *Sos2*/+ and normal sibling immature tassels. The expression of DR5-RFP also seemed to have increased fluorescence in *Sos2/*+ plants (Figure 2D, lower panel) compared to normal siblings (Figure 2D, upper panel), specifically in the SM/SPMs. This discrepancy between IAA levels measured by LC-MS and what was observed with the DR5-RFP auxin response marker could be due to the time of day in which plants were collected and imaged,

or frozen for hormone analysis, as auxin has been shown to be regulated by the circadian clock in *Arabidopsis* (Covington & Harmer, 2007). Alternatively, as mentioned previously, auxin response may be increased in *Sos2* mutants and the decreased levels when tassels are ground up is due to the decreased number of AM produced in *Sos2.*

The hormones, giberrellic acid (GA), salicylic acid (SA), and jasmonic acid (JA) were also measured in the hormone panel. Of the eleven GA's measured, five were not detected in either mutant or normal tissues, and GA20/GA9, GA intermediaries (Li et al., 2019), had no statistically significant differences between *Sos2*/+ tassels and normal siblings. Four GA intermediaries: GA12, GA19, GA24, and GA53 (Li et al., 2019), all were significantly decreased in *Sos2*/+ mutants compared to normal siblings (data not shown). Both SA and JA were not statistically significantly different between mutant and normal tissues.

Sos2 *and* Sos3 *mutants have more phenotypic variability than* Sos1

There are currently three semi-dominant *Suppressor of sessile spikelets* mutants: *Sos1* (Doebley et al., 1995; Wu et al., 2009), *Sos2* (Chapter 2, Results), and *Sos3* (Blythe and Guthrie, unpublished). The *Sos1* mutation acts in a traditional semi-dominant fashion; heterozygous mutants have an increase in the number of single spikelets due to the suppression of sessile spikelet, as determined by SEM analysis (Johnson, 2017; Wu et al., 2009). Homozygous mutants have a complete suppression of sessile spikelets in both ears and tassels (Johnson, 2017; Wu et al., 2009). There is very little phenotypic variability in these

lines, and the suppression of sessile spikelets in the *Sos1* mutants is the phenotype for which this class of maize mutants is named.

Sos2 mutants also see a decreased in the number of paired spikelets in tassels and ears, and an increased number of single spikelets, resulting in uneven kernel row pairing in the ear, and interspersed paired and single spikelets in the tassel (Chapter 2, Results). In addition, *Sos2* mutants have a wide range of phenotypic variability – tassels can have many short branches or no branches at all, and the main spike can be present or absent. Severe *Sos2* heterozygous ears are ball-shaped or fail to form at all inside developed husk leaves. *Sos2* homozygous mutants are even more severe, in that a majority fail to germinate, and the few that do germinate, die after leaf three emergence as a seedling (Chapter 2, Results).

Sos3 mutants also display a decrease in the number of paired spikelets in the ears and tassels of heterozygous mutants. However, contrasting to the name of the mutant phenotype, the sessile spikelet is not necessarily always suppressed in the tassel – occasionally the pedicellate spikelet is suppressed instead (Fig. 3I), and from here forward the single spikelet phenotype will be described as so, or as a suppression of paired-spikelets. The phenotype becomes much more severe in homozygotes, with the starkest phenotype being the formation of crater-like indentations and barren patches on the main rachis of tassels and ears and the reverse germ orientation of kernels on ears (Fig. 3C). In addition, *Sos3* phenotypes display a wide range of phenotypic variability (Supplemental Fig. 2), similar to the phenotypic variability seen in *Sos2/+* mutants. In addition, the aborted spikelet

phenotype seen in *Sos2/+* tassels was also seen in *Sos3/+* and *Sos3/Sos3* tassels. This phenotypic analysis indicates that that *Sos3* plants are also deficient in meristem initiation or maintenance pathways.

Previously published mapping data of *Sos1* places the mutation on chromosome 4 (Johnson, 2017; Wu et al., 2009), and the *Sos2* mutation on chromosome 10 (Chapter 2, Figure 5). Preliminary mapping data suggest that the *Sos3* mutation may be on chromosome 1 (Blythe honors thesis), however, more recent whole genome sequencing data shows similar genomic signatures in *Sos2* and *Sos3* introgressed into the W22-acr non-reference line (Supplemental Fig. 1). This information, paired with phenotypic similarities, leads to the hypothesis that *Sos2* and *Sos3* might be allelic to each other.

A complementation test was performed between all three *Sos* mutants. As all *Sos* mutants are dominant, complementation is detected by the presence of normal plants in the self of the trans-heterozygote rather than in the F1 as in a recessive mutant. Unfortunately, the F1 trans-heterozygote could not be successfully selfed in the quantity necessary for a true complementation test to occur as *Sos1/+;Sos2/+, Sos2/+;Sos3/+,* and *Sos1/+;Sos3/+* trans-heterozygote reproductive organs were either not present, greatly reduced, or susceptible to mold before harvest.

Increased similarity in Sos2 and Sos3 gene expression compared to Sos1

To test if *Sos1* and *Sos3* were similar to *Sos2* at a transcriptional level, as well as to assess their roles in hormone regulatory pathways, an RNA-seq analysis

was performed on immature, field grown tassels. The *Sos1* phenotype is suppressed in the W22-acr non-reference genetic background, which is recessive for the *anthocyaninless1* (*a*) *colored alurone1* (*c*), and *colored1* (*r*) pigmentation genes resulting in yellow kernels, so this mutation has been introgressed into the B73 genetic background. *Sos2* and *Sos3* mutants are stable in the W22-acr non-reference background and have been fully introgressed. Tassels were pooled based on phenotypes, RNA extracted and sent for sequence analysis. Reads from *Sos* and normal siblings were aligned to the appropriate background: B73 for *Sos1/+* and normal siblings, and W22-ACR (reference) for *Sos2/+* and *Sos3/+* and normal sibling genomes. Differential expression was assessed via EdgeR (Robinson et al., 2009).

Due to the differences in the predicted genes between the B73_v3 and W22-ACR reference genomes, only the genes that had convertible gene IDs could be used to determine relationships based on transcript expression in subsequent statistical analysis in R. Of the total number of 21,183 expressed genes in *Sos2* and 20,533 expressed genes in *Sos3,* only 16,878 and 16,487 genes had B73_v3 gene IDs, respectively (Supplemental Workbook 1). Of the 21,577 genes expressed in *Sos1* aligned to B73_v3, 17,022 genes had W22-ACR gene IDs associated. Since *Sos1* RNAseq analysis only found four down-regulated genes (*Zmpin1a*, *zim4* and uncharacterized genes GRMZM2G131421 and GRMZM2G404375) to be DE with the FDR < 0.05 threshold, and two up-regulated genes (GRMZM2G173989 and GRMZM2G478779 both uncharacterized), the total expressed genes in each mutant were used for the comparisons below.

When the total expressed genes of all three *Sos* mutants were compared to each other using B73 and converted B73 gene IDs, 70.6% (15,808) of these genes were shared between the three mutants (Fig. 4A). These genes include general growth and development genes, as well as those vital to tassel development. 5,440 genes were expressed specific to *Sos1,* 188 genes specific to *Sos2*, and 44 specific to *Sos3* in this study

Based on expressed genes, there was more overlap between *Sos2* and *Sos3* (2.7%, 594 genes) than with *Sos1* and *Sos2* (1.3%, 288 genes) or *Sos1* and *Sos3* (0.2%, 41 genes; Fig. 4A). This could mean that the *Sos2* and *Sos3* mutations affect similar pathways and therefore shared direct and indirect targets represented by the overlapping genes. However, it is also possible that because *Sos2* and *Sos3* share a genetic background that is different than *Sos1* (W22 non-reference versus B73), some of these genes are genetic background specific.

To determine the relationship between the *Sos* mutants based on transcript expression patterns, the logfold change values of all gene expressed in *Sos1, Sos2,* and *Sos3,* including the 71.2% shared genes, were compared using heatmap2 in R. Results showed *Sos2* and *Sos3* transcript expression patterns, based on logfold change of all expressed genes, were overall more similar than that of *Sos1* (Supplemental Figure 3). Since *Sos2* and *Sos3* shared the most genes in common, the DEG of these two mutants determined by EdgeR, FDR < 0.05 were compared. *Sos2* had significantly more DEGs than *Sos3* (2,785 versus 365, respectively). Of those, there was a 145 gene overlap (Fig. 4B).

Sos mutant phytohormone-specific gene expression varied

Since *Sos2* mutants had changes in cytokinin and auxin levels, known genes within these phytohormone pathways were mined, and expression patterns were compared. Genes for cytokinin biosynthesis, degradation, and response were mined, and expression was compared between the three *Sos* mutants (Fig. 4D). As a whole, *Sos2* saw the most DE compared to *Sos1* and *Sos3* (Fig. 4D), in cytokinin response. This agrees with the TCS-tdTomato confocal analysis as this transgenic marker used reflects cytokinin response. Of the genes involved in CK biosynthesis, *ZmLONELY GUY7* (*ZmLOG7*) was significantly down regulated. As *ZmLOG7* is responsible for catalyzing cytokinin precursors into active CK, this result supports the significant increase of CK intermediaries found in the hormone analysis. Further supporting the increased levels of cytokinin seen in *Sos2* mutants from confocal and hormone analysis, two genes involved in CK degradation (*ckx12* and *cko*) were significantly down regulated in *Sos2* mutants as well (Fig. 4D).

Sos2 mutants had decreased levels of auxin and possible altered expression of ZmPIN1a and DR5 (Fig. 2C-D), AUX-IAAs proteins are degraded in response to auxin so that auxin response factors (ARFs) can initiate transcription of downstream auxin responsive genes (Salehin et al., 2015). The AUX-IAAs themselves are targets of ARFs and are induced in the presence of auxin. There are 33 AUX-IAAs in maize with overlapping expression (Ludwig et al., 2013), and of these seven were DE in *Sos2* (Fig 4E). Four AUX-IAAs were significantly up-regulated, and two were significantly down regulated (Fig 4E). While not much is known about these seven AUX/IAAs in maize specifically, they do have specificity to *Sos2* function when compared to *Sos1* and *Sos3.* Together, the transcriptomic

results described for *Sos2* and the results from the hormone and confocal analysis show that auxin is incorrectly regulated in *Sos2* mutants.

Of the subset of auxin genes analyzed (Fig 4E) of genes, only Zm*pin1a* was differentially expressed in *Sos1* and *Sos2* ($p < 0.05$, FDR < 0.05), and locally significant in *Sos3* ($p < 0.05$). Interestingly, *Zmpin1* was up-regulated in *Sos1* mutants and down-regulated in *Sos2* and *Sos3* mutants, indicating that all three *Sos* mutants have disruption of either auxin level or transport, however, it is opposite in *Sos1* mutants compared to *Sos2* and *Sos3*, again highlighting expression differences of genes between *Sos2* and *Sos2/Sos3*.

As the *Sos3/Sos3* phenotype is also reminiscent of auxin mutants such as *bif2, ba1,* and *ba2* (Gallavotti et al., 2004; McSteen & Hake, 2001; McSteen et al., 2007; Yao et al., 2019), due to the barren patches and craters seen in tassels and ears (Figure 1C,F,I; Supplemental Figure 1), an increase in DEG involved in auxin was hypothesized. Of the genes involved in auxin biosynthesis and transport, one was significantly DE (*baf1*) and three were locally significant (*vt2, pin1,* and *bif2*), but all were up-regulated. Since *Sos3/+* tassels were used in this analysis, it can be predicted that all four of these gene would be even more significantly DE in *Sos3/Sos3* mutants.

DISCUSSION

Previous studies indicated that *Sos2* mutants functioned in the CLV-WUS meristem maintenance pathway, partially due to their reproductive phenotypes and similarity to the *Sos1* mutant which is caused by overexpression of *Zmcle7*

(Johnson, 2017). However, recent evidence indicates that *sos2* may act in the REV-STM pathway (Chapter 2, Discussion) to regulate meristem maintenance. This pathway has strong links to cytokinin regulatory pathways within meristems and prompted the exploration of the relationship between *Sos2* mutants and phytohormone pathways.

Results from Chapter 2 indicate the *Sos2* mutation is possibly caused by overexpression of a *LITTLE ZIPPER 4-like* gene, *ZmZPR4-like*, on the short arm of chromosome 10. In *Arabidopsis,* ZPR4 negatively regulates HD-ZIPII activity in the SAM by physically binding to these HD-ZIPIII transcription factors making them non-functional (Kim et al., 2008). HD-ZIPIII proteins are linked to the cytokinin biosynthesis pathway (reviewed in Sessa et al, 2018). A specific example of this in *Arabidopsis* is the positive regulation of ISOPENTYLTRANSFERASE7 (IPT7), the protein responsible for the rate-limiting step of cytokinin biosynthesis, by PHABULOSA (PHB), one of the five HD-ZIPIII proteins in *Arabidopsis*. Therefore, over-expression of *ZPR4* should cause a decrease in *PHB* and cytokinin levels in *Arabidopsis.*

The downstream effects of ZmZPR proteins on the cytokinin pathway are not known in monocots, but it can still be hypothesized that *Sos2* mutants will have altered cytokinin levels when compared to normal as meristem maintenance is affected. Our studies show that precursor forms of active cytokinins, cZR and tZR, were up regulated in *Sos2* tassels, supported by increased expression of TCS-TdTomato marker lines, not down as hypothesized in *Arabidopsis.* Interestingly, *ipt* genes in *Sos2* mutants are not significantly differentially expressed compared

to normal, but *ZmLOG7* was significantly down regulated. The transition of tZR and cZR to the active forms of cytokinin tZ and cZ is catalyzed by *log7* (Tokunaga et al., 2012). The down regulation of *Zmlog7* would be predicted to bottleneck the transition of these CK precursory structures into active cytokinins. Alternatively, *log7* could be decreased due to the increase of tZR and cZR in *Sos2* mutants. These alterations in the cytokinin biosynthesis pathway will need subsequent analysis to better understand how ZPR genes function within this pathway in maize.

To understand the spatial distribution of cytokinin in *Sos2* mutants, the expression of the cytokinin inducible reporter line TCS-tdTomato, reflecting type-B ARR transcriptional response was analyzed by confocal microscopy (Zürcher et al., 2013). The results appeared to show that the CK response in *Sos2* mutants was broader than that of normal siblings – and this response was increased in *Sos2* severe tassels. The increased cytokinin response domain may be due to an increased in biosynthesis of the cytokinin intermediates, although there is no evidence that these are involved in signaling. These data support a connection between the *Sos2* meristem maintenance and cytokinin regulatory pathways.

Since cytokinin and auxin hormone pathways act antagonistically, it is not surprising that the same hormone assay that was used to measure cytokinins found a significant decreased in IAA, the primary active form of auxin in plants. In addition to this, seven AUX/IAA proteins in *Sos2* mutants were differentially expressed, three down regulated (IAA11. IAA26, and IAA25), and four up-regulated (IAA2, IAA23, IAA28 and IAA4) which are responsive to IAA. However,

both the PIN-YFP and DR5-RFP auxin transport and auxin response transgenic lines seemed to show an increase in expression, specifically at the axillary meristem sites (SPM and SM), compared to normal siblings. This could mean that auxin biosynthesis is interrupted, or the feedback within the system is compensating for a decrease in active auxins in *Sos2* mutants. In the case of ZmPIN1a-YFP expression, this result was supported by our RNA-seq analysis, in which *ZmPIN1* was differentially up-regulated. The discrepancy in these results may be resolved by performing a Western analysis on the ZmPIN1a and DR5 constructs in *Sos2* immature tassels, and this assay should be pursued in future studies.

It was hypothesized that *Sos2* and *Sos3* would be more closely related in expression patterns than *Sos1* based on similarities in phenotypic variation and in whole-genome sequencing signatures. As expected, *Sos2* and *Sos3* mutants had more shared expressed genes, and more similar expression levels of these genes compared to *Sos1* mutants. Both *Sos2* and *Sos3* mutants had more differentially expressed genes in the auxin and cytokinin pathways than *Sos1,* indicating they have more similar functions than *Sos1*. This, taken with the similar genetic signatures seen in whole genome sequencing, and phenotypic variability seen in both mutants provides evidence that these two genes function in the same, similar, or overlapping molecular pathways.

This RNA-seq analysis uncovered a few different avenues of study to further understand how the *Sos* mutants effect plant development, specifically in their interactions with phytohormones. While *Sos2* had more genes differentially

expressed related to the cytokinin pathway, *Sos3* had more genes differentially expressed related to the auxin pathway. Surprisingly, *Sos1* mutants did not see any obvious perturbations in any phytohormone pathway. This could be because *Sos1/+* mutants were used in this RNA-seq analysis, as the *Sos1* heterozygous phenotype is more comparable to the *Sos2* and *Sos3* heterozygous phenotypes for comparison across mutants. Having only one mutant *Sos1* allele might not be enough to show differential expression of genes involved in phytohormone signaling and response.

Moving forward, phytohormone assays need to be performed in *Sos1* and *Sos3* to better compare the physiological changes happening at the tissue level in these three *Sos* mutants. In addition, if *Sos1* and *Sos3* mutations are to be analyzed for their individual effects on immature tassel development, I would recommend performing another RNA-seq analysis with *Sos1* and *Sos3* homozygous mutants, with the understanding that analyzing transcriptomics of increasingly severe mutants make comparing RNA-seq results between mutants – with biological relevance – increasingly difficult.

METHODS

Hormone Analysis

Samples were grown in the ECPGF under the following conditions: average day temp 86^{o}F, night temp 65^{o}F, lights on 16 hours between 6 am and 10 pm with average light between 1000 and 1300 PAR. Plants were grown in 4-inch pots and watered with DI water until leaf 4, then repotted into 3 gallon pots at 3 plants per

pot and watered with Jack's fertilizer 20-20-20 daily. The first batch of plants was planted on 12/17/2019 and tassel meristems were excised on 1/7/2020 (29 days), the second batch was planted on 1/15/2020 and tassel meristems were excised on 2/17/2020 (33 days), the third batch was planted on 1/22/2020 and tassel meristems were excised on 2/18/2020 (28 days). Excised immature tassel meristems ranged between 3 mm to 11 mm in size (where the IM had not collapsed) and were flash-frozen in liquid nitrogen and stored at -80 until sample submission. All three batches were pooled to minimize for batch effects, tissue was ground, and samples were sent to the University of Nebraska – Lincoln Proteomics and Metabolomics Facility for hormone extraction and analysis by LC-MS/MS. Samples were normalized based on internal standards D5Iaa, D5tZ, D5tZR, D6ABA, D2JA, D4SA, D2GA1, D2GA12, and GR24 to account for experimental variation and hormone extraction/ionization efficiency.

Fluorescent and confocal analysis

Plants were grown in either the Sears Plant Growth Facility or ECPGF for three to five weeks before tassels were excised for imaging. TCS-tdTomato, PIN-YFP and DR5-RFP stocks were obtained from the Maize Cell Genomics Consortium. The plants containing the construct of interest were crossed and backcrossed to *Sos2* for at least three generations. These lines were treated with BASTA to ensure they contained the construct and genotyped for either the YFP or RFP fluorescent marker using the following primer pairs: YFP (Forward: 5' – GACCACATGAAGCAGCACGAC – 3, Reverse: 5' – GAGCTGCACGCTGCCGTC – 3') and RFP (Forward: 5'- CGA GGA CGT CAT CAA GGA GT -3', Reverse: 5'-

CCC ATG GTC TTC TTC TGC AT -3'). Samples were mounted in water on glass slides and imaged on an Olympus BX61 microscope with bright field, darkfield, and fluorescent optic options. Images were captured on an Olympus XC10 digital camera using a Dell PC with CallSans image capture and analysis software.

Phenotypic analysis

All mature plants were grown from seed to maturity at the University of Missouri Genetics farm (May to August). Phenotypes were previously described for *Sos1* in (Wu et al, 2009 and Johnson 2017), *Sos2* in Chapter 2, Figure 1, and *Sos3* (Blythe and Guthrie, unpublished) following the methods outlined in the respective documents.

Plants used for SEM were grown in either the Sears Greenhouse or in the field during the summer and dissected three to five weeks after sowing. Greenhouse conditions were set to 16-hour day, 8-hour night periods with average daily temperatures set to 87 degrees Fahrenheit and average evening temperatures to 67 degrees Fahrenheit. Tissue was than fixed in FAA, dehydrated, and critical point dried by the University of Missouri Electron Microscopy Core. The meristems were subsequently mounted on stubs and sputter coated using the Emitech K575x Sputter Coater to cover the samples in a 0.01um conductive layer of platinum and imaged on an FEI Quanta 600F Scanning Electron Microscope in the MU SEM Core.

RNA-seq analysis

Transcriptomic analysis of *Sos2* is described in detail in Chapter 2 Methods, and *Sos1* and *Sos3* plants were analyzed with this same method, repeated here. Plants were grown for four weeks in the Missouri 2019 field season at the MU Genetics Farm. Tassels were excised, phenotyped (*Sos1*/+, *Sos2*/+, *Sos3*/+, and respective normal siblings), measured, and flash frozen in liquid nitrogen. Three replicates of six tassels of each phenotypic class were pooled and RNA was extracted using the Qiagen RNA extraction kit. RNA was then sent to Psomogen for library prep and sequencing (paired-end reads, 150bp insertion size, TruSeq Stranded mRNA LT Sample Prep) on the Illumina NovaSeq6000 S4 sequencer. FastQ files were downloaded for subsequent DE analysis. Reads were first trimmed with Trimmomatic-0.36 (Bolger et al., 2014) software and aligned using bwa-0.7.12 (Li & Durbin, 2009): *Sos1*/+ and normal siblings were aligned to B73-reference_v3, *Sos2*/+ and normal siblings as well as and *Sos3*/+ and normal siblings were aligned to the W22-ACR-reference version 1 (Springer et al., 2018). Aligned raw read counts were counted via htseq2 (Anders et al., 2015), and differential expression was performed using EdgeR with standard parameters (Robinson et al., 2009). An FDR correction value of < 0.05 was used to determine significance.

AUTHOR CONTRIBUTIONS

KG designed experiments, collected and analyzed data, wrote results, and advised CN and AB. CN and AB were involved in data collection and analysis. PM oversaw project as the primary investigator.

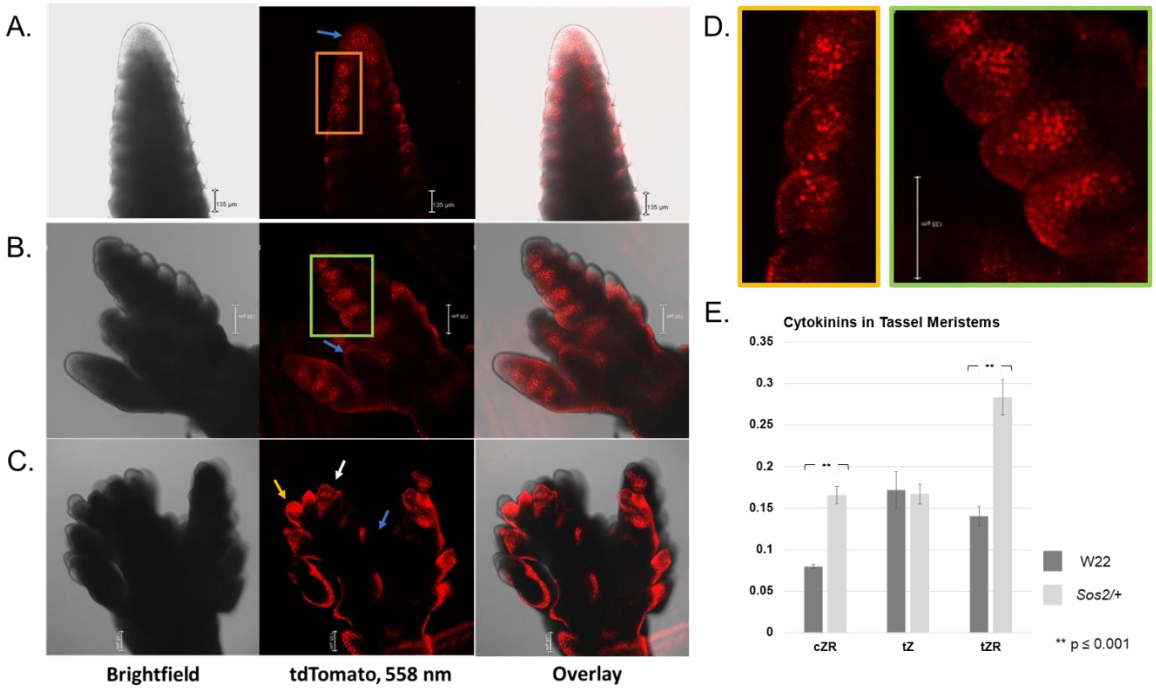

Figure 1: Cytokinin response and hormone levels in immature tassel meristems of *Sos2*/+ and normal siblings. **A.** Cytokinin response of immature normal tassels using nuclear localized, TCS-tdTomato confocal marker, orange box around SMs, **B.** Cytokinin response in *Sos2*/+ typical and **C**. *Sos2*/+ severe immature tassels using nuclear localized TCS-tdTomato confocal marker, green box around SMs, **A-C.** From left to right: Brightfield, TCS-tdTomato (558nm), Overlay. IM denoted with blue arrow, SM marked with orange arrow, undefined meristem marked with white arrow. **C.** Close up of SPMs of normal (left) and SMs of *Sos2*/+ typical (right); The TCS-tdtomato expression pattern is expanded in *Sos2*/+ typical SMs. **D.** Cytokinin measurements via LC-MS in normal sibling vs *Sos2*/+ mutants; trans-Zeatin Riboside (tZR) and cis-Zeatin Riboside (cZR) are cytokinin intermediates, trans-Zeatin (tZ) is an active form of cytokinin; Significance determined by Student's T Test, $p < 0.001$, scale bar = 135 nm in **A, B, C, D.**

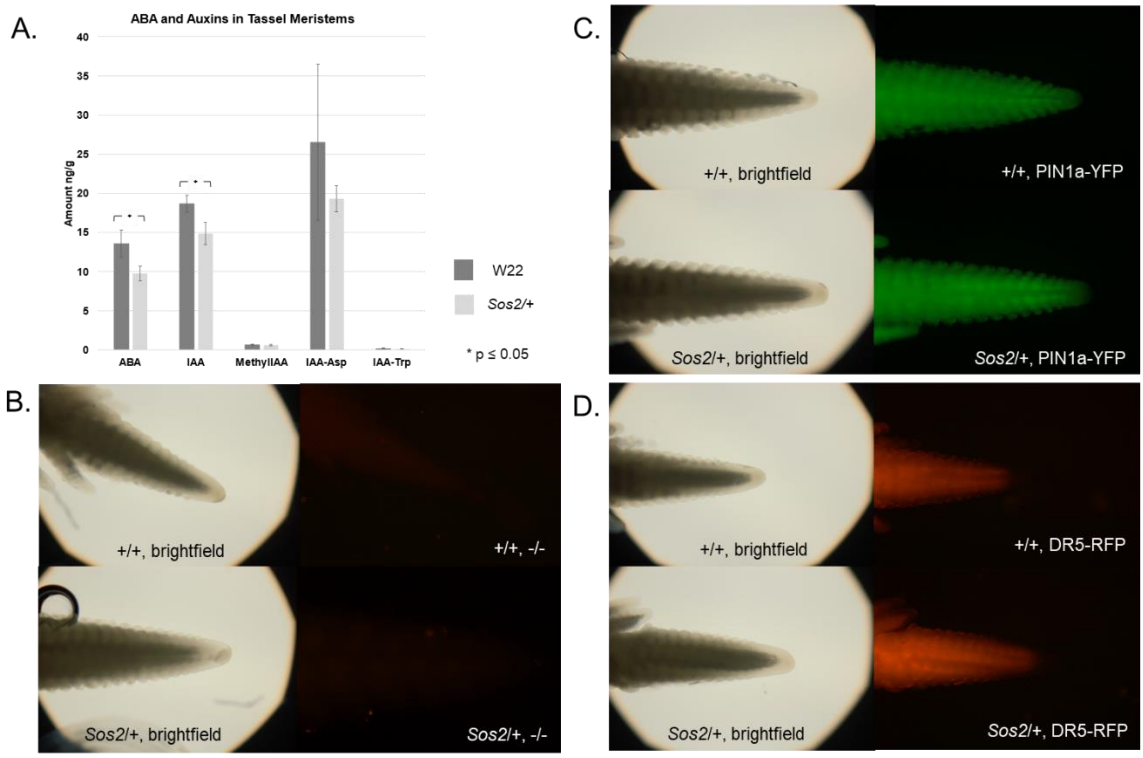

Figure 2: Auxin levels, transport and response in immature tassel meristems of *Sos2/+* and normal siblings. **A.** ABA and Auxin hormone levels measured via LC-MS; IAA is the active and most common form of auxin in plants, Methyl-IAA, IAA-ASP and IAA-Trp are auxin derivatives. Significance determined by Student's T-Test, $p < 0.05$. **B.** Fluorescence of Basta susceptible (non-transgenic) immature tassel as a negative control, **C.** Fluorescence of Basta resistant (transgenic) immature tassel showing ZmPIN1a-YFP expression marking auxin transport, **D.** Fluorescence of Basta resistant (transgenic) immature tassel showing DR5-RFP expression, marking auxin response, **B-D.** Normal siblings (top), *Sos2/+* siblings (bottom); brightfield (left) and PIN-YFP/DR5-RFP fluorescent imaging (right), 4x objective.

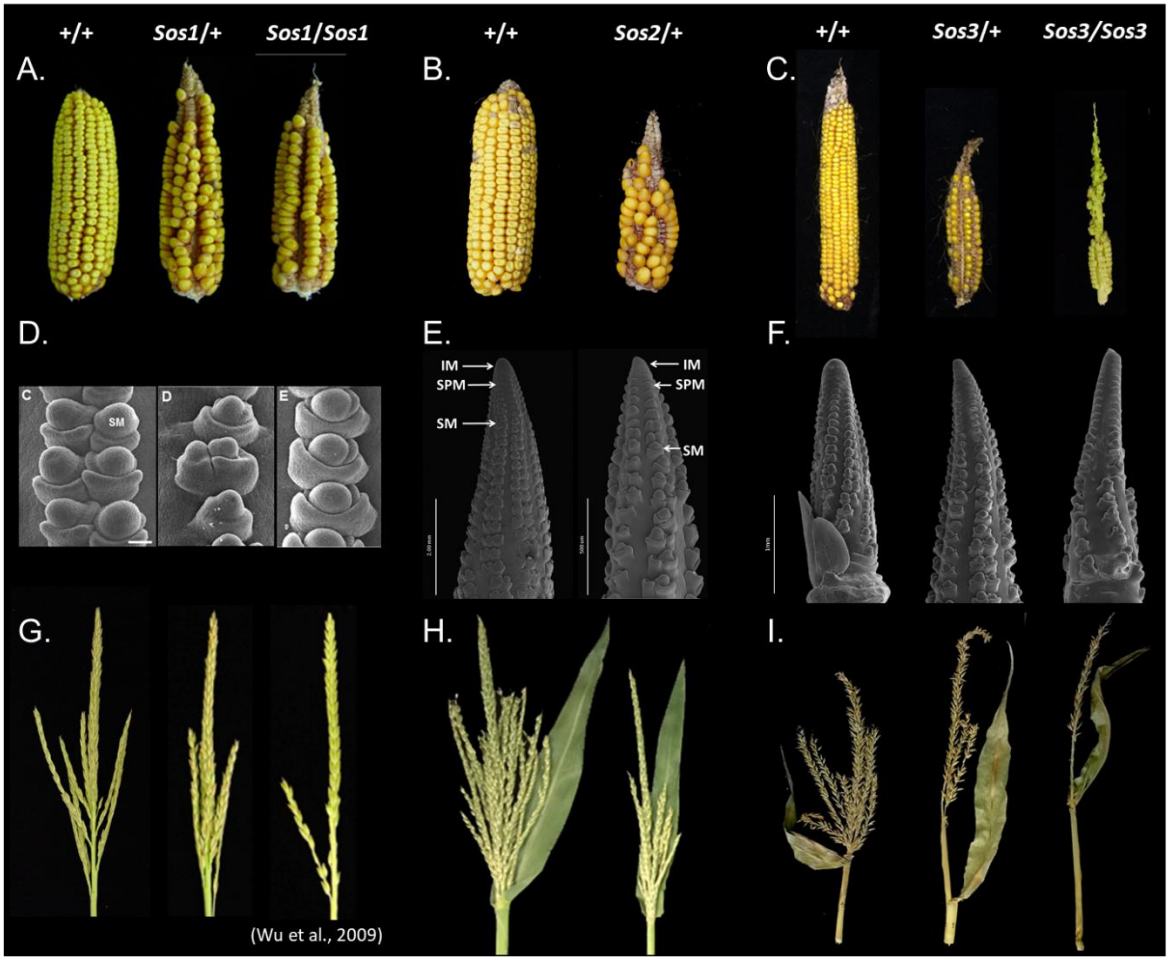

Figure 3: Phenotypic comparison of *Sos1, Sos2*, and *Sos3* mutants. **A-C.** Mature ear phenotypes, **D-F.** SEM images of immature ears, **G-I.** Mature tassel phenotypes. **A.** Normal B73 sib ears compared to *Sos1/+* which have an increase in single spikelet (kernel) production and *Sos1/Sos1* ears are entirely composed of single spikelets (kernels) (Wu et al. 2009). **B.** Normal W22 sib ears compared to *Sos2/+* with show a partial increase in single spikelets along the length of the cob (Chapter 2). *Sos2/Sos2* plants are seedling lethal and not imaged. **C.** Normal W22 sib ears compared to *Sos3/+* show partial to full production of single spikelets along the length of the cob and *Sos3/Sos3* with reverse germ orientation of kernel and barren phenotypes (Blythe and Guthrie, unpublished). **D.** SEM of the SPMs of

normal siblings compared to *Sos1/+* and *Sos1/Sos1* mutants showing formation of single or paired SM (Wu et al. 2009). **E.** Immature ear SEM of normal siblings compared to *Sos2/+* mutants showing formation of single or paired SM (Chapter 2). **F.** Immature ear SEM of normal siblings compared to *Sos3/+* and *Sos3/Sos3* mutants showing formation of single or paired SM (Blythe and Guthrie, unpublished). **G.** Normal sib tassels compared to *Sos1/+* tassels with decreased branching and suppression of sessile spikelets on the main rachis (Wu et al. 2009). **H.** Normal sib tassels compared to *Sos2/+* tassels, which show decreased branching and branch length, decreased production of paired spikelets and increase in single spikelets, and production of aborted spikelets (Chapter 2). **I.** Normal sib tassels compared to *Sos3/+* tassels which also have decreased branching and decreased production of paired spikelets and increase in single spikelets, and *Sos3/Sos3* tassels which show no branching, and are mostly composed of single spikelets and barren patches along the main rachis (Blythe and Guthrie, unpublished).

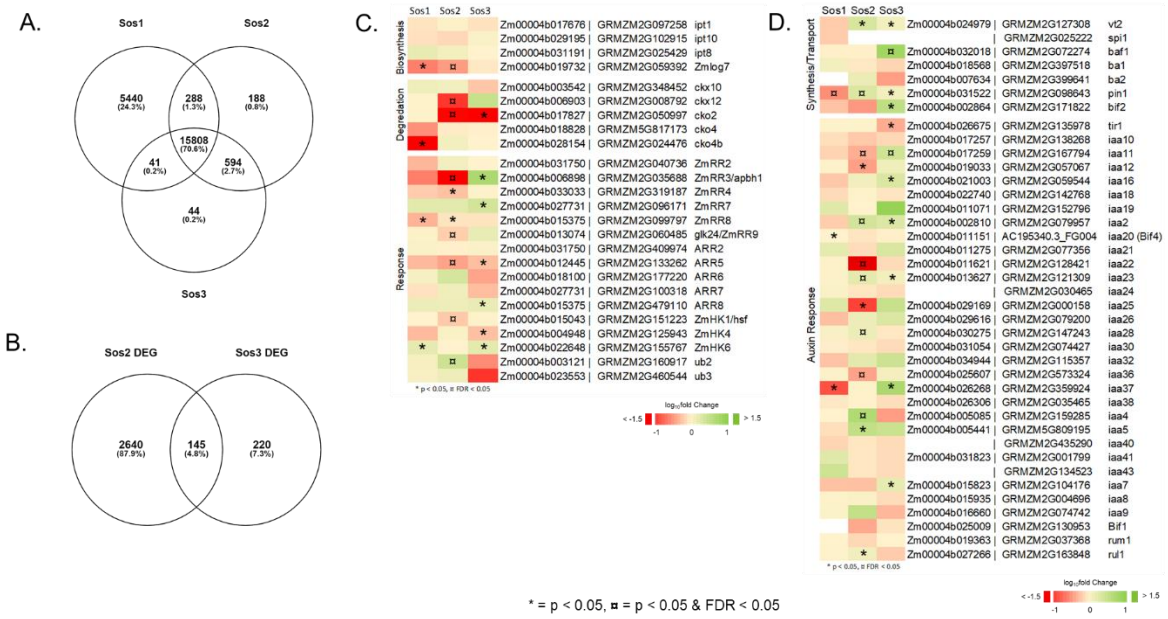

Figure 4: RNA-seq comparison of *Sos* mutants. **A.** Overlap of total expressed genes in *Sos1, Sos2,* and *Sos3* immature tassels. **B.** Overlap between the significantly differentially expressed genes in *Sos2* and *Sos3*. **C.** Expression of select cytokinin related genes in *Sos1, Sos2* and *Sos3* separated into biosynthesis, degradation, and response genes. **D.** Expression of known auxin related genes in *Sos1, Sos2,* and *Sos3*. **C-D.** Differentially expressed genes are denoted by ¤ (FDR 0.05), locally significant genes denoted by * (p 0.05).

Supplemental Figure 1: *Sos3* whole genome sequencing analysis compared to *Sos2* in W22-acr (non reference), aligned to W22-ACR reference genome. Graphs are made on a 100bp sliding window, y-axis = SNP allele frequency, x-axis = physical position on chromosome. Boxes denote overlapping genetic signatures (regions of SNPs in the *Sos2* and *Sos3* genomes that are 100% not like W22-reference).

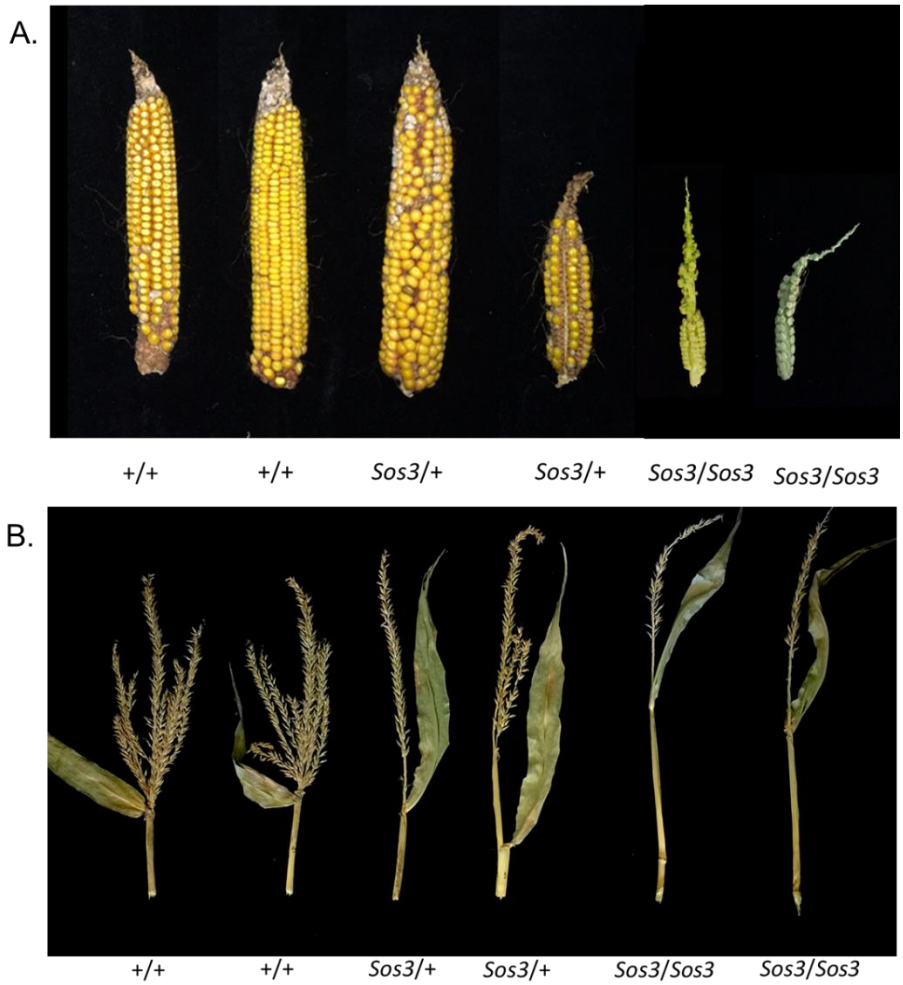

Supplemental Figure 2: Variation in the *Sos3* reproductive phenotypes. **A.** *Sos3* mutant ear phenotypes compared to normal. **B.** *Sos3* mutant tassel phenotypes compared to normal (Blythe and Guthrie, unpublished)

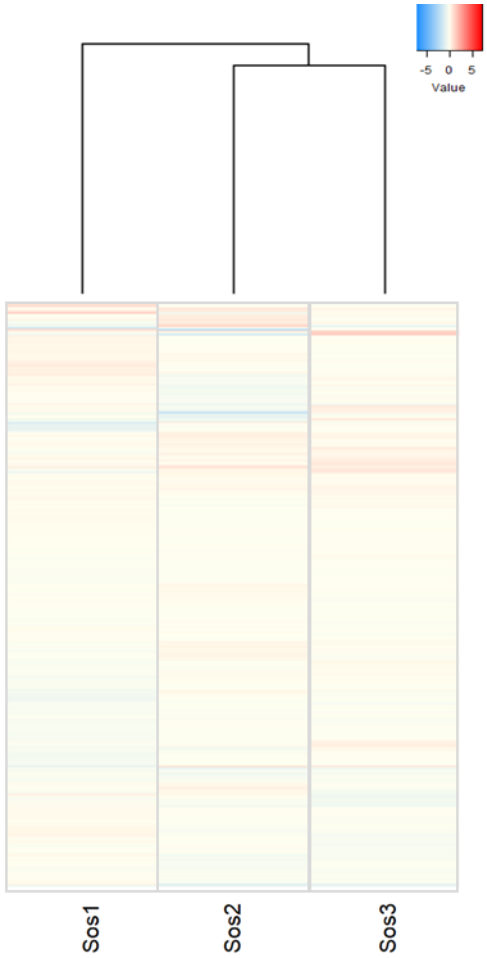

Supplemental Figure 3: Heatmap and dendrogram of the total expressed genes *Sos1, Sos2,* and *Sos3* immature tassels to depict relationships between all three mutants.

WORKS CITED

Anders, S., Pyl, P. T., & Huber, W. (2015). HTSeq-A Python framework to work with high-throughput sequencing data. *Bioinformatics*, *31*(2), 166–169. https://doi.org/10.1093/bioinformatics/btu638

Bolduc, N., & Hake, S. (2009). The maize transcription factor KNOTTED1 directly regulates the gibberellin catabolism gene ga2ox1. *Plant Cell*, *21*(6), 1647–1658. https://doi.org/10.1105/tpc.109.068221

Bolduc, N., Yilmaz, A., Mejia-Guerra, M. K., Morohashi, K., O'Connor, D., Grotewold, E., & Hake, S. (2012). Unraveling the KNOTTED1 regulatory network in maize meristems. *Genes and Development*, *26*(15), 1685–1690. https://doi.org/10.1101/gad.193433.112

Bolger, A. M., Lohse, M., & Usadel, B. (2014). Trimmomatic: A flexible trimmer for Illumina sequence data. *Bioinformatics*, *30*(15), 2114–2120. https://doi.org/10.1093/bioinformatics/btu170

Coenen, C., & Lomax, T. L. (1997). Auxin-cytokinin interactions in higher plants: Old problems and new tools. In *Trends in Plant Science* (Vol. 2, Issue 9, pp. 351–356). Elsevier Ltd. https://doi.org/10.1016/S1360-1385(97)84623-7

Covington, M. F., & Harmer, S. L. (2007). The circadian clock regulates auxin signaling and responses in Arabidopsis. *PLoS Biology*, *5*(8), 1773–1784. https://doi.org/10.1371/journal.pbio.0050222

D'Agostino, I. B., Deruère, J., & Kieber, J. J. (2000). Characterization of the response of the Arabidopsis response regulator gene family to cytokinin. *Plant Physiology*, *124*(4), 1706–1717. https://doi.org/10.1104/pp.124.4.1706

Doebley, J., Stec, A., & Kent, B. (1995). Suppressor of Sessile spikelets 1 (Sos1): A Dominant Mutant Affecting Inflorescence Development in Maize. *American Journal of Botany*, *82*(5), 571. https://doi.org/10.2307/2445415

Gallavotti, A., Yang, Y., Schmidt, R. J., & Jackson, D. (2008). The relationship between auxin transport and maize branching. *Plant Physiology*, *147*(4), 1913–1923. https://doi.org/10.1104/pp.108.121541

Gallavotti, A., Zhao, Q., Kyozuka, J., Meeley, R. B., Ritter, M. K., Doebley, J. F., Pè, M. E., & Schmidt, R. J. (2004). The role of barren stalk1 in the architecture of maize. *Nature*, *432*(7017), 630–635. https://doi.org/10.1038/nature03148

Giullni, A., Wang, J., & Jackson, D. (2004). Control of phyllotaxy by the cytokinin-inducible response regulator homologue ABPHYL1. *Nature*, *430*(7003), 1031–1034. https://doi.org/10.1038/nature02778

Gordon, S. P., Chickarmane, V. S., Ohno, C., & Meyerowitz, E. M. (2009). Multiple feedback loops through cytokinin signaling control stem cell number within the Arabidopsis shoot meristem. *Proceedings of the National Academy of Sciences of the United States of America*, *106*(38), 16529–16534. https://doi.org/10.1073/pnas.0908122106

Jasinski, S., Piazza, P., Craft, J., Hay, A., Woolley, L., Rieu, I., Phillips, A., Hedden, P., & Tsiantis, M. (2005). KNOX action in Arabidopsis is mediated by coordinate regulation of cytokinin and gibberellin activities. *Current Biology*, *15*(17), 1560–1565. https://doi.org/10.1016/j.cub.2005.07.023

Johnson, E. (2017). *Evolution and development of the paired spikelet trait in maize and other grasses (Poaceae)*.

Kerstetter, R. A., Laudencia-Chingcuanco, O., Smith, L. G., & Hake, S. (1997). Loss-of-function mutations in the maize homeobox gene, knotted1, are defective in shoot meristem maintenance. *Development*, *124*(16), 3045–3054. https://doi.org/10.1242/dev.124.16.3045

Kim, Y. S., Kim, S. G., Lee, M., Lee, I., Park, H. Y., Pil, J. S., Jung, J. H., Kwon, E. J., Se, W. S., Paek, K. H., & Park, C. M. (2008). HD-ZIP III activity is modulated by competitive inhibitors via a feedback loop in Arabidopsis shoot apical meristem development. *Plant Cell*, *20*(4), 920–933. https://doi.org/10.1105/tpc.107.057448

Lee, B. H., Johnston, R., Yang, Y., Gallavotti, A., Kojima, M., Travençolo, B. A. N., Costa, L. D. F., Sakakibara, H., & Jackson, D. (2009). Studies of aberrant phyllotaxy1 mutants of maize indicate complex interactions between auxin and cytokinin signaling in the shoot apical meristem 1. *Plant Physiology*, *150*(1), 205–216. https://doi.org/10.1104/pp.109.137034

Li, C., Zheng, L., Wang, X., Hu, Z., Zheng, Y., Chen, Q., Hao, X., Xiao, X., Wang, X., Wang, G., & Zhang, Y. (2019). Comprehensive expression analysis of Arabidopsis GA2-oxidase genes and their functional insights. *Plant Science*, *285*, 1–13. https://doi.org/10.1016/j.plantsci.2019.04.023

Li, H., & Durbin, R. (2009). Fast and accurate short read alignment with Burrows-Wheeler transform. *Bioinformatics*, *25*(14), 1754–1760. https://doi.org/10.1093/bioinformatics/btp324

Ludwig, Y., Zhang, Y., & Hochholdinger, F. (2013). The maize (Zea mays L.) AUXIN/INDOLE-3-ACETIC ACID gene family: Phylogeny, synteny, and unique root-type and tissue-specific expression patterns during development. *PLoS ONE*, *8*(11), 78859. https://doi.org/10.1371/journal.pone.0078859

McSteen, P., & Hake, S. (2001). Barren inflorescence2 regulates axillary meristem development in the maize inflorescence. *Development*, *128*(15), 2881–2891. https://doi.org/10.1242/dev.128.15.2881

McSteen, Paula, Malcomber, S., Skirpan, A., Lunde, C., Wu, X., Kellogg, E., & Hake, S. (2007). barren inflorescence2 encodes a co-ortholog of the Pinoid serine/threonine kinase and is required for organogenesis during inflorescence and vegetative development in maize. *Plant Physiology*, *144*(2), 1000–1011. https://doi.org/10.1104/pp.107.098558

Robinson, M. D., McCarthy, D. J., & Smyth, G. K. (2009). edgeR: A Bioconductor package for differential expression analysis of digital gene expression data. *Bioinformatics*, *26*(1), 139–140. https://doi.org/10.1093/bioinformatics/btp616

Salehin, M., Bagchi, R., & Estelle, M. (2015). ScfTIR1/AFB-based auxin perception: Mechanism and role in plant growth and development. *Plant Cell*, *27*(1), 9–19. https://doi.org/10.1105/tpc.114.133744

Shimizu-Sato, S., Tanaka, M., & Mori, H. (2009). Auxin-cytokinin interactions in the control of shoot branching. In *Plant Molecular Biology* (Vol. 69, Issue 4, pp. 429–435). Springer. https://doi.org/10.1007/s11103-008-9416-3

Skirpan, A., Wu, X., & McSteen, P. (2008). Genetic and physical interaction suggest that BARREN STALK1 is a target of BARREN INFLORESCENCE2 in maize inflorescence development. *Plant Journal*, *55*(5), 787–797. https://doi.org/10.1111/j.1365-313X.2008.03546.x

Skylar, A., & Wu, X. (2011). Regulation of Meristem Size by Cytokinin Signaling. In *Journal of Integrative Plant Biology* (Vol. 53, Issue 6, pp. 446–454). John Wiley & Sons, Ltd. https://doi.org/10.1111/j.1744-7909.2011.01045.x

Springer, N. M., Anderson, S. N., Andorf, C. M., Ahern, K. R., Bai, F., Barad, O., Barbazuk, W. B., Bass, H. W., Baruch, K., Ben-Zvi, G., Buckler, E. S., Bukowski, R., Campbell, M. S., Cannon, E. K. S., Chomet, P., Kelly Dawe, R., Davenport, R., Dooner, H. K., Du, L. H., … Brutnell, T. P. (2018). The maize w22 genome provides a foundation for functional genomics and transposon biology. *Nature Genetics*, *50*(9), 1282–1288. https://doi.org/10.1038/s41588-018-0158-0

Steeves, Taylor A; Sussex, I. M. (1989). *Patterns in Plant Development*.

Su, Y. H., Liu, Y. B., & Zhang, X. S. (2011). Auxin-cytokinin interaction regulates meristem development. In *Molecular Plant* (Vol. 4, Issue 4, pp. 616–625). Oxford University Press. https://doi.org/10.1093/mp/ssr007

Sun, J., Niu, Q. W., Tarkowski, P., Zheng, B., Tarkowska, D., Sandberg, G., Chua, N. H., & Zuo, J. (2003). The Arabidopsis AtIPT8/PGA22 gene encodes an isopentenyl transferase that is involved in de novo cytokinin

biosynthesis. *Plant Physiology*, *131*(1), 167–176. https://doi.org/10.1104/pp.011494

Takei, K., Sakakibara, H., & Sugiyama, T. (2001). Identification of Genes Encoding Adenylate Isopentenyltransferase, a Cytokinin Biosynthesis Enzyme, in Arabidopsis thaliana. *Journal of Biological Chemistry*, *276*(28), 26405–26410. https://doi.org/10.1074/jbc.M102130200

To, J. P. C., Haberer, G., Ferreira, F. J., Deruère, J., Mason, M. G., Schaller, G. E., Alonso, J. M., Ecker, J. R., & Kieber, J. J. (2004). Type-A Arabidopsis response regulators are partially redundant negative regulators of cytokinin signaling. *Plant Cell*, *16*(3), 658–671. https://doi.org/10.1105/tpc.018978

Tokunaga, H., Kojima, M., Kuroha, T., Ishida, T., Sugimoto, K., Kiba, T., & Sakakibara, H. (2012). Arabidopsis lonely guy (LOG) multiple mutants reveal a central role of the LOG-dependent pathway in cytokinin activation. *Plant Journal*, *69*(2), 355–365. https://doi.org/10.1111/j.1365-313X.2011.04795.x

Wu, Q., Luo, A., Zadrozny, T., Sylvester, A., & Jackson, D. (2013). Fluorescent protein marker lines in maize: Generation and applications. *International Journal of Developmental Biology*, *57*(6–8), 535–543. https://doi.org/10.1387/ijdb.130240qw

Wu, X., Skirpan, A., & McSteen, P. (2009). Suppressor of sessile spikelets1 functions in the ramosa pathway controlling meristem determinacy in maize. *Plant Physiology*, *149*(1), 205–219. https://doi.org/10.1104/pp.108.125005

Xie, M., Chen, H., Huang, L., O'Neil, R. C., Shokhirev, M. N., & Ecker, J. R. (2018). A B-ARR-mediated cytokinin transcriptional network directs hormone cross-regulation and shoot development. *Nature Communications*, *9*(1), 1–13. https://doi.org/10.1038/s41467-018-03921-6

Yao, H., Skirpan, A., Wardell, B., Matthes, M. S., Best, N. B., McCubbin, T., Durbak, A., Smith, T., Malcomber, S., & McSteen, P. (2019). The barren stalk2 Gene Is Required for Axillary Meristem Development in Maize. *Molecular Plant*, *12*(3), 374–389. https://doi.org/10.1016/j.molp.2018.12.024

Zürcher, E., Tavor-Deslex, D., Lituiev, D., Enkerli, K., Tarr, P. T., & Müller, B. (2013). A robust and sensitive synthetic sensor to monitor the transcriptional output of the cytokinin signaling network in planta. *Plant Physiology*, *161*(3), 1066–1075. https://doi.org/10.1104/pp.112.211763

CHAPTER 4:

Transcriptome analysis reveals distinct roles of *barren inflorescence2, barren stalk1,* and *barren stalk2* in regulation of axillary meristem development

Katy Guthrie, Sidharth Sen, Norman Best, Michaela S. Matthes, Janlo M. Robil, Trupti Joshi, Paula McSteen

ABSTRACT

Axillary meristems (AMs) produce shoots or flowers enabling lateral outgrowth in plants. The maize mutants *barren inflorescence2* (*bif2*), *barren stalk1* (*ba1*), and *barren stalk2* (*ba2*) fail to initiate AMs and hence can be used to identify AM specific genes. This study utilized transcriptome analysis of two stages of inflorescence development, 1 mm tip and base of young developing tassels, where AMs on the periphery of the inflorescence meristem are initiating and maturing respectively. A total of 304 differentially expressed genes (DEG) were identified in *ba1, bif2,* and *ba2* mutants compared to normal but only 34 genes showed overlap between the mutants in the tip and 89 genes overlapped in the base. Weighted Gene Co-Expression Analysis (WGCNA) produced seven co-expression modules in the base and five in the tip, all predominantly consisting of genes up or down regulated in a specific mutant, further indicating that *ba1*, *bif2*, and *ba2* play predominantly unique roles in AM development. Overall, this study shows that the regulatory roles of *ba1, bif2,* and *ba2,* are predominantly unique and are more extensive than previously studied auxin-response related responses.

INTRODUCTION

Overall plant development is directed from groups of stem cells called meristems. Meristems enable the continued production of organs throughout the lifetime of the plant. In grasses, the wide variety of reproductive inflorescence phenotypes are due to the production of different types of axillary meristems (AMs) from the inflorescence meristem (IM) (Kyozuka, 2014). In maize, there are two types of AM formed from an IM; branch meristems (BMs), which give rise to the long branches at the base of the inflorescence; and spikelet pair meristems (SPMs) that give rise to short branches called spikelets which are the unit of grass inflorescence architecture (Pautler et al., 2013). The SPM then produce two spikelet meristems (SMs) which produce two floral meristems (FMs) that produce the floral organs. Regulation of sexual organ development then gives rise to separate male flowers in the apical tassel and female flowers in the axillary ear inflorescences (Irish, 1996).

Two domains, the boundary domain (BD) and suppressed bract domain, have been identified by gene expression patterns, and are essential for AM initiation. The upper/adaxial BD separates the AM from the apical meristem and the lower/abaxial leaf domain (called a bract in the inflorescence) which is suppressed in many species and referred to as the suppressed bract (SB) (Long & Barton, 2000; Žádníková & Simon, 2014). The plant growth hormone auxin primarily plays a role during reproductive development to regulate AM initiation while outgrowth is regulated by many additional hormones and the environment (McSteen, 2009; Wang et al., 2014).

Transport of auxin, along with local auxin biosynthesis, to areas on the periphery of the IM has been shown to be required for AM initiation during the formation of flower primordia (Reinhardt et al., 2003; Yamaguchi et al., 2013). Maize mutants that fail to synthesize, transport, or signal auxin fail to produce BM and SPM from the flanks of the IM (Barazesh et al., 2009; Barazesh & McSteen, 2008; Gallavotti et al., 2008; Gallavotti et al., 2008; Galli et al., 2015; Matthes et al., 2019; McSteen & Hake, 2001; Phillips et al., 2011; Wu & McSteen, 2007). Mutants that can correctly perceive auxin will produce SBs but fail to initiate AMs in the axils of SBs (Gallavotti et al., 2004; Ritter et al., 2002; Yao et al., 2019).

A mutant in this latter class, *barren stalk1 (ba1),* gives rise to mature tassels that are predominately barren, except for enlarged SBs, with no branches or spikelets formed along the periphery, and plants completely fail to produce ears (Fig. 1) (Gallavotti et al., 2004; Ritter et al., 2002). The *ba1* gene encodes a basic Helix-Loop-Helix (bHLH) transcription factor (Gallavotti et al., 2004), and the expression of *ba1* transcripts is one of the first to be seen in the BD required for AM initiation (Galli et al., 2015; Woods et al., 2011). Auxin Response Factors (ARFs) directly regulate the expression of *ba1* (Fig. 1) indicating that *ba1* acts downstream of auxin signaling (Barazesh & McSteen, 2008; Gallavotti et al., 2008; Galli et al., 2015; Wu & McSteen, 2007).

Similar to *ba1*, *barrenstalk2* (*ba2*) mutants produce SBs but not AMs (Yao et al., 2019). Mature tassels produce fewer branches and spikelets particularly at the base of the main rachis resulting in a barren area with regular SB protrusions (Fig. 1) (Yao et al., 2019). The gene responsible for the *ba2* phenotype is

orthologous to LAX PANICLE2 (LAX2) in rice, which encodes a nuclear protein that physically interacts with the rice BA1 ortholog LAX1 (Tabuchi et al., 2011; Yao et al., 2019). Biochemical and genetic analyses indicate that *ba2* physically and genetically interacts with *ba1* in maize and has overlapping functions in the same pathway (Skirpan et al., 2008; Yao et al., 2019). The *ba2* transcripts accumulate on the periphery of the IM preceding AM outgrowth, but once AMs initiate, transcripts are detected in the AM and developing floral organs (Fig. 1) (Yao et al., 2019). While *ba1* transcripts are restricted to the BD throughout development (Gallavotti et al., 2004), research in rice indicates that LAX1 protein is detected in the AM after initiation (Kyozuka et al., 2002; Oikawa & Kyozuka, 2009).

Mutants of *barren inflorescence2 (bif2)* also make very few branches and spikelets causing the majority of the main rachis to be barren, but unlike *ba1* and *ba2* mutants, regular protrusions are not seen because *bif2* regulates auxin transport (Fig. 1) (McSteen et al., 2007; McSteen & Hake, 2001; Wu & McSteen, 2007). The *bif2* gene encodes a Serine/Threonine kinase orthologous to *Arabidopsis* PINOID (PID), and functions in phosphorylation of the maize PINFORMED1 (PIN1) ortholog, ZmPIN1a (McSteen et al., 2007; Skirpan et al., 2009). In addition, BIF2 is detected in the nucleus and phosphorylates BA1 *in vitro* (Fig. 1) (Skirpan et al., 2008). Transcripts of *bif2* accumulate in all AMs, organ primordia, and vasculature during inflorescence development (McSteen et al., 2007) indicating that *bif2* plays wider roles than AM establishment. Evidence for this is also provided by genetic interactions which show that *bif2* plays unique and overlapping roles with *ba1* and *ba2* (McSteen et al., 2007; Yao et al., 2019).

Previous transcriptome studies have identified many of the genes expressed in immature tassel and ear primordia (Bolduc et al., 2012; Eveland et al., 2014; Walley et al., 2016). These studies have been instrumental in understanding the overall changes in gene regulation at different stages in tassel and ear growth, but more research is needed to determine the early transcriptional response in the maize inflorescence, specifically the subset of genes that are needed for the development of AM, and respective BD and SB domains. The goal of this study was to identify components of the AM development pathway by determining transcript abundance changes when known steps of AM development were perturbed utilizing transcriptome analysis of early and late stages of development of *bif2, ba1*, and *ba2* inflorescences compared to normal. The tissue at the tip of the tassel meristem represents a younger developmental stage than that of the base and allows the study of changes in gene regulation over developmental time. Tip tissue contains the IM and establishing BD, SB, and SPM, while base tissue contains already established BD and SB and maturing/elongating SPM (in the process of producing SM); comparing both stages can identify genes involved in AM initiation versus maturation. Through this process, we discovered that DEGs in *ba1*, *bif2,* and *ba2* mutants were much more specific to the individual mutant than shared among all three mutants, indicating that these three genes act primarily independently in AM development.

RESULTS

DEG in *ba1, bif2, and ba2 are largely unique to individual mutants*

To identify genes expressed in AMs, we dissected the tip and base of immature 3-4.5mm tassel primordia of *ba1, bif2,* and *ba2* mutants compared to B73 grown in the field*.* After RNA extraction and library prep, reads from all three replicates for *ba1*, *ba2,* and *bif2* had an average of 94% mapping rate to the v4 B73 reference genome. A dendrogram and principal component analysis (PCA) grouped the samples by replicate instead of by genotype (Supplemental Fig. 1). This is likely reflective of the variations in the environment of the field-grown materials and therefore batch effect was included in subsequent EdgeR analysis.

A differential gene expression analysis of the samples was conducted with EdgeR (Robinson et al., 2009) using generalized linear model (GLM) as described in the methods section, to identify a total of 420 unique DEGs in the tip between all three mutants, and 752 unique DEGs in the base compared with B73 (Fig. 2a). In *ba1*, a total of 231 genes were up-regulated and 316 genes down-regulated between the tip and base; with 42 of the up-regulated genes and 52 down-regulated genes overlapping in both (Fig. 2a, 2b). The *ba2* mutant had a total of 206 genes up-regulated and 291 genes down-regulated in the tip and the base; with 58 up-regulated genes and 55 down-regulated genes overlapping in both (Fig. 2a, 2b). *bif2* had 155 DEGs up-regulated and 105 down-regulated in the tip and the base; with 56 up-regulated genes and 22 down-regulated genes shared between the tip and the base (Fig. 2a, 2b). These findings indicate that there is a large subset of DEGs that overlap between *ba1, bif2,* and *ba2* tip and base tissue, which are likely involved in general tassel development, while genes more directly related to AM, SBs and BD establishment would be DE only at the tip (Fig. 2).

As all three mutants are characterized by the absence of axillary meristems (McSteen & Hake, 2001; Ritter et al., 2002; Yao et al., 2019), we tested if any DEGs were shared in tip samples. Surprisingly, there was only one shared up-regulated gene, and no shared down-regulated genes (Fig. 2c). The one shared gene was Zm00001d044815, a gene with 46% sequence similarity to *Arabidopsis* gene, *AtBOBBER1* (*AtBOB1*), a heat shock protein (HSP) shown to be essential to all stages of development, including inflorescence development (Jurkuta et al., 2009; Kaplinsky, 2009; Perez et al., 2009). Unlike most HSP, *bob1* transcripts are expressed throughout development, even under normal temperatures, although transcripts are elevated under high-heat conditions. *bob1* mutants fail to establish auxin gradients throughout development, impairing axillary meristem production, and at reproductive maturity, *bob1* mutant inflorescences are pin-like with few to no floral axillary meristems on the periphery (Kaplinsky, 2009; Perez et al., 2009). This provides evidence of crosstalk between auxin signaling and thermo-regulatory pathways and indicates an essential role of *BOB1* in the establishment of axillary maxima. Increased expression of Zm00001d044815 in *ba1, bif2,* and *ba2* may be compensatory in nature, and support an essential function of this HSP in the overall auxin regulatory pathway required for axillary meristem development.

Additionally, HSP studies in *Arabidopsis* have highlighted the roles of HSP as co-chaperones in the auxin pathway. Specifically, HSP90 has been shown to interact with the TIR/AFB complex, stabilizing the complex during high temperatures, allowing auxin signaling to continue as temperatures fluctuate (Donato & Geisler, 2019; Wang et al., 2016). Another study found that HSP90

functions to localize TIR1 in the nucleus and can buffer against auxin-related phenotypes when mutations occur in the TIR1 receptor (Donato & Geisler, 2019; Watanabe et al., 2017). A conserved co-chaperone of HSP90, with structural similarity to AtBOB1, p23, has been found to be involved in the localization of auxin transporter PIN1 and subsequent cell division in root meristems (D'Alessandro et al., 2015; Kaplinsky, 2009). Altered auxin distribution in p23 mutants, and increased auxin signaling phenotypes when HSP90 binding is perturbed highlight the growing importance of HSP on maintaining the auxin signaling pathway in meristems. While these studies focus on *Arabidopsis* root development, a recent study suggest these patterns may be conserved in maize IM development as well. The *needle1* mutant displays severe IM defect reminiscent of auxin regulatory mutants *Bif1/Bif4* in a temperature-dependent manner: at high temperatures, a strong *ndl1* phenotype was observed, which includes barren inflorescences, and at mild temperature, no phenotype was seen (Liu et al., 2019). Genetic analysis with known players in the auxin signaling pathway indicate synergistic interactions, and further analysis found a decrease in auxin levels in *ndl1* mutants, indicating crosstalk between *ZmNDL1* and the auxin regulatory pathway (Liu et al., 2019). This study, supported by the roles of HSP in *Arabidopsis* root development, and an increased expression of *AtBOB1-like* HSP, Zm00001d044815 in *ba1, bif2,* and *ba2,* provide a basis for future analysis of the role of HSP in axillary meristem development.

As physical and genetic interactions were previously identified between *ba1* and *ba2* and between *ba1*and *bif2* (Skirpan et al., 2008, 2009), we also tested

whether there were any DEGs that were shared between two of the three mutants. Between *ba1* and *ba2*, 14 DEGs were shared in the tip and 51 DEGs in the base; *ba1* and *bif2* shared 11 DEGs in the tip and 16 DEGs in the base; and *ba2* and *bif2* mutants shared seven DEGs in the tip and 11 DEGs in the base (Fig. 2b). Interestingly, many of shared DEGs were involved in responses to environment. For example, between *ba1* and *ba2,* three DEGs that were upregulated were shared, two of which (Zm00001d016070 and Zm00001d045678) were annotated as BCL-2 ASSOCIATED ATHANOGENE (BAG) proteins, a family of stress response proteins that are expressed in response to temperature change, and have been show to bind heat-shock proteins (Wang, 2018). In *ba2* and *bif2*, the *Zmcalnexin homolog1* (*Zmclx1* - Zm00001d003857), a gene involved in monitoring correct protein folding during stress (Crofts & Denecke, 1998; del Bem, 2011; Kwiatkowski et al., 1995), which is phosphorylated in normal tassels (Walley et al., 2016), was shared. This, in combination with Zm00001d044815, described above, indicates an increased sensitivity to temperature changes in *ba1, bif2,* and *ba1* mutants.

Several transcription factors and processes related to cell cycle were DE in two out of three mutants. Two genes that were downregulated in *ba1* and *ba2* tips included *histone H3.2* and *histone acetyl transferase* (Zm00001d003725). In *ba2* and *bif2*, a gene with 64% sequence similarity to cell cycle regulator, CELL DIVISION CYCLE 48 (*At*CDC48; Zm00001d032117), was upregulated in both tip and base. In *ba1* and *bif2*, a transcription factor, *tcp-transcription factor11* (*Zmtcptf11*; Zm00001d032217), in the same family as *teosinte branched1* (*tb1*),

which functions in AMs, was downregulated in both the tip and the base tissue (Doebley et al., 1995).

In the base tissue, there were four genes that were up-regulated in all three mutants, including Zm00001d044815 (similar to *AtBOB1*), which was also DE in the tip (Fig. 2b). Many genes involved in environmental stress response were also up-regulated in two of the three mutants similar to younger, developing, tip tissue. There were 59 genes down-regulated in two of the three mutants. *ba1* and *ba2* down-regulated genes had the most overlap with 54 genes in common (Fig. 2c). This included six transcription factors: *Zmzdh1, Zmzdh2, Zmmads43, Zmthx15, Zmc3h42* and *Zmtcptf11* (Zm00001d049000, Zm00001d020460, Zm00001d011748, Zm00001d003549, Zm00001d008356, Zm00001d032217, respectively) which were downregulated and *sbp29* (Zm00001d021573) which was upregulated (Fig. 4).

One of the maize genes with previously known functions in axillary meristem development that was DE in the data set was *Zmbarrenstalk fastigiate1* (*Zmbaf1*), which has previously been shown to be expressed in the BD of maize inflorescences (Gallavotti et al., 2011). The *baf1* transcript was down-regulated in *bif2* tip and in *ba1* base tissue in our data set. This result indicates that the BD may be absent in *bif2* and supports previous research showing the *bif2* functions early in development of AMs (McSteen et al., 2007; McSteen & Hake, 2001). Previous studies have also shown that *Zmbaf1* regulates *ba1* and that *baf1* is still expressed at the tip of *ba1* tassels (though the base was not examined) (Gallavotti et al.,

2011). As Zm*baf1* is expressed later in development in SMs, before FMs arise, decreased *Zmbaf1* expression in the *ba1* base may be due to the fact that *ba1* mutants are missing SPM and SM at the base.

In summary, 83% or more of DEGs were unique to each mutant at the tip, and 72% or more or DEGs were unique to each mutant at the base (Fig. 2) highlighting the unique roles of *ba1, bif2,* and *ba2* in maize inflorescence development. Gene Ontology (GO) (Du et al., 2010) and MAPMAN (Usadel et al., 2009) analysis on these DEGs was not particularly informative (transcriptional response and phosphorylation were enriched terms); therefore, further bioinformatic analysis was utilized to provide additional insights into processes affected in the mutants.

Co-Expression Analysis (WGCNA) of DEG at the tip primarily clustered genes by mutant

A co-expression analysis was conducted using WGCNA (Langfelder & Horvath, 2008) on the DEGs in the tip and the base separately, which resulted in five co-expression modules in the tip (M1-M5), consisting of 420 genes (Fig 5a) and seven co-expression modules in the base (M6-M12), consisting of 752 genes (Fig 5a). In this co-expression analysis, the modules primarily grouped genes that were DE in one of the three mutants of interest (*ba1, bif2,* or *ba2*). This indicates that co-expressed genes may provide more information about what pathways *ba1, bif2,* and *ba2* regulate than what developmental pathways are shared among all three during BD, SB, and AM initiation. Genes in each of these modules are

discussed below, including genes known to be involved in maize lateral organ development, as well as additional genes that had no previously known function in tassel development.

The tip-specific, red module (M1) is largely composed of *ba2* up-regulated DEGs (Fig. 2). This was one of the few modules that displayed GO enrichment which was for protein kinase activity (GO:0004672). A kinase of interest that was upregulated in *ba2* in the M1 module, was Zm00001d053676, with sequence similarity to members of the *Arabidopsis* STRUBBELIG family (SRF) of eight leucine rich repeat, receptor-like kinases (LRR-RLKs). SRF proteins are involved in control of cell division plane signaling (Eyüboglu et al., 2007; Vaddepalli et al., 2011). Basic local alignment search tool (BlastP) analysis showed that Zm00001d053676 shared 33% sequence similarity to *AtSRF2* in Arabidopsis. *AtSRF2* was originally characterized as an atypical RLK shown to be expressed in inflorescence meristems, flower primordia, and flower organ development via RNA *in situ* hybridization (Chevalier et al., 2005; Eyüboglu et al., 2007). Atypical LRR-RLKs play important roles in moderating cell-to-cell communication to direct overall growth and development and regulate hormones in *Arabidopsis* (Wu et al., 2016). Interestingly, this gene was also found to be upregulated in *ba2* bases and down regulated in *ba1* bases indicating that it may also play an important role in maize inflorescence development.

Another gene of interest in the M1 module, is Zm00001d041926, with 26% sequence similarity to *Arabidopsis* bHLH transcription factor, LONESOME HIGHWAY (LHW). This gene was found to be upregulated in both *ba2* tip and

base. The best-known function of *LHW* is to regulate the pool of stem cells which will differentiate into vasculature in the roots (Ohashi-Ito & Bergmann, 2007). In *Arabidopsis*, LHW also forms a heterodimer with another bHLH transcription factor, TARGET OF MONOPTEROS5 (TMO5) which regulates cytokinin biosynthesis, important in embryonic root initiation (Katayama et al., 2015; Schlereth et al., 2010). TMO5, is a target of MONOPTEROS, an ARF involved in auxin signaling in the root (Hardtke & Berleth, 1998; Schlereth et al., 2010). Interestingly, *Zmbhlh56* (Zm00001d028504), which is 34% similar to *AtTMO5*, was downregulated in *ba1* tip and base. Identification of these two genes in our transcriptomic data indicates that they may play a role in tassel meristems in maize.

The cyan module (M2) contains DEGs mostly found to be down regulated in the *ba2* mutant (Fig. 3). Within this module, Zm00001d005908, which has many predicted ARF binding sites (seven repressor ARFs and seven activator ARFs). A similar (43.09%) gene in *Arabidopsis, AtRECEPTOR-LIKE PROTEIN2* (*AtRLP2*), is expressed in shoot and root meristems and plays a role in transmitting the CLAVATA3 (CLV3) CLE signaling peptide, independently and in parallel with CLV1 and CLV2 receptors, aiding meristem maintenance (Kinoshita et al., 2010). This gene was also found to be down regulated in the *ba2* bases (M11 – black), indicating that it may be important in AM maintenance.

Transcription factors of interest were also members of the M2 module. This includes another SBP-like transcription factor, down-regulated in *ba2* called *neighbor of tga1* (*not1;*Zm00001d049824), a paralog of and bound by *teosinte glume architecture1* (*tga1*), most commonly known for its key role in kernel

evolution from teosinte to maize (Preston et al., 2012; Wang et al., 2015). Mutants for both *tga1* and *not1* have ears with elongated glumes that occasionally produce second ears, as well as longer ear shoots, and/or lateral branches (Dorweiler & Doebley, 1997; Wang et al., 2015). The DE of this gene in *ba2* tassels indicates that it may play a role in tassels as well as in ears. Another transcription factor in this module that was down-regulated in *ba2* and up-regulated in *ba1* was *Zmmads39* (Zm00001d050897), which is co-orthologous to *AtAGAMOUS-like 16* (*AtAGL16*) a member of the MADS-box transcription factor family. While there is a published function of *AtAGL16* in controlling flowering time (Hu et al., 2014), there are three other members of the same clade of *AGL* MADS-box transcription factors which are expressed strongly in root meristems. The DE of this transcription factor in *ba1* and *ba2* tips indicates that it may play a role in tassel meristems in maize.

The yellow module (M3) contains DEGs from all three mutants (Fig. 3) and both tissues, most of which are down-regulated, with one exception being Zm00001d044815, the *AtBOB1*-like gene previously described, which is up-regulated in all three mutants. Several transcription factors, that were previously mentioned, were members of the module including *baf1* which is down regulated in *bif2*, *tcptf11* which is downregulated in *ba1* and *bif2,* and *bhlh56* which is downregulated in *ba1*.

In addition, the M3 module also contains *Zmphosphate regulatory homolog80, Zmbnl*/*pho80* (Zm00001d016070), which are genes that contain a BAG domain characterized in *Arabidopsis* to play a role as a molecular chaperone of proteins in response to biotic and abiotic stress (Kabbage & Dickman, 2008;

Mehdi Kabbage et al., 2016). While Zm00001d016070 is up-regulated in *ba2* tip tissue and found to be co-expressed in the M3 module, five other BAG domain containing proteins were found to be co-expressed in five different modules: Zm00001d005246 (*ba1* down-regulated, tip, M5), Zm00001d046131 (*ba2* up-regulated, tip, M1), Zm00001d045678 (*ba1, ba2* up-regulated, base, M12), Zm00001d005246 (*ba1*, down-regulated, bases, M6), and Zm00001d051689 (*ba2* down-regulated, base, M9). The BAG protein family is diverse and evolutionarily conserved between humans and plants (Kabbage & Dickman, 2008). The number of BAG proteins in this data set indicate some play an important role in AM development.

In the green module (M4), a majority of DEGs were composed of *bif2* up and down regulated genes (Fig. 2). Within these, ten transcription factors were found including *dof29* which is 40% similar to TARGET of MONOPTEROS6, *ereb168*, *tcp23* and *myb125* which are upregulated and *gras27* and *bhlh147* which are downregulated in *bif2*. The DOF proteins induced by plant hormones are involved in tissue differentiation and regulation of metabolism (Noguero et al., 2013). *ZmMYB125* is in the S16 clade, as defined by Du et al, 2012, of maize MYB transcription factors that lack introns in the protein coding sequence (Du et al., 2012). In general, members of this clade are involved in secondary metabolism, and other members of the MYB family of transcription factors in *Arabidopsis* have been shown to be involved in control of AM formation (Ambawat et al., 2013).

ZmNAC100, Zm00001d041886, a NAC transcription factor within a clade shown to be involved in response to infectious pathogens in maize also in M4

(Voitsik et al., 2013) was found to be up regulated in *bif2* tips and is up regulated in *bif2* base tissue (M10) implying this gene is repressed by *bif2* throughout tassel development. The NAC transcription factor family is large, diverse, and highly redundant, and has been shown to be involved in hormone signaling, protein-protein interactions, and cross-talk between these functions (Puranik et al., 2012). Two other NAC transcription factors were found to be co-expressed in other modules: *ZmNAC84* (Zm00001d041791, down-regulated in *ba1* base, M12) and *ZmNAC74* (Zm00001d013151, down-regulated, *ba2* base, M11). These two NAC transcription factors are found in two different clades as defined by Voitsik et al. 2013. Although not well characterized, the altered expression of these transcription factors in *ba1* and *ba2* indicate that they may play an important role in AM development.

The maroon module (M5) consisted of 70 up-regulated and 24 down-regulated genes in *ba1* tips (Fig. 3). Within this module, a maize gene *Zmsquamosa-binding protein29,* (*Zmsbp29*), was found to be up-regulated. This is of interest as *Zmsbp29* has been shown to be differentially expressed in *Zmunbranched3* (*Zmub3*) mutants, and the promotor of the *Zmsbp29* gene can be bound and regulated by *Zmub3* (Du et al., 2017). The *Zmub3* gene is a member of the SQUAMOSA promotor binding protein-like (SPL) family, that functions in the initiation of AM primordia in both vegetative and reproductive tissue through regulation of cytokinin biosynthesis and the size of the IM (Chuck et al., 2014; Du et al., 2017), and orthologous *ub3* genes in rice have roles in initiation of SM meristems from the IM (Lu et al., 2013; Miura et al., 2010). Also found to be co-

expressed with *Zmsbp29* is *Zmrbr3 (*Zm00001d031678) (Sabelli et al., 2005) 58% similar to *Arabidopsis RETINOBLASTOMA-RELATED1* (*AtRBR1*) gene involved in cell-cycle regulation via ARF mediated cytokinin signaling (Nowack et al., 2012; Perilli et al., 2013). As *Zmrbr3* was significantly down regulated in *ba1*, this cell division/differentiation cascade may be an indirect target of *ba1*, as AM initiation and subsequent development has been hindered. Another maize gene, Zm00001d003040, has 33% sequence similarity to *Arabidopsis* BARD1, which is a target of WUSCHEL (WUS) (Han et al., 2008), was also downregulated in *ba2* tips likely as an indirect result of altered AM maintenance.

Co-Expression Analysis (WGCNA) of DEG at the base primarily clustered genes by mutant

Similar to the co-expression modules found in the tip through WGCNA, bases co-expression modules also primarily clustered by mutant. The first co-expression module, M6 (lime), in the base primarily contained DEGs in *bif2* mutants (58 genes up-regulated, 8 down-regulated). There were 41.5% of the DEGs in M6 also found in M4 in the tip (Fig. 5b), including the transcription factors *Zmereb168, Zmnac100, Zmdof29, Zmmyb125,* and *Zmlim10* all of which were upregulated in *bif2* mutants. Other DEGs upregulated in *bif2* mutant bases in M6 relate to the cell cycle, such as Zm00001d029215, whose ortholog (with 58% sequence similarity) in *Arabidopsis*, At*VILLIN2* (*AtVLN2*), is involved in actin bundling during the development of the phragmoplast during cytokinesis (van der Honing et al., 2012), and Zm00001d005495, a gene with 74% sequence similarity to *Arabidopsis* RAB GTPase11C, a member of a group of GTPases involved in

cytokinesis during cell division (Asaoka et al., 2013). This could indicate that *bif2* mutants, which are missing axillary meristems, have defects in cell division.

The hot-pink module (M7) is primarily composed of DEGs that are down-regulated in *ba1, bif2,* and *ba2,* highlighting a common function of these three genes (Fig.3). As mentioned previously, the *baf1* gene was down regulated in *ba1* and *bif2.* In addition, two TCP, *Zmtcptf11* and *Zmtcp15*, and were down-regulated in *ba1* bases*,* M7, and *Zmtcp11* was also down-regulated in *bif2* bases. Both *Zmtcp11* and *Zmtcp15* are together in the same phylogenetic subclade within the *cycloidea/teosinte branched1* clade, suggesting that they may be paralogs (Chai et al., 2017). Both *Zmtcp11* and *Zmtcp15* show their highest expression in developing maize ear and tassels (Chai et al., 2017; Viola et al., 2013), and control AM outgrowth in the axillary buds and floral transition in *Arabidopsis* (Li, 2015). Also, within this module was Zm00001d031759, a gene with 39% sequence similarity to *AtINDETERMINATE (ID)-DOMAIN D14* (*AtIDD14*). *At*IDD14, in conjunction with *At*IDD15 and *At*IDD16, function to control lateral organ development specifically by promoting transcription of auxin transport and synthesis genes (Cui et al., 2013). These examples suggest the genes in this module may be DE due to the absence of AMs in *ba1, bif2,* and *ba2.*

The blue module (M8) is primarily comprised of *ba1* regulated genes, with 6 genes being up-regulated and 139 down-regulated in *ba1* (Fig. 3). Genes involved in JA biosynthesis and response were found in this module, including *Zmtasselseed2* (*Zmts2*), which encodes a short-chain alcohol dehydrogenase, that was down-regulated in *ba1* (DeLong et al., 1993). The *Zmts2* mutant has been

previously shown to be involved jasmonic acid (JA) synthesis or signaling and required for pistil abortion in the floral meristem (Acosta et al., 2009). The maize gene *12-oxo-phytodienic acid reductase5* (*Zmopr5*) was down-regulated in *ba1* and *ba2* bases and may also be involved in JA biosynthesis due to high sequence similarity with *Zmopr7* and *Zmopr8*, known to be involved in this pathway (Yan et al., 2012). In addition, the *Zmlipoxygenase11* (*Zmlox11*) transcript was also down-regulated in *ba1* bases and may also have a potential involvement in JA biosynthesis (Christensen et al., 2015; Ogunola et al., 2017).

The M8 module also had slight GO enrichment for transcription initiation factor activity (GO:0016986), and a transcription factor of interest in this module includes maize *ZIM-transcription factor 13* (*Zmzim13*), which was downregulated in *ba1* bases. The *Zmzim13* gene has 38.69% sequence similarity to *AtJAZ1* in *Arabidopsis,* which is involved in JA signaling by transcriptional repression of JA response (Thines et al., 2007), further supporting the hypothesis that *ba1* affects JA metabolism. Transcriptional expression of *AtJAZ1* in Arabidopsis is stimulated by auxin (Grunewald et al., 2009). This is very intriguing as *ba1* is a direct target of the maize ZmARFs (Galli et al., 2015), and *Zmzim13* has 13 predicted ARF binding sites (seven repressors and five activators) within a 2kb region up/downstream of the gene. This suggests a possible link between auxin and JA regulation in the *ba1* mutant. When transcripts were visualized via RNA *in situ* hybridization (Fig. 6), *Zmzim13* was shown to be expressed in AMs in normal tassels, starting at the initiation of AMs at the tip of the tassel (Fig. 6a). The decrease in *Zmzim13* transcripts seen in *ba1* mutants could be due to the fact that

ba1 entirely lack AMs (Fig. 6b) and *bif2* has a decreased number of AMs (Fig. 6c). Consistent with the hypothesis above, *Zmarf9* is up regulated in *ba1* within this same co-expression module. *ZmARF9* is within the B clade of activator ARFs, and while less is known about ARFs within this clade, it has been suggested that clade B ARFs are involved in the fine-tuning regulation of auxin signaling, in a tissue specific manner (Matthes et al., 2019). As *Zmarf9* is expressed in AMs and vasculature of immature tassels of maize (Galli et al., 2015) and is upregulated in *ba1* mutants, this indicates that repression of Zm*arf9* and JA may be important in axillary meristem development.

The orange module (M9) contained DEG that were mostly up regulated in *ba2* mutant bases (Fig. 2) which had a high percentage of overlap with the M1 tip module. Genes with sequence similarity to *AtBOB1, AtLHW,* and *AtSRF*, were all down regulated and discussed previously in the M1 tip module. Similar to M1 there was GO enrichment for protein kinase activity (GO:0004672) in the M9 module. Within the genes enriched was, Zm00001d039931 with very high sequence identity (93%) to *WALL-ASSOCIATED RECEPTOR-LIKE KINASE 1* (*OsWAK1*) in rice. While the best-known function of *OsWAK1* is in plant defense, other RLKs, such as *AtCLAVATA1, AtBAM1/2*, and *ZmCRINKLY4,* have many developmental roles (DeYoung et al., 2006; Li & Durbin, 2009), and further investigation into Zm00001d039931 may find roles in AM establishment and development as well.

In the M10 grey module, Zm00001d003349, a gene with 47.32% sequence similarity to *Arabidopsis CYTOCHROME P-450 724A1* (*AtCYP724A1*) was down-regulated in *ba2* mutant bases. The *AtCYP724A1* gene in Arabidopsis is involved

in brassinosteriod (BR) biosynthesis, whereas overexpression of the transcript can complement *dwarf4* mutants, the rate-limiting step in BR biosynthesis (Zhang et al., 2012). Furthermore, the *bristleless1* (*Svbsl1*) mutant in *Setaria viridis* encodes an ortholog to *AtCYP724A1*, and results in altered inflorescence development and a suppression of bristle development in the panicle (Yang et al., 2018). The *Svbsl1* transcript accumulates in the boundary area between the meristem and developing organs within the panicle indicating that BR is synthesized in the BD (Yang et al., 2018). In *Arabidopsis*, *CUP-SHAPED COTYLEDON* (*CUC*) and *LATERAL ORGAN BOUNDARIES* (*LOB*) mutants exclude BR from BDs (Bell et al., 2012; Gendron et al., 2012). The down regulation of Zm00001d003349 in *ba2* mutants implicates BR function in BDs in inflorescence development in maize.

Additionally, Zm00001d016370, a DEG found in *ba2*, was down regulated in the M10 grey co-expression module. This gene is 45% similar to *POLTERGEIST-LIKE1* (*AtPLL1*) in *Arabidopsis*, a protein phosphatase that functions to regulate *WUS* expression by *CLAVATA* signaling in SAMs and FMs (Song et al., 2006) providing another link to defects in AM maintenance in *ba2* mutants. The *Zmpebp24* (Zm00001d021135) transcript was also down-regulated in *ba2* within this module. This gene is involved in controlling flowering time, as increased expression of this gene causes delayed flowering in maize (Azodi et al., 2020; Danilevskaya et al., 2008). As these genes have identified functions in flowering, M10 may be a down-stream response to *ba1* mutants being unable to produce AM.

DEGs of interest in the black M11 module that are up-regulated in *ba1* mutants (Fig. 2) include Zm00001d048185 and Zm00001d044327 with 42% and 38% sequence similarity to *Arabidopsis SLEEPY1* (*AtSLY1*) and *LONELY-GUY7* (*AtLOG7),* respectively. *AtSLY1* has been shown to regulate gibberellic acid via repression of DELLA-containing proteins that inhibit gibberellic acid (GA) response (McGinnis et al., 2003), and *AtLOG7* regulates meristem size in *Arabidopsis* by activating the cytokinin pathway (Kurakawa et al., 2007; Tokunaga et al., 2012). These two genes suggest *ba1* mutants have downstream effects on hormone regulation.

Furthermore, the maize *auxin-response factor24* (*Zmarf24*) transcription factor, which is a part of the Class B group of ARFs that generally act as transcriptional repressors (Galli et al., 2018; 2015) was upregulated in *ba1* in M11. Specifically, *Zmarf24* belongs to the ETTIN (ETT) subclade of ARF repressors, which act atypically in that the direct binding of indole-acetic-acid (IAA) to the ETT/ARF is enough to release repression of the corresponding transcription factor (Simonini et al., 2016). Interestingly, genetic analysis in *Arabidopsis* between ETT and *AtBOB1* indicates that ETT genes may also act downstream of *AtBOB1.* The up regulation of both *Zmarf24* and Zm00001d044815 (similar to *bob1* in *Arabidopsis*) in *ba1* support this finding, and the previously discussed importance of auxin and thermo-regulatory pathway crosstalk in axillary meristem development (Silverblatt-Buser et al., 2018). Furthermore, ETT complexes have been hypothesized to regulate two separate sets of DEGs as direct binding by IAA can turn repression on or off (Simonini et al., 2016). This means the M11 module

may be reflecting the downstream effects of *ba1* regulation and is additionally supported by the enrichment of ZmARF binding in *ba1* downregulated genes.

Also co-expressed within M11 was Zm00001d003040, which was up-regulated in *ba1* and down-regulated in *ba2*. As mentioned previously, this gene is orthologous to AtBARD1 that functions to repress WUS expression to the organizing center in the SAM (Han et al., 2008). It is possible this gene is also important in organizing the AM. This, along with Zm00001d005908, was also down regulated in *ba2* tips and discussed in the M2 module description above indicates that *ba1* and *ba2* may also function to regulate axillary meristem maintenance pathways.

The M12 purple module in the base was also primarily composed of DEG from the *ba1* mutant; 67 up- and 11 down-regulated, with genes that are involved in hormone regulation (Fig. 3). For instance, maize *ABA-Insensitive40* (*Zmabi40)*, a member of the ABI3/VP1-like transcription factor family known to be involved in ABA regulation during seed development and controlling apical dominance (Mönke et al., 2012) was up-regulated in *ba1*. ABA has been known to inhibit axillary bud outgrowth at increased levels, and *Zmabi40* is in the ABI3 class of ABA inhibitors that are upregulated when ABA levels are high in dormant axillary buds (Shimizu-Sato & Mori, 2001). As AM initiation and subsequent development is inhibited in *ba1* mutants, the up-regulation of *Zmabi40* in this module hints at an indirect role of *ba1* in regulating ABA and/or apical dominance-related responses during tassel development.

In addition to *Zmabi40,* two MYB transcription factors, *Zmmyb56* and *Zmmyb28* were also up regulated in *ba1* bases in the M12 module. While *Zmmyb56* and *Zmmyb28* are not within the same clade of MYB transcription factors in maize (Du et al., 2012), they both have *Arabidopsis* orthologs (*AtMYB59* and *AtMYB16,* respectively) that are involved in meristem development (Ambawat et al., 2013). *At*MYB59 is a negative regulator of calcium signaling and aids in regulation of the cell cycle in root meristems (Ambawat et al., 2013; Fasani et al., 2019). A recent study noted an increase of *AtMYB59* expression in leaves in response to ABA treatment (Fasani et al., 2019), and *Atmyb59* mutants differentially down-regulated AtSPL5*,* a SQUAMOSA-BINDING LIKE protein that is involved in plant growth and development (Cardon et al., 1999; Preston & Hileman, 2013). Interestingly, *ZmSBP29*, which was mentioned previously as also upregulated in *ba1* bases in the M11 module is orthologous to *AtSPL4,* which is closely related to *AtSPL5* (Preston & Hileman, 2013). *Zmsbp29* and *Zmmyb56* are also upregulated in *bif2* bases. Finally, *AtMYB16* encodes a MIXTA-like MYB transcription factor to control petal development (Ambawat et al., 2013), and is likely an indirect target of *bif2* as the base tissue was primarily where flowers would be formed and are absent in *bif2* mutants.

DISCUSSION

The DEG of *ba1, bif2,* and *ba2* in IM and AM development were analyzed in this study in order to better understand what genes are involved in BD, SB, and AM establishment versus development. Previous studies of *ba1, bif2,* and *ba2* show these genes have been shown to respond to auxin (Gallavotti et al., 2004;

McSteen & Hake, 2001; McSteen et al., 2007; Yao et al., 2019). While we initially hypothesized that DEGs would be co-expressed based on regulatory pathways impacted by an inhibition of a specific step in the auxin response pathway, we found that co-expression analysis clustered DEGs into modules based on a specific mutant and furthermore by up or down regulated expression patterns. This finding suggests a much more comprehensive and complex network of regulation unique to each mutant than what was previously known.

WGCNA performed on both the tip and the base identified modules that were primarily composed of an individual mutant's, up or down regulated genes indicating unique roles of *ba1, bif2,* and *ba2* in the regulation of BD, SB, and AM establishment. The genes present in these modules offer some insight as to how *ba1, bif2,* and *ba2* regulate AM development to follow up with in subsequent experiments. In the developmentally younger tip tissue, where AMs are still being formed from the IM, modules contained genes pertaining to cell division and differentiation, abiotic and biotic stress, as well as genes pertaining to transcription factors that are either directly or are orthologous to genes involved in regulating meristem maintenance genes. Modules with similarly expressed genes were found in the base tissue co-expression networks, although the lack of overlap between the modules in the tip and the base indicates *ba1, ba2,* and *bif2* have differential regulation of transcription throughout inflorescence development (Fig. 2b). Additionally, base modules also contained biosynthesis genes related to JA, ABA, Auxin, and BRs. These may be indirect effects of *ba1, ba2,* and *bif2* regulation as

base tissue is developmentally older, and the genes mis-regulated in the tip may be affecting downstream hormone pathways as the inflorescence matures.

In summary, our results indicate that *ba1, bif2,* and *ba2* regulate a wide array of direct and indirect responses during the development of AMs than was previously known. The outcome of our study outlines a much more detailed picture of the overall regulation of AM development, and that, even though *ba1, bif2,* and *ba2* interact with each other to regulate AM establishment, they each act to regulate a subset of genes unique to each mutant to control tassel development.

METHODS

Plant Growth and RNA Extraction

Segregating families (3:1 and 1:1) of *ba1*, *ba2,* and *bif2* mutants, introgressed more than 5 times into the B73 inbred background, were grown, along with B73 controls, during the summer for ~three weeks at the MU Genetics Farm in Columbia, MO in different field seasons (Rep1- July 2013; Rep2- September 2013; Rep3- July 2014). The *ba1-ref*, *ba2-3112,* and *bif2-77* alleles were utilized and genotyped as previously described (Gallavotti et al., 2004; McSteen et al., 2007). The plants were labeled, leaves numbered and when 10-12 leaves were visible (v9-v11), tassels ranging from 3-4.5mm in size were dissected, branches removed from the base, and the main spike sectioned into thirds: tip 1mm, middle 1-3mm, and base 1mm (Fig. 2). Frozen tip tissue (IM/SPM) and base tissue (SPM/SM) from 10-14 plants were pooled, and RNA was extracted using a NucleoSpin RNA Plant kit (Macherey-Nagel, Duren, Germany). Libraries for

Replicate 1 and Replicate 3 were constructed using the TruSeq mRNA Library Prep kit (Illumina, San Diego, CA). The library for Replicate 2 was prepped via NEBNext Ultra RNA kit (New England Biolabs, Ipswich, MA). Single-end 1 x 100 bp reads were sequenced on the Illumina HiSeq 2500 sequencing system for replicates 1 and 2, replicate 3 sequenced single-end 1 x 75 bp reads on the Illumina NextSeq 500.

RNA-seq Data Analysis

RNA-seq data analysis of raw reads fastq files was conducted using an in-house developed informatics pipeline. This pipeline consists of processing fastq files for quality control using the fastqc tool (http://www.bioinformatics.babraham.ac.uk/projects/fastqc/) and removes low quality reads and trim adaptor sequences using trim-galore (http://www.bioinformatics.babraham.ac.uk/projects/trim_galore/). The trimmed fastq files were then indexed and aligned to the reference maize genome v4 B73 genome (downloaded from maizegdb.org/) using the TopHat2 Alignment tool (Kim et al., 2013) and then the counts of reads aligned to genes was calculated using htseq-count tool (Anders et al., 2015).

Differential Expression Genes Analysis

DEG were analyzed with the EdgeR Bioconductor package using standard parameters, normalizing for batch effects, and using a General Linear Model (GLM) to account for variation for sample collection time and differences in sequencing methods (McCarthy et al., 2012; Robinson et al., 2009). The analysis

included a design matrix to account for variation and results were filtered by a false discovery rate (FDR) of 0.05 and a log2 fold change value cutoff of 2 (Robinson et al., 2009). Gene names and annotations were obtained from Maize GDB (Lawrence et al., 2004). The DEGs were also uploaded to the Maize KB database within KBCommons (Zeng et al., 2019) and incorporated into its in-house developed Differential Expression Suite of Tools for web-based access for filtering and annotating the DEGs interactively. Arabidopsis and Rice gene and annotation lists were obtained from Gramene (www.gramene.org), and orthologs determined via BLAST using nucleotide sequence (Altschul et al., 1990). The web-based AgriGO (Du et al., 2010) and PANTHER (Mi et al., 2017) gene-ontology tools were used to further analyze gene function with significance threshold set at a p-value of 0.05 and a minimum number of mapping entries set at three. Venn diagrams were used to compare DEGs lists with Venny, an on-line visualization tool (Oliveros, n.d.). Heat maps to compare changes based on fold change in gene expression were produced via hierarchical clustering and heatmap.2 functions in the R package ‘gplots’ (Howe et al., 2011).

Weighted Gene Co-Expression Network Analysis (WGCNA)

The comprehensive WGCNA R package was utilized to determine modules of co-expressed genes based on TMM-normalized read count values (Langfelder & Horvath, 2008; Zhang & Horvath, 2005). A unique list of DEGs was compiled from all three mutants, tip and base, for input. Significance was determined using a log fold (2) expression value cut off and false positive test correction for multiple

hypothesis was performed using false discovery rate (FDR) (Langfelder & Horvath, 2008; Storey et al., 2004).

AUTHOR CONTRIBUTIONS

KG, NBB and MSM performed wet lab experiments; KG, SS, NBB and performed bioinformatic analysis; KG, NBB, MSM, JLR, and PM interpreted the data; KG, NBB and JMR made the figures; KG lead writing of manuscript with contributions from all authors; PM and TJ supervised the research.

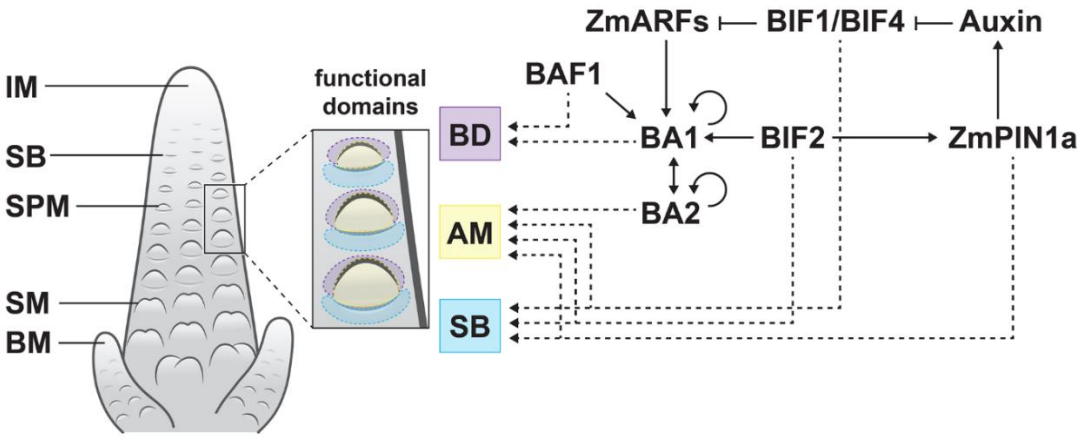

Figure 1: Model for axillary meristem formation in maize as depicted in a cartoon of tassel meristem (modified from Yao et al 2018). Axillary meristems initiate between an adaxial boundary domain (BD) and an abaxial suppressed bract (SB) domain. The transcription factor BAF1 regulates the transcription of BA1 (Gallavotti et al., 2011). The Aux/IAA repressors BIF1 and BIF4 bind ZmARF transcription factors, which bind to the BA1 promoter (Galli et al., 2015). BIF2 phosphorylates ZmPIN1a (Skirpan et al., 2009) and BA1 (Skirpan et al., 2008). Direct interactions are depicted with a solid arrow; functions based on expression or mutant phenotype are depicted with dashed arrows.

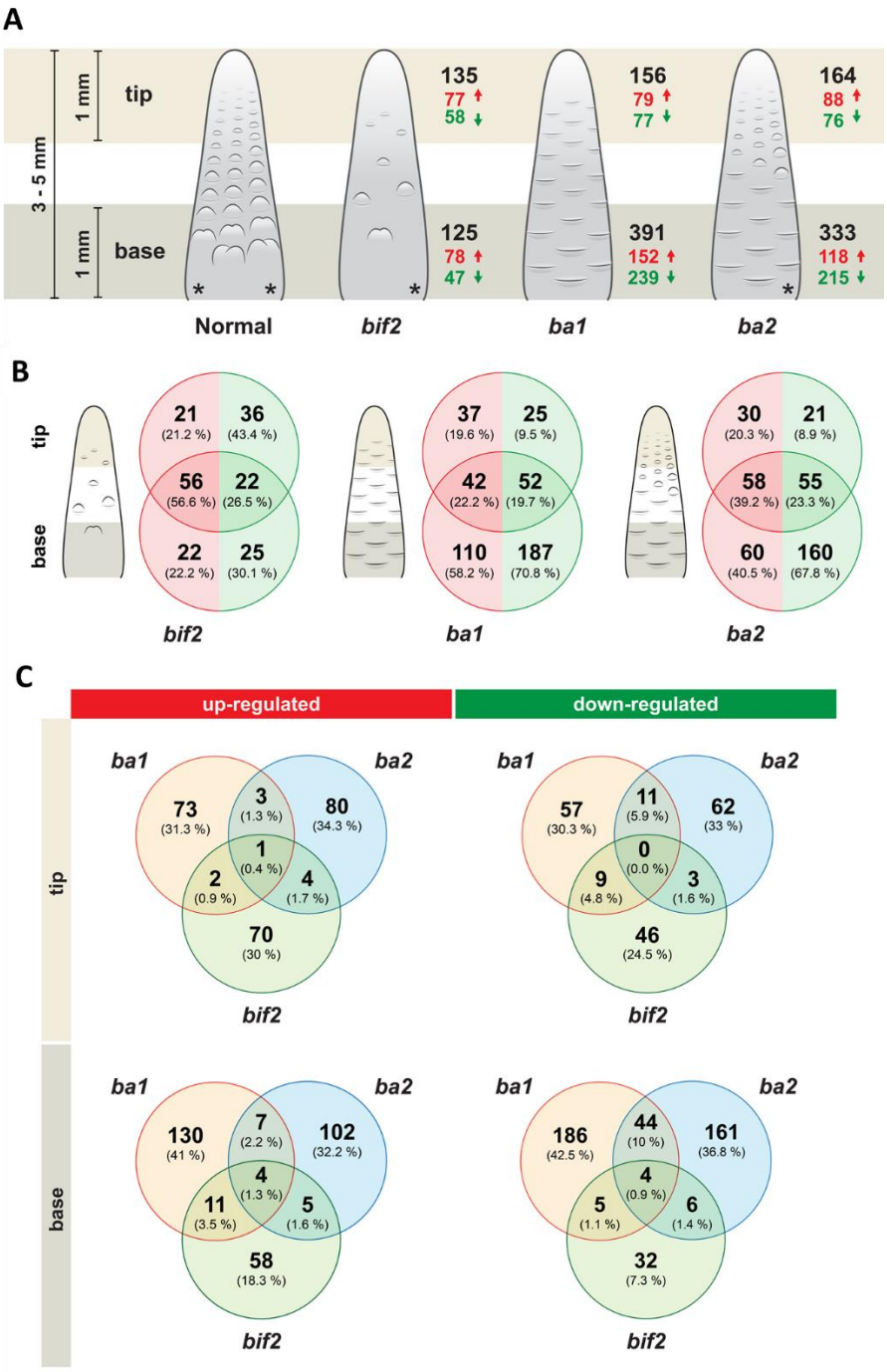

Figure 2: Cartoon depiction of *ba1*, *bif2,* and *ba2* phenotypes and experimental design. A) differentially expressed genes found within the tip and base of *ba1, bif2,* and *ba2* compared to normal (B73). Green numbers indicate the number of DEG up-regulated, and red numbers indicate the number of genes down-regulated. B)

cartoon depiction of the DEG for *ba1, bif2,* and *ba2* respectively, compared tip to base. Green numbers indicate the number of DEG up-regulated, and red numbers indicate the number of genes down-regulated. C) Venn's Diagrams of DEG overlap among *bif2, ba1* and *ba2* mutants separated out by up- and down-regulated genes in the tip and base of tassel meristems

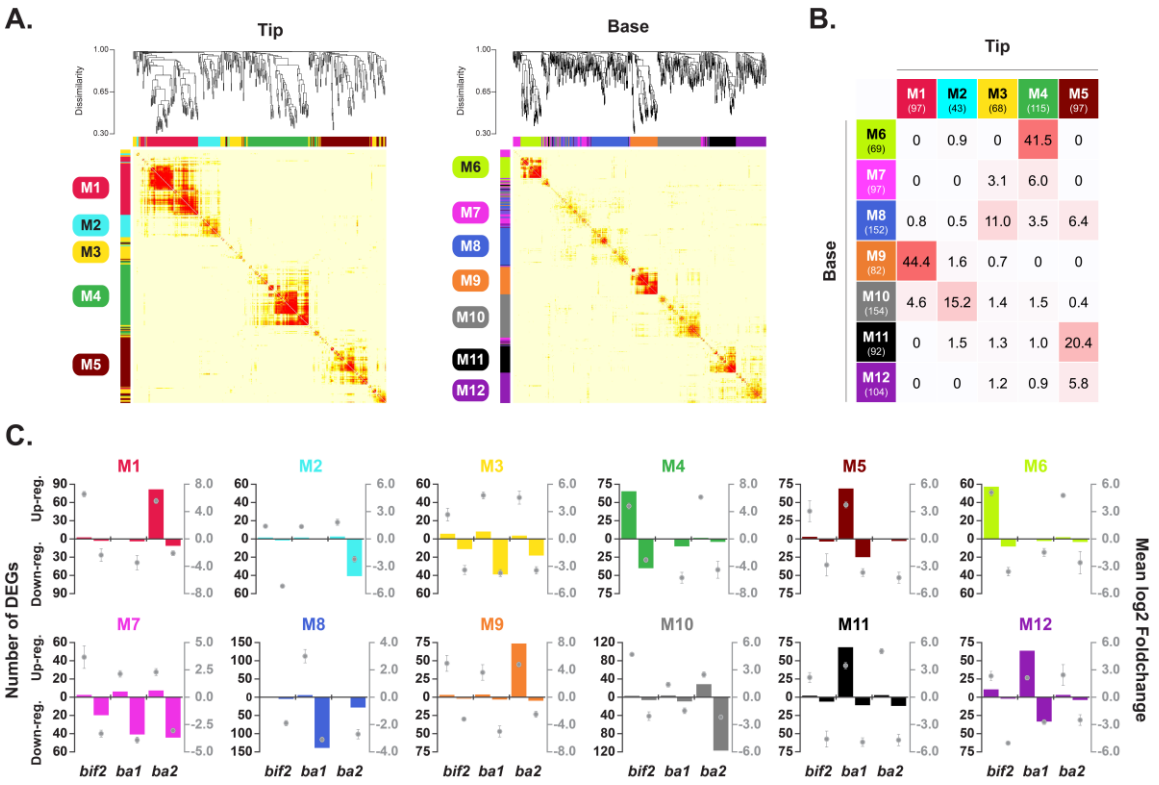

Figure 3: Weighted Gene Co-Expression Analysis (WGCNA) of the tip and bases. A) base (left) WGCNA produced co-expression modules M1-M7 and tip WGCNA produced M8-M12 (right) co-expression modules. B) up- and down-regulated DEG within clusters M1-M12 separated out by mutant C) Comparison of overlap between modules M1-M7 found in the base to modules M8-M12 found in the tip. Numbers in parentheses represent the number of DEG found within one module, numbers in table represent the percentages of overlap between modules being compared.

A.

Replicate 1	No. of pooled meristem		12	12	10	12
	Tip	Sample ID	PM10	PM11	PM12	PM13
		No. of reads	58,960,917	60,837,596	58,349,849	48,848,298
		% read coverage	95.6%	94.7%	94.3%	94.2%
	Base	Sample ID	PM14	PM15	PM16	PM17
		No. of reads	62,039,774	59,390,278	44,441,977	48,799,551
		% read coverage	95.7%	95.3%	95.4%	94.4%
Replicate 2	No. of pooled meristem		14	14	14	14
	Tip	Sample ID	PM18	PM19	PM20	PM21
		No. of reads	57,023,214	57,743,678	47,130,430	50,789,256
		% read coverage	96.9%	95.9%	95.9%	95.1%
	Base	Sample ID	PM22	PM23	PM24	PM25
		No. of reads	58,725,212	49,367,848	52,292,111	55,280,808
		% read coverage	97%	96.2%	96.0%	95.1%
Replicate 3	No. of pooled meristem		12	12	12	12
	Tip	Sample ID	PM26	PM27	PM28	PM29
		No. of reads	57,699,512	53,235,989	61,311,177	58,327,123
		% read coverage	98.2%	97.5%	97.5%	96.8%
	Base	Sample ID	PM30	PM31	PM32	PM33
		No. of reads	61,248,162	55,522,374	58,661,831	60,272,463
		% read coverage	98.2%	97.6%	97.6%	96.8%

B.

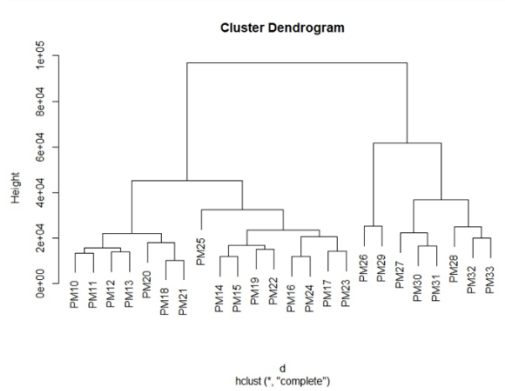

C.

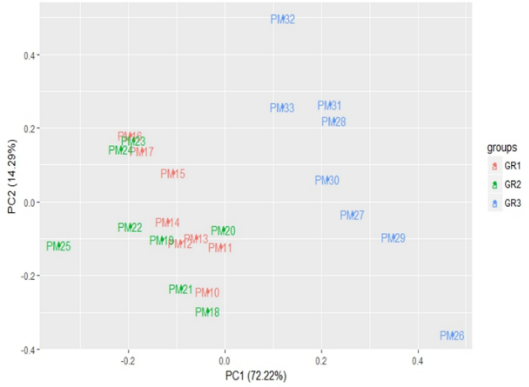

Supplemental Figure 1: Analysis of sample replicates A) Overview of percentage coverage of library reads to Maize Genome_V4 in each pooled sample used in this analysis. All pooled samples had over 94% read coverage. Comparison of replicate similarity, B) cluster dendrogram clusters replicates PM10-13, PM13, PM20-21 on a branch closely related containing replicates PM14-15, PM16-17, PM23-25 while replicates PM26-PM33 cluster outside, C) PCA plots of replicates.

WORKS CITED

Acosta, I. F., Laparra, H., Romero, S. P., Schmelz, E., Hamberg, M., Mottinger, J. P., Moreno, M. A., & Dellaporta, S. L. (2009). tasselseed1 Is a Lipoxygenase Affecting Jasmonic Acid Signaling in Sex Determination of Maize. *Science*, *323*(5911), 262–265. https://doi.org/10.1126/SCIENCE.1164645

Altschul, S. F., Gish, W., Miller, W., Myers, E. W., & Lipman, D. J. (1990). Basic local alignment search tool. *Journal of Molecular Biology*, *215*(3), 403–410. https://doi.org/10.1016/S0022-2836(05)80360-2

Ambawat, S., Sharma, P., Yadav, N. R., & Yadav, R. C. (2013). MYB transcription factor genes as regulators for plant responses: an overview. *Physiology and Molecular Biology of Plants*, *19*(3), 307–321. https://doi.org/10.1007/S12298-013-0179-1

Anders, S., Pyl, P. T., & Huber, W. (2015). HTSeq-A Python framework to work with high-throughput sequencing data. *Bioinformatics*, *31*(2), 166–169. https://doi.org/10.1093/bioinformatics/btu638

Asaoka, R., Uemura, T., Ito, J., Fujimoto, M., Ito, E., Ueda, T., & Nakano, A. (2013). Arabidopsis RABA1 GTPases are involved in transport between the trans-Golgi network and the plasma membrane, and are required for salinity stress tolerance. *The Plant Journal*, *73*(2), 240–249. https://doi.org/10.1111/TPJ.12023

Azodi, C. B., Pardo, J., VanBuren, R., de los Campos, G., & Shiu, S.-H. (2020). Transcriptome-Based Prediction of Complex Traits in Maize. *The Plant Cell*, *32*(1), 139–151. https://doi.org/10.1105/TPC.19.00332

Barazesh, S., & McSteen, P. (2008). Barren inflorescence1 Functions in Organogenesis During Vegetative and Inflorescence Development in Maize. *Genetics*, *179*(1), 389–401. https://doi.org/10.1534/GENETICS.107.084079

Barazesh, S., Nowbakht, C., & McSteen, P. (2009). sparse inflorescence1, barren inflorescence1 and barren stalk1 Promote Cell Elongation in Maize Inflorescence Development. *Genetics*, *182*(1), 403. https://doi.org/10.1534/GENETICS.108.099390

Bell, E. M., Lin, W., Husbands, A. Y., Yu, L., Jaganatha, V., Jablonska, B., Mangeon, A., Neff, M. M., Girke, T., & Springer, P. S. (2012). Arabidopsis LATERAL ORGAN BOUNDARIES negatively regulates brassinosteroid accumulation to limit growth in organ boundaries. *Proceedings of the National Academy of Sciences*, *109*(51), 21146–21151. https://doi.org/10.1073/PNAS.1210789109

Bolduc, N., Yilmaz, A., Mejia-Guerra, M. K., Morohashi, K., O'Connor, D., Grotewold, E., & Hake, S. (2012). Unraveling the KNOTTED1 regulatory network in maize meristems. *Genes & Development*, *26*(15), 1685–1690. https://doi.org/10.1101/GAD.193433.112

Cardon, G., Höhmann, S., Klein, J., Nettesheim, K., Seedler, H., & Huijser, P. (1999). Molecular characterisation of the Arabidopsis SBP-box genes. *Gene*, *237*(1), 91–104. https://doi.org/10.1016/S0378-1119(99)00308-X

Chai, W., Jiang, P., Huang, G., Jiang, H., & Li, X. (2017). Identification and expression profiling analysis of TCP family genes involved in growth and development in maize. *Physiology and Molecular Biology of Plants*, *23*(4), 779–791. https://doi.org/10.1007/S12298-017-0476-1

Chevalier, D., Batoux, M., Fulton, L., Pfister, K., Yadav, R. K., Schellenberg, M., & Schneitz, K. (2005). STRUBBELIG defines a receptor kinase-mediated signaling pathway regulating organ development in Arabidopsis. *PNAS*, *102*(25), 9074–9079. https://doi.org/10.1073/PNAS.0503526102

Christensen, S. A., Huffaker, A., Kaplan, F., Sims, J., Ziemann, S., Doehlemann, G., Ji, L., Schmitz, R. J., Kolomiets, M. v., Alborn, H. T., Mori, N., Jander, G., Ni, X., Sartor, R. C., Byers, S., Abdo, Z., & Schmelz, E. A. (2015). Maize death acids, 9-lipoxygenase–derived cyclopente(a)nones, display activity as cytotoxic phytoalexins and transcriptional mediators. *Proceedings of the National Academy of Sciences*, *112*(36), 11407–11412. https://doi.org/10.1073/PNAS.1511131112

Chuck, G. S., Brown, P. J., Meeley, R., & Hake, S. (2014). Maize SBP-box transcription factors unbranched2 and unbranched3 affect yield traits by regulating the rate of lateral primordia initiation. *PNAS*, *111*(52), 18775–18780. https://doi.org/10.1073/PNAS.1407401112

Crofts, A. J., & Denecke, J. (1998). Calreticulin and calnexin in plants. *Trends in Plant Science*, *3*(10), 396–399. https://doi.org/10.1016/S1360-1385(98)01312-0

Cui, D., Zhao, J., Jing, Y., Fan, M., Liu, J., Wang, Z., Xin, W., & Hu, Y. (2013). The Arabidopsis IDD14, IDD15, and IDD16 Cooperatively Regulate Lateral Organ Morphogenesis and Gravitropism by Promoting Auxin Biosynthesis and Transport. *PLOS Genetics*, *9*(9), e1003759. https://doi.org/10.1371/JOURNAL.PGEN.1003759

D'Alessandro, S., Golin, S., Hardtke, C. S., Schiavo, F. lo, & Zottini, M. (2015). The co-chaperone p23 controls root development through the modulation of auxin distribution in the Arabidopsis root meristem. *Journal of Experimental Botany*, *66*(16), 5113. https://doi.org/10.1093/JXB/ERV330

Danilevskaya, O. N., Meng, X., Selinger, D. A., Deschamps, S., Hermon, P., Vansant, G., Gupta, R., Ananiev, E. v., & Muszynski, M. G. (2008). Involvement of the MADS-Box Gene ZMM4 in Floral Induction and Inflorescence Development in Maize. *Plant Physiology*, *147*(4), 2054–2069. https://doi.org/10.1104/PP.107.115261

del Bem, L. E. (2011). The evolutionary history of calreticulin and calnexin genes in green plants. *Genetica*, *139*(2), 255–259. https://doi.org/10.1007/S10709-010-9544-Y

DeLong, A., Calderon-Urrea, A., & Dellaporta, S. L. (1993). Sex determination gene TASSELSEED2 of maize encodes a short-chain alcohol dehydrogenase required for stage-specific floral organ abortion. *Cell*, *74*(4), 757–768. https://doi.org/10.1016/0092-8674(93)90522-R

DeYoung, B. J., Bickle, K. L., Schrage, K. J., Muskett, P., Patel, K., & Clark, S. E. (2006). The CLAVATA1-related BAM1, BAM2 and BAM3 receptor kinase-like proteins are required for meristem function in Arabidopsis. *The Plant Journal*, *45*(1), 1–16. https://doi.org/10.1111/J.1365-313X.2005.02592.X

Doebley, J., Stec, A., & Gustus, C. (1995). Teosinte Branched1 and the Origin of Maize: Evidence for Epistasis and the Evolution of Dominance. *Genetics*, *141*(1), 333. /pmc/articles/PMC1206731/?report=abstract

Donato, M. di, & Geisler, M. (2019). HSP90 and co-chaperones: a multitaskers' view on plant hormone biology. *FEBS Letters*, *593*(13), 1415–1430. https://doi.org/10.1002/1873-3468.13499

Dorweiler, J. E., & Doebley, J. (1997). Developmental analysis of teosinte glume architecture1: A key locus in the evolution of maize (Poaceae). *American Journal of Botany*, *84*(10), 1313–1322. https://doi.org/10.2307/2446130

Du, H., Feng, B.-R., Yang, S.-S., Huang, Y.-B., & Tang, Y.-X. (2012). The R2R3-MYB Transcription Factor Gene Family in Maize. *PLOS ONE*, *7*(6), e37463. https://doi.org/10.1371/JOURNAL.PONE.0037463

Du, Y., Liu, L., Li, M., Fang, S., Shen, X., Chu, J., & Zhang, Z. (2017). UNBRANCHED3 regulates branching by modulating cytokinin biosynthesis and signaling in maize and rice. *The New Phytologist*, *214*(2), 721–733. https://doi.org/10.1111/NPH.14391

Du, Z., Zhou, X., Ling, Y., Zhang, Z., & Su, Z. (2010). agriGO: A GO analysis toolkit for the agricultural community. *Nucleic Acids Research*, *38*(SUPPL. 2), W64. https://doi.org/10.1093/nar/gkq310

Eveland, A. L., Goldshmidt, A., Pautler, M., Morohashi, K., Liseron-Monfils, C., Lewis, M. W., Kumari, S., Hiraga, S., Yang, F., Unger-Wallace, E., Olson, A., Hake, S., Vollbrecht, E., Grotewold, E., Ware, D., & Jackson, D. (2014).

Regulatory modules controlling maize inflorescence architecture. *Genome Research*, *24*(3), 431. https://doi.org/10.1101/GR.166397.113

Eyüboglu, B., Pfister, K., Haberer, G., Chevalier, D., Fuchs, A., Mayer, K. F., & Schneitz, K. (2007). Molecular characterisation of the STRUBBELIG-RECEPTOR FAMILY of genes encoding putative leucine-rich repeat receptor-like kinases in Arabidopsis thaliana. *BMC Plant Biology 2007 7:1*, *7*(1), 1–24. https://doi.org/10.1186/1471-2229-7-16

Fasani, E., DalCorso, G., Costa, A., Zenoni, S., & Furini, A. (2019). The Arabidopsis thaliana transcription factor MYB59 regulates calcium signalling during plant growth and stress response. *Plant Molecular Biology*, *99*(6), 517–534. https://doi.org/10.1007/S11103-019-00833-X

Gallavotti, A, Barazesh, S., Malcomber, S., Hall, D., Jackson, D., Schmidt, R. J., & McSteen, P. (2008). sparse inflorescence1 encodes a monocot-specific YUCCA-like gene required for vegetative and reproductive development in maize. *PNAS*, *105*(39), 15196–15201. https://doi.org/10.1073/PNAS.0805596105

Gallavotti, Andrea, Malcomber, S., Gaines, C., Stanfield, S., Whipple, C., Kellogg, E., & Schmidt, R. J. (2011). BARREN STALK FASTIGIATE1 Is an AT-Hook Protein Required for the Formation of Maize Ears. *The Plant Cell*, *23*(5), 1756. https://doi.org/10.1105/TPC.111.084590

Gallavotti, Andrea, Yang, Y., Schmidt, R. J., & Jackson, D. (2008). The relationship between auxin transport and maize branching. *Plant Physiology*, *147*(4), 1913–1923. https://doi.org/10.1104/pp.108.121541

Gallavotti, Andrea, Zhao, Q., Kyozuka, J., Meeley, R. B., Ritter, M. K., Doebley, J. F., Pè, M. E., & Schmidt, R. J. (2004). The role of barren stalk1 in the architecture of maize. *Nature*, *432*(7017), 630–635. https://doi.org/10.1038/nature03148

Galli, M., Liu, Q., Moss, B. L., Malcomber, S., Li, W., Gaines, C., Federici, S., Roshkovan, J., Meeley, R., Nemhauser, J. L., & Gallavotti, A. (2015). Auxin signaling modules regulate maize inflorescence architecture. *Proceedings of the National Academy of Sciences*, *112*(43), 13372–13377. https://doi.org/10.1073/PNAS.1516473112

Gendron, J. M., Liu, J.-S., Fan, M., Bai, M.-Y., Wenkel, S., Springer, P. S., Barton, M. K., & Wang, Z.-Y. (2012). Brassinosteroids regulate organ boundary formation in the shoot apical meristem of Arabidopsis. *Proceedings of the National Academy of Sciences*, *109*(51), 21152–21157. https://doi.org/10.1073/PNAS.1210799110

Grunewald, W., Vanholme, B., Pauwels, L., Plovie, E., Inzé, D., Gheysen, G., & Goossens, A. (2009). Expression of the Arabidopsis jasmonate signalling repressor JAZ1/TIFY10A is stimulated by auxin. *EMBO Reports*, *10*(8), 923. https://doi.org/10.1038/EMBOR.2009.103

Han, P., Li, Q., & Zhu, Y.-X. (2008). Mutation of Arabidopsis BARD1 Causes Meristem Defects by Failing to Confine WUSCHEL Expression to the Organizing Center. *The Plant Cell*, *20*(6), 1482. https://doi.org/10.1105/TPC.108.058867

Howe, E. A., Sinha, R., Schlauch, D., & Quackenbush, J. (2011). RNA-Seq analysis in MeV. *Bioinformatics*, *27*(22), 3209–3210. https://doi.org/10.1093/BIOINFORMATICS/BTR490

Hu, J. Y., Zhou, Y., He, F., Dong, X., Liu, L. Y., Coupland, G., Turck, F., & de Meaux, J. (2014). miR824-Regulated AGAMOUS-LIKE16 Contributes to Flowering Time Repression in Arabidopsis. *The Plant Cell*, *26*(5), 2024–2037. https://doi.org/10.1105/TPC.114.124685

Irish, E. E. (1996). Regulation of sex determination in maize. *BioEssays*, *18*(5), 363–369. https://doi.org/10.1002/BIES.950180506

Jurkuta, R. J., Kaplinsky, N. J., Spindel, J. E., & Barton, M. K. (2009). Partitioning the Apical Domain of the Arabidopsis Embryo Requires the BOBBER1 NudC Domain Protein. *The Plant Cell*, *21*(7), 1957–1971. https://doi.org/10.1105/TPC.108.065284

Kabbage, M, & Dickman, M. B. (2008). The BAG proteins: a ubiquitous family of chaperone regulators. *Cellular and Molecular Life Sciences*, *65*(9), 1390–1402. https://doi.org/10.1007/S00018-008-7535-2

Kabbage, Mehdi, Kessens, R., & Dickman, M. B. (2016). A plant Bcl-2-associated athanogene is proteolytically activated to confer fungal resistance. *Microbial Cell*, *3*(5), 224. https://doi.org/10.15698/MIC2016.05.501

Kaplinsky, N. J. (2009). Temperature compensation of auxin dependent developmental patterning. *Plant Signaling & Behavior*, *4*(12), 1157. https://doi.org/10.4161/PSB.4.12.9949

Katayama, H., Iwamoto, K., Kariya, Y., Asakawa, T., Kan, T., Fukuda, H., & Ohashi-Ito, K. (2015). A Negative Feedback Loop Controlling bHLH Complexes Is Involved in Vascular Cell Division and Differentiation in the Root Apical Meristem. *Current Biology*, *25*(23), 3144–3150. https://doi.org/10.1016/J.CUB.2015.10.051

Kim, D., Pertea, G., Trapnell, C., Pimentel, H., Kelley, R., & Salzberg, S. L. (2013). TopHat2: accurate alignment of transcriptomes in the presence of

insertions, deletions and gene fusions. *Genome Biology 2013 14:4*, *14*(4), 1–13. https://doi.org/10.1186/GB-2013-14-4-R36

Kinoshita, A., Betsuyaku, S., Osakabe, Y., Mizuno, S., Nagawa, S., Stahl, Y., Simon, R., Yamaguchi-Shinozaki, K., Fukuda, H., & Sawa, S. (2010). RPK2 is an essential receptor-like kinase that transmits the CLV3 signal in Arabidopsis. *Development*, *137*(22), 3911–3920. https://doi.org/10.1242/DEV.048199

Kurakawa, T., Ueda, N., Maekawa, M., Kobayashi, K., Kojima, M., Nagato, Y., Sakakibara, H., & Kyozuka, J. (2007). Direct control of shoot meristem activity by a cytokinin-activating enzyme. *Nature 2006 445:7128*, *445*(7128), 652–655. https://doi.org/10.1038/nature05504

Kwiatkowski, B. A., Zielińska-Kwiatkowska, A. G., Migdalski, A., Kleczkowski, L. A., & Wasilewska, L. D. (1995). Cloning of two cDNAs encoding calnexin-like and calreticulin-like proteins from maize (Zea mays) leaves: identification of potential calcium-binding domains. *Gene*, *165*(2), 219–222. https://doi.org/10.1016/0378-1119(95)00537-G

Kyozuka, J. (2014). Grass Inflorescence: Basic Structure and Diversity. *Advances in Botanical Research*, *72*, 191–219. https://doi.org/10.1016/B978-0-12-417162-6.00007-9

Kyozuka, J., Komatsu, K., Okamoto, N., Maekawa, M., & Shimamoto, K. (2002). The LAX PANICLE (LAX) gene of rice is required for axillary meristem initiation in the inflorescence. *Plant and Cell Physiology*, *43*.

Langfelder, P., & Horvath, S. (2008). WGCNA: an R package for weighted correlation network analysis. *BMC Bioinformatics 2008 9:1*, *9*(1), 1–13. https://doi.org/10.1186/1471-2105-9-559

Lawrence, C. J., Dong, Q., Polacco, M. L., Seigfried, T. E., & Brendel, V. (2004). MaizeGDB, the community database for maize genetics and genomics. *Nucleic Acids Research*, *32*(Database issue). https://doi.org/10.1093/NAR/GKH011

Li, H., & Durbin, R. (2009). Fast and accurate short read alignment with Burrows-Wheeler transform. *Bioinformatics*, *25*(14), 1754–1760. https://doi.org/10.1093/bioinformatics/btp324

Liu, Q., Galli, M., Liu, X., Federici, S., Buck, A., Cody, J., Labra, M., & Gallavotti, A. (2019). NEEDLE1 encodes a mitochondria localized ATP-dependent metalloprotease required for thermotolerant maize growth. *Proceedings of the National Academy of Sciences of the United States of America*, *116*(39), 19736. https://doi.org/10.1073/PNAS.1907071116

Long, J., & Kathryn Barton, M. (2000). *Initiation of Axillary and Floral Meristems in Arabidopsis*. https://doi.org/10.1006/dbio.1999.9572

Lu, Z., Yu, H., Xiong, G., Wang, J., Jiao, Y., Liu, G., Jing, Y., Meng, X., Hu, X., Qian, Q., Fu, X., Wang, Y., & Li, J. (2013). Genome-Wide Binding Analysis of the Transcription Activator IDEAL PLANT ARCHITECTURE1 Reveals a Complex Network Regulating Rice Plant Architecture. *The Plant Cell*, *25*(10), 3743–3759. https://doi.org/10.1105/TPC.113.113639

Matthes, M. S., Best, N. B., Robil, J. M., Malcomber, S., Gallavotti, A., & McSteen, P. (2019). Auxin EvoDevo: Conservation and Diversification of Genes Regulating Auxin Biosynthesis, Transport, and Signaling. *Molecular Plant*, *12*(3), 298–320. https://doi.org/10.1016/J.MOLP.2018.12.012

McCarthy, D. J., Chen, Y., & Smyth, G. K. (2012). Differential expression analysis of multifactor RNA-Seq experiments with respect to biological variation. *Nucleic Acids Researchcids Research*, *40*(10), 4288–4297. https://doi.org/10.1093/NAR/GKS042

McGinnis, K. M., Thomas, S. G., Soule, J. D., Strader, L. C., Zale, J. M., Sun, T., & Steber, C. M. (2003). The Arabidopsis SLEEPY1 Gene Encodes a Putative F-Box Subunit of an SCF E3 Ubiquitin Ligase. *The Plant Cell*, *15*(5), 1120–1130. https://doi.org/10.1105/TPC.010827

McSteen, P., & Hake, S. (2001). barren inflorescence2 regulates axillary meristem development in the maize inflorescence. *Development*, *128*(15), 2881–2891. https://doi.org/10.1242/DEV.128.15.2881

McSteen, P, Malcomber, S., Skirpan, A., Lunde, C., Wu, X., Kellogg, E., & Hake, S. (2007). barren inflorescence2 Encodes a co-ortholog of the PINOID serine/threonine kinase and is required for organogenesis during inflorescence and vegetative development in maize. *Plant Physiology*, *144*(2), 1000–1011. https://doi.org/10.1104/PP.107.098558

McSteen, Paula. (2009). Hormonal Regulation of Branching in Grasses. *Plant Physiology*, *149*(1), 46–55. https://doi.org/10.1104/PP.108.129056

McSteen, Paula, Malcomber, S., Skirpan, A., Lunde, C., Wu, X., Kellogg, E., & Hake, S. (2007). barren inflorescence2 encodes a co-ortholog of the Pinoid serine/threonine kinase and is required for organogenesis during inflorescence and vegetative development in maize. *Plant Physiology*, *144*(2), 1000–1011. https://doi.org/10.1104/pp.107.098558

Mi, H., Huang, X., Muruganujan, A., Tang, H., Mills, C., Kang, D., & Thomas, P. D. (2017). PANTHER version 11: expanded annotation data from Gene Ontology and Reactome pathways, and data analysis tool enhancements.

Nucleic Acids Research, *45*(D1), D183–D189. https://doi.org/10.1093/NAR/GKW1138

Miura, K., Ikeda, M., Matsubara, A., Song, X.-J., Ito, M., Asano, K., Matsuoka, M., Kitano, H., & Ashikari, M. (2010). OsSPL14 promotes panicle branching and higher grain productivity in rice. *Nature Genetics 2010 42:6*, *42*(6), 545–549. https://doi.org/10.1038/ng.592

Mönke, G., Seifert, M., Keilwagen, J., Mohr, M., Grosse, I., Hähnel, U., Junker, A., Weisshaar, B., Conrad, U., Bäumlein, H., & Altschmied, L. (2012). Toward the identification and regulation of the Arabidopsis thaliana ABI3 regulon. *Nucleic Acids Research*, *40*(17), 8240–8254. https://doi.org/10.1093/NAR/GKS594

Noguero, M., Atif, R. M., Ochatt, S., & Thompson, R. D. (2013). The role of the DNA-binding One Zinc Finger (DOF) transcription factor family in plants. *Plant Science*, *209*, 32–45. https://doi.org/10.1016/J.PLANTSCI.2013.03.016

Nowack, M. K., Harashima, H., Dissmeyer, N., Zhao, X., Bouyer, D., Weimer, A. K., de Winter, F., Yang, F., & Schnittger, A. (2012). Genetic framework of cyclin-dependent kinase function in Arabidopsis. *Developmental Cell*, *22*(5), 1030–1040. https://doi.org/10.1016/J.DEVCEL.2012.02.015

Ogunola, O. F., Hawkins, L. K., Mylroie, E., Kolomiets, M. v., Borrego, E., Tang, J. D., Williams, W. P., & Warburton, M. L. (2017). Characterization of the maize lipoxygenase gene family in relation to aflatoxin accumulation resistance. *PLOS ONE*, *12*(7), e0181265. https://doi.org/10.1371/JOURNAL.PONE.0181265

Ohashi-Ito, K., & Bergmann, D. C. (2007). Regulation of the Arabidopsis root vascular initial population by LONESOME HIGHWAY. *Development*, *134*(16), 2959–2968. https://doi.org/10.1242/DEV.006296

Oikawa, T., & Kyozuka, J. (2009). Two-Step Regulation of LAX PANICLE1 Protein Accumulation in Axillary Meristem Formation in Rice. *The Plant Cell*, *21*(4), 1095–1108. https://doi.org/10.1105/TPC.108.065425

Oliveros, J. C. (n.d.). *VENNY. An interactive tool for comparing lists with Venn Diagrams*. Retrieved July 14, 2021, from https://bioinfogp.cnb.csic.es/tools/venny/

Pautler, M., Tanaka, W., Hirano, H. Y., & Jackson, D. (2013). Grass meristems I: shoot apical meristem maintenance, axillary meristem determinacy and the floral transition. *Plant & Cell Physiology*, *54*(3), 302–312. https://doi.org/10.1093/PCP/PCT025

Perez, D. E., Hoyer, J. E., Johnson, A. I., Moody, Z. R., Lopez, J., & Kaplinsky, N. J. (2009). BOBBER1 is a noncanonical Arabidopsis small heat shock

protein required for both development and thermotolerance. *Plant Physiology*, *151*(1), 241–252. https://doi.org/10.1104/PP.109.142125

Perilli, S., Perez-Perez, J. M., di Mambro, R., Peris, C. L., Díaz-Triviño, S., del Bianco, M., Pierdonati, E., Moubayidin, L., Cruz-Ramírez, A., Costantino, P., Scheres, B., & Sabatini, S. (2013). RETINOBLASTOMA-RELATED Protein Stimulates Cell Differentiation in the Arabidopsis Root Meristem by Interacting with Cytokinin Signaling. *The Plant Cell*, *25*(11), 4469–4478. https://doi.org/10.1105/TPC.113.116632

Phillips, K., Skirpan, A. L., Liu, X., Christensen, A., Slewinski, T. L., Hudson, C., Barazesh, S., Cohen, J. D., Malcomber, S., & McSteen, P. (2011). vanishing tassel2 encodes a grass-specific tryptophan aminotransferase required for vegetative and reproductive development in maize. *The Plant Cell*, *23*(2), 550–566. https://doi.org/10.1105/TPC.110.075267

Preston, J. C., Wang, H., Kursel, L., Doebley, J., & Kellogg, E. A. (2012). The role of teosinte glume architecture (tga1) in coordinated regulation and evolution of grass glumes and inflorescence axes. *New Phytologist*, *193*(1), 204–215. https://doi.org/10.1111/J.1469-8137.2011.03908.X

Preston, J., & Hileman, L. (2013). Functional Evolution in the Plant SQUAMOSA-PROMOTER BINDING PROTEIN-LIKE (SPL) Gene Family. *Frontiers in Plant Science*, *0*(APR), 80. https://doi.org/10.3389/FPLS.2013.00080

Puranik, S., Sahu, P. P., Srivastava, P. S., & Prasad, M. (2012). NAC proteins: regulation and role in stress tolerance. *Trends in Plant Science*, *17*(6), 369–381. https://doi.org/10.1016/J.TPLANTS.2012.02.004

Reinhardt, D., Pesce, E.-R., Stieger, P., Mandel, T., Baltensperger, K., Bennett, M., Traas, J., Friml, J., & Kuhlemeier, C. (2003). Regulation of phyllotaxis by polar auxin transport. *Nature 2003 426:6964*, *426*(6964), 255–260. https://doi.org/10.1038/nature02081

Ritter, M. K., Padilla, C. M., & Schmidt, R. J. (2002). The maize mutant barren stalk1 is defective in axillary meristem development. *American Journal of Botany*, *89*(2), 203–210. https://doi.org/10.3732/AJB.89.2.203

Robinson, M. D., McCarthy, D. J., & Smyth, G. K. (2009). edgeR: A Bioconductor package for differential expression analysis of digital gene expression data. *Bioinformatics*, *26*(1), 139–140. https://doi.org/10.1093/bioinformatics/btp616

Sabelli, P. A., Dante, R. A., Leiva-Neto, J. T., Jung, R., Gordon-Kamm, W. J., & Larkins, B. A. (2005). RBR3, a member of the retinoblastoma-related family from maize, is regulated by the RBR1/E2F pathway. *Proceedings of the National Academy of Sciences*, *102*(37), 13005–13012. https://doi.org/10.1073/PNAS.0506160102

Schlereth, A., Möller, B., Liu, W., Kientz, M., Flipse, J., Rademacher, E. H., Schmid, M., Jürgens, G., & Weijers, D. (2010). MONOPTEROS controls embryonic root initiation by regulating a mobile transcription factor. *Nature 2010 464:7290*, *464*(7290), 913–916. https://doi.org/10.1038/nature08836

Shimizu-Sato, S., & Mori, H. (2001). Control of Outgrowth and Dormancy in Axillary Buds. *Plant Physiology*, *127*(4), 1405–1413. https://doi.org/10.1104/PP.010841

Silverblatt-Buser, E. W., Frick, M. A., Rabeler, C., & Kaplinsky, N. J. (2018). Genetic Interactions Between BOB1 and Multiple 26S Proteasome Subunits Suggest a Role for Proteostasis in Regulating Arabidopsis Development. *G3*, *8*(4), 1379–1390. https://doi.org/10.1534/G3.118.300496

Simonini, S., Deb, J., Moubayidin, L., Stephenson, P., Valluru, M., Freire-Rios, A., Sorefan, K., Weijers, D., Friml, J., & Østergaard, L. (2016). A noncanonical auxin-sensing mechanism is required for organ morphogenesis in Arabidopsis. *Genes & Development*, *30*(20), 2286–2296. https://doi.org/10.1101/GAD.285361.116

Skirpan, A., Culler, A. H., Gallavotti, A., Jackson, D., Cohen, J. D., & McSteen, P. (2009). BARREN INFLORESCENCE2 Interaction with ZmPIN1a Suggests a Role in Auxin Transport During Maize Inflorescence Development. *Plant and Cell Physiology*, *50*(3), 652–657. https://doi.org/10.1093/PCP/PCP006

Skirpan, A., Wu, X., & McSteen, P. (2008). Genetic and physical interaction suggest that BARREN STALK1 is a target of BARREN INFLORESCENCE2 in maize inflorescence development. *Plant Journal*, *55*(5), 787–797. https://doi.org/10.1111/j.1365-313X.2008.03546.x

Song, S.-K., Lee, M. M., & Clark, S. E. (2006). POL and PLL1 phosphatases are CLAVATA1 signaling intermediates required for Arabidopsis shoot and floral stem cells. *Development*, *133*(23), 4691–4698. https://doi.org/10.1242/DEV.02652

Storey, J. D., Taylor, J. E., & Siegmund, D. (2004). Strong control, conservative point estimation and simultaneous conservative consistency of false discovery rates: a unified approach. *Journal of the Royal Statistical Society: Series B (Statistical Methodology)*, *66*(1), 187–205. https://doi.org/10.1111/J.1467-9868.2004.00439.X

Tabuchi, H., Zhang, Y., Hattori, S., Omae, M., Shimizu-Sato, S., Oikawa, T., Qian, Q., Nishimura, M., Kitano, H., Xie, H., Fang, X., Yoshida, H., Kyozuka, J., Chen, F., & Sato, Y. (2011). LAX PANICLE2 of rice encodes a novel nuclear protein and regulates the formation of axillary meristems. *The Plant Cellell*, *23*(9), 3276–3287. https://doi.org/10.1105/TPC.111.088765

Thines, B., Katsir, L., Melotto, M., Niu, Y., Mandaokar, A., Liu, G., Nomura, K., He, S. Y., Howe, G. A., & Browse, J. (2007). JAZ repressor proteins are targets of the SCF(COI1) complex during jasmonate signalling. *Nature*, *448*(7154), 661–665. https://doi.org/10.1038/NATURE05960

Tokunaga, H., Kojima, M., Kuroha, T., Ishida, T., Sugimoto, K., Kiba, T., & Sakakibara, H. (2012). Arabidopsis lonely guy (LOG) multiple mutants reveal a central role of the LOG-dependent pathway in cytokinin activation. *Plant Journal*, *69*(2), 355–365. https://doi.org/10.1111/j.1365-313X.2011.04795.x

Usadel, B., Poree, F., Nagel, A., Lohse, M., Czedik-Eysenberg, A., & Stitt, M. (2009). A guide to using MapMan to visualize and compare Omics data in plants: a case study in the crop species, Maize. *Plant Cell Environment*, *32*(9), 1211–1229. https://doi.org/10.1111/J.1365-3040.2009.01978.X

Vaddepalli, P., Fulton, L., Batoux, M., Yadav, R. K., & Schneitz, K. (2011). Structure-Function Analysis of STRUBBELIG, an Arabidopsis Atypical Receptor-Like Kinase Involved in Tissue Morphogenesis. *PLOS ONE*, *6*(5), e19730. https://doi.org/10.1371/JOURNAL.PONE.0019730

van der Honing, H. S., Kieft, H., Emons, A. M. C., & Ketelaar, T. (2012). Arabidopsis VILLIN2 and VILLIN3 Are Required for the Generation of Thick Actin Filament Bundles and for Directional Organ Growth. *Plant Physiology*, *158*(3), 1426–1438. https://doi.org/10.1104/PP.111.192385

Viola, I. L., Güttlein, L. N., & Gonzalez, D. H. (2013). Redox modulation of plant developmental regulators from the class I TCP transcription factor family. *Plant Physiology*, *162*(3), 1434–1447. https://doi.org/10.1104/PP.113.216416

Voitsik, A.-M., Muench, S., Deising, H. B., & Voll, L. M. (2013). Two recently duplicated maize NAC transcription factor paralogs are induced in response to Colletotrichum graminicola infection. *BMC Plant Biology 2013 13:1*, *13*(1), 1–16. https://doi.org/10.1186/1471-2229-13-85

Walley, J. W., Sartor, R. C., Shen, Z., Schmitz, R. J., Wu, K. J., Urich, M. A., Nery, J. R., Smith, L. G., Schnable, J. C., Ecker, Joseph. R., & Briggs, S. P. (2016). Integration of omic networks in a developmental atlas of maize. *Science*, *353*(6301), 814–818. https://doi.org/10.1126/SCIENCE.AAG1125

Wang, H., Studer, A. J., Zhao, Q., Meeley, R., & Doebley, J. F. (2015). Evidence That the Origin of Naked Kernels During Maize Domestication Was Caused by a Single Amino Acid Substitution in tga1. *Genetics*, *200*(3), 965–974. https://doi.org/10.1534/GENETICS.115.175752

Wang, R., Zhang, Y., Kieffer, M., Yu, H., Kepinski, S., & Estelle, M. (2016). HSP90 regulates temperature-dependent seedling growth in Arabidopsis by

stabilizing the auxin co-receptor F-box protein TIR1. *Nature Communications 2016 7:1*, *7*(1), 1–11. https://doi.org/10.1038/ncomms10269

Wang, Y., Wang, J., Shi, B., Yu, T., Qi, J., Meyerowitz, E. M., & Jiao, Y. (2014). The Stem Cell Niche in Leaf Axils Is Established by Auxin and Cytokinin in Arabidopsis. *The Plant Cell*, *26*(5), 2055–2067. https://doi.org/10.1105/TPC.114.123083

Watanabe, E., Mano, S., Hara-Nishimura, I., Nishimura, M., & Yamada, K. (2017). HSP90 stabilizes auxin receptor TIR1 and ensures plasticity of auxin responses. *Plant Signaling & Behavior*, *12*(5), e1311439. https://doi.org/10.1080/15592324.2017.1311439

Woods, D. P., Hope, C. L., & Malcomber, S. T. (2011). Phylogenomic analyses of the BARREN STALK1/LAX PANICLE1 (BA1/LAX1) genes and evidence for their roles during axillary meristem development. *Molecular Biology and Evolution*, *28*(7), 2147–2159. https://doi.org/10.1093/MOLBEV/MSR036

Wu, X., & McSteen, P. (2007). The role of auxin transport during inflorescence development in maize (Zea mays, Poaceae). *American Journal of Botany*, *94*(11), 1745–1755. https://doi.org/10.3732/AJB.94.11.1745

Wu, Y., Xun, Q., Guo, Y., Zhang, J., Cheng, K., Shi, T., He, K., Hou, S., Gou, X., & Li, J. (2016). Genome-Wide Expression Pattern Analyses of the Arabidopsis Leucine-Rich Repeat Receptor-Like Kinases. *Molecular Plant*, *9*(2), 289–300. https://doi.org/10.1016/J.MOLP.2015.12.011

Yamaguchi, N., Wu, M. F., Winter, C. M., Berns, M. C., Nole-Wilson, S., Yamaguchi, A., Coupland, G., Krizek, B. A., & Wagner, D. (2013). A molecular framework for auxin-mediated initiation of flower primordia. *Developmental Cell*, *24*(3), 271–282. https://doi.org/10.1016/J.DEVCEL.2012.12.017

Yan, Y., Christensen, S., Isakeit, T., Engelberth, J., Meeley, R., Hayward, A., Emery, R. J., & Kolomiets, M. V. (2012). Disruption of OPR7 and OPR8 reveals the versatile functions of jasmonic acid in maize development and defense. *The Plant Cell*, *24*(4), 1420–1436. https://doi.org/10.1105/TPC.111.094151

Yang, J., Thames, S., Best, N. B., Jiang, H., Huang, P., Dilkes, B. P., & Eveland, A. L. (2018). Brassinosteroids modulate meristem fate and differentiation of unique inflorescence morphology in Setaria viridis. *Plant Cell*, *30*(1), 48–66. https://doi.org/10.1105/TPC.17.00816

Yao, H., Skirpan, A., Wardell, B., Matthes, M. S., Best, N. B., McCubbin, T., Durbak, A., Smith, T., Malcomber, S., & McSteen, P. (2019). The barren stalk2 Gene Is Required for Axillary Meristem Development in Maize.

Molecular Plant, *12*(3), 374–389. https://doi.org/10.1016/J.MOLP.2018.12.024

Žádníková, P., & Simon, R. (2014). How boundaries control plant development. *Current Opinion in Plant Biology*, *17*(1), 116–125. https://doi.org/10.1016/J.PBI.2013.11.013

Zeng, S., Lyu, Z., Narisetti, S. R. K., Xu, D., & Joshi, T. (2019). Knowledge Base Commons (KBCommons) v1.0: A multi OMICS' web-based data integration framework for biological discoveries. *Proceedings - 2018 IEEE International Conference on Bioinformatics and Biomedicine, BIBM 2018*, 589–594. https://doi.org/10.1109/BIBM.2018.8621369

Zhang, B., & Horvath, S. (2005). A general framework for weighted gene co-expression network analysis. *Statistical Applications in Genetics and Molecular Biology*, *4*(1). https://doi.org/10.2202/1544-6115.1128

Zhang, R., Xia, X., Lindsey, K., & da Rocha, P. S. (2012). Functional complementation of dwf4 mutants of Arabidopsis by overexpression of CYP724A1. *Journal of Plant Physiology*, *169*(4), 421–428. https://doi.org/10.1016/J.JPLPH.2011.10.013

CHAPTER 5:

Conclusions and Future Directions

Katy Guthrie

SUMMARY AND DISCUSSION

Patterns in development are repeated, even across species and kingdoms. In plants, patterns of development repeat regularly, to continuously produce organs throughout their lifetime via proper regulation of meristems. When regulation fails to happen, morphological alterations, such as enlarged meristems or altered organ number, can occur. For instance, loss-of-function mutations in the maize *CLAVATA* mutants *fasciated ear2 (fea2), thick tassel dwarf2 (td1),* and *compact plant2 (ct2)* all result in enlarged ear meristems compared to normal siblings (Bommert et al., 2005, 2013; Taguchi-Shiobara et al., 2001). While studies of these genes in one meristem type can usually be used to inform another type within the same species, or even across species (e.g. using information from *Arabidopsis* to inform maize meristem development), there are aspects of these pathways that are unique, both within meristem types, and between species. Identifying when information can be extrapolated, and areas where information is still needed, was the goal of Chapter 1.

In Chapter 1, I reviewed the canonical *CLAVATA-WUS* pathway which controls meristem maintenance in maize and other species and also discussed additional pathways such as, LITTLE ZIPPERs (ZPRs), a class of small signaling proteins, that competitively bind to and inhibit HD-ZIPIII transcription factors, to prevent the induction of SHOOTMERISTEMLESS (STM), a KNOX1-like transcription factor, and regulate meristem size in Arabidopsis (Kim et al., 2008; Wenkel et al., 2007). A study of a *ZPR* gene in tomato, *defective tomato meristem1*

(*dtm1*) found that *dtm1* functioned to regulate the expression domain of tomato members of the *CLAVATA*-*WUS* pathway, again supporting a role of these ZPR proteins in meristem maintenance. While *zpr* genes were reported to be differentially expressed in the maize *wus1* mutant, *Barren inflorescence 3* (Bif3) (Chen et al., 2021), no functional analysis of these genes in maize has been reported. My review of the literature only found three papers studying the function of ZPR proteins in meristem maintenance pathways, all done in dicots, highlighting holes in our understanding of meristem maintenance pathways that require further research.

The semi-dominant class of maize developmental mutants, *Suppressor of sessile spikelets* (*Sos*) has three members *Sos1, Sos2* and *Sos3.* Previous studies into the founding member of this class, *Sos1* identified a role in meristem maintenance, specifically through the maize *CLAVATA* pathway (Johnson, 2017), however, the *Sos2* mutants had not been characterized until this study. The similarity in phenotype, specifically the reduction in the number of paired spikelets during ear and tassel development, led to the hypothesis that *Sos2* also functions in meristem maintenance. When double mutant analyses were performed with *td1, fea2,* and *ct2*, it was found that *Sos2* did function in the maize *CLAVATA* pathway, but differently than *Sos1*. While genetic evidence suggested that *Sos1* signals through the *td1* and *fea2;td1* complexes (Johnson, 2017), genetic evidence indicated that *Sos2* signals through *fea2* but not the *td1* pathway (Chapter 2). FEA2 is a member of multiple protein complexes in maize so which of these pathways is impacted by *Sos2* requires further study.

The *Sos2* gene location was mapped to the short arm of chromosome 10 using fine mapping and whole-genome sequencing, to a region in the W22-ACR genome containing 23 genes. Since semi-dominant mutants are inherently dose-dependent, and only a single copy of a mutated gene is necessary to see alterations in phenotype, it is likely *Sos3* is a hypermorphic or neomorphic mutation (Muller, 1932). This is supported by previously published studies on dominant and semi-dominant mutants in maize, such as *Fascicled ear1, Rolled leaf 1, Tasselseed5* and *Barren inflorescence3* (Chen et al., 2021; Du et al., 2021; Juarez et al., 2004; Lunde et al., 2019). To determine if any of the 23 genes were mis-regulated, indicative of a hyper or neomorph, expression of genes differentially expressed in *Sos2/+* immature tassels was overlaid on sequencing data. When this is done, it was found that only two genes were differentially expressed at an absolute logfold value of 1 or more: *ZmZPR4-like* (up regulated over 3-fold) and *ZmZCN3-like/PEBP3* (down-regulated just over 1-fold). Due to the dramatic increase in expression, known roles of *ZPR* genes in meristem maintenance from previously published studies, and similarity in early meristem termination phenotypes – which is seen in *Arabidopsis* when *ZPR* proteins are over-expressed (Wenkel et al., 2007), and in *Sos2* homozygotes and sporadically in *Sos2* heterozygotes, it is likely that *ZmZPR4-like* is the candidate gene for the *Sos2* phenotype. However, both *ZmZCN3-like/PEBP3* and *golden kernel5* (*glk5*) genes were both differentially down-regulated in *Sos2* mutants compared to normal, and also fall within our fine mapping window. While our results potentially mark the first time evidence has been provided for a role of *ZPR* genes in meristem maintenance

in maize, and monocots in general, it will be important to verify that these two other genes are not responsible for the *Sos2* phenotype.

In *Arabidopsis,* the ZPR/HD-ZP III/STM regulatory pathway intersects with the cytokinin biosynthesis pathway during development (Kim et al., 2008; Wenkel et al., 2007; Zhang et al., 2017). Determining if *Sos2* also impacted phytohormone pathways was reported in Chapter 3. It was found that cytokinin intermediates were significantly up regulated compared to normal siblings, and the most prevalent active form of auxin, IAA, was significantly decreased. Commonalities between all three *Sos* mutant phenotypes lead to the hypothesis that *Sos1* and *Sos3* may also regulate phytohormone pathways, and an RNA-seq analysis was used to uncover similarities and differences between *Sos1, Sos2,* and *Sos3.* While *Sos1* did not have differential expression of very many genes (the phenotype is weak in tassels) and was ultimately inconclusive, *Sos3* did have differential expression in many auxin-related genes. Based on the phenotypic similarity of *Sos3* with auxin mutants, it would be interesting to follow up on this result in *Sos3* and determine if it's impact on auxin regulation overlaps that of *Sos2*.

Chapter 3 did uncover some inconsistencies between the defects in *Sos2* in maize compared with previously published work on ZPR's in *Arabidopsis.* For example: ZPR3/4 competitively bind HD-ZIP III transcription factors making them nonfunctional (Kim et al., 2008). Some HD-ZIP III TFs, such as REVOLUTA, directly induce expression of *STM* (Shi et al., 2016), as well as cytokinin biosynthesis, which in turn activates *WUS1* expression (Zhang et al., 2017). It can be hypothesized that over-expression of ZPR proteins would lead to decreased

expression of *STM* and *WUS1* in *Arabidopsis.* In *Sos2/+,* there was a significant decrease in *Zmwus1* expression consistent with the hypothesis made from studies in *Arabidopsis* and tomato, however *knotted1 (STM* ortholog) was significantly increased in *Sos2/+* tassels, inconsistent with what was hypothesized from *Arabidopsis* studies. Furthermore, it can be hypothesized that overexpression of ZPR proteins would lead to decreased cytokinin, while in *Sos2/+* there was evidence of increased cytokinin or cytokinin signaling by hormone measurements, reporter assays and transcriptome analysis. It is important to note again that while information from one species can be used to inform studies of meristem maintenance in other species, it is likely that genes could function differently in different species or in different meristems. Therefore, Chapter 2 and 3 open up a new area of research on meristem maintenance in maize to be further investigated in the future.

In Chapter 4, the role of auxin was extensively analyzed in three maize auxin mutants: *ba1, bif2,* and *ba2* (Gallavotti et al., 2004; McSteen & Hake, 2001; Yao et al., 2019). RNA-seq and subsequent WGCNA found that each of these three mutants, while sharing some similarity in phenotype, ultimately had unique direct and indirect targets. This highlighted how much still needs to be learned about auxin regulation during axillary meristem initiation.

FUTURE DIRECTIONS

Follow up analysis needs to be performed to confirm the results from Chapter 2. To validate the RNA-seq results, RNA *in situ* hybridization with

ZmZPR4-like and *ZmWUS1* will be performed in immature tassels. We can expect to see an increased *ZmZPR4-like* expression domain in *Sos2* compared to normal siblings, and decreased *ZmWUS1* domain in an antagonistic pattern to each other. In addition, qRT-PCR would be a beneficial way to confirm the changes in transcript expression seen in my RNA-seq analysis as well, and primers have been designed to perform this experiment in the future. To confidently prove that either *ZmZPR4-like, ZCN3-like,* or the *glk5* gene underlies the *Sos2* mutant phenotype, recapitulation of the *Sos2* phenotype by over-expression of the *ZmZPR4-like* and *ZCN3-like* genes in normal plants would be necessary. The results of this experiment, taken with the results published in this study, will be the basis of future grants to research the underlying *Sos2* gene function in meristem maintenance.

In order to determine which *fea2* signaling complexes *Sos2* functions through, *Sos2;ZmCRN* double mutant analysis will need to be analyzed. If *Sos2* does function through the *fea2;ZmCRN* signaling complex, then we can expect *Sos2/+;ZmCRN/ZmCRN* double mutants to have fasciated IMs in tassels and ears. Genetic material for this double mutant analysis has been created and is currently being bulked to perform this study. Additional genetic materials have been developed to assess the role of *Sos2* in the determinacy pathway, i.e. the *ramosa* pathway, and preliminary results indicate additive interactions with both *ramosa1* and *ramosa2* indicating the *Sos2* gene and the *ramosa* genes act in different pathways. These results would need to be confirmed with a quantitative analysis in future field seasons. Genetic material is also available or in the process of being backcrossed for the following double mutant studies: *Sos2;bd1, Sos2;tls1,*

*Sos2;kn1-r1, Sos2;fea3, Sos2;fea4-ba*CL, Sos2;fea4-ref, Sos2,Rld1, Sos2;Hsf* and *Sos2;cr4.*

Chapter 3 explored the impacts of the *Sos* mutants on the auxin and cytokinin regulatory pathways. Both *Sos2* and *Sos3* mutants had disruptions in these pathways, as evidenced by RNA-seq analysis. It would be interesting to follow up this study with additional experiments, such as a Western analysis with ZmPIN1a-YFP and DR5-RFP in immature *Sos2* tassels, as well as an LC-MS hormone assay of *Sos3* immature tassels. Both of these assayas, combined with the RNA-seq analysis, would shed light on the roles of the *Sos2* and *Sos3* genes on phytohormone regulation during tassel development. The major results of the transcriptomic analysis in Chapter 4 was that mutants with hypothesized overlapping functions in the auxin regulatory pathway due to similarities in AM phenotype, actually had more unique transcriptomic profiles that previously thought. This mirrors the results of the RNA-seq analysis in Chapter 3, in that while the *Sos* mutants which have similar phenotypic characteristics had different expression profiles. Taking this into account, it would be interesting to perform a WGCNA on the three *Sos* mutants using the RNA-seq analysis in Chapter 3 to take a more comprehensive look at the co-expression of *Sos* direct and indirect targets. Chapter 4 is being submitted for publication soon but follow-up studies could involve validating some of the many transcription factors identified as being downstream of auxin.

An obvious follow up to the *Sos2* and *Sos3* gene function comparison studies is complementation testing and *Sos1, Sos2,* and *Sos3* genetic interaction

studies, as we know *Sos1* maps to a different location than *Sos2* and *Sos3* (Johnson, 2017). These genetic experiments were initiated in the 2017 field season, however all three *Sos* mutants have decreased seed set due to the production of single spikelets (kernels) in ears. Double heterozygous plants often had poor pollen production or failed to make ears with enough kernels for subsequent studies or failed to make ears altogether. The inability to self double heterozygous *Sos* mutants, in addition to low seed production made analyzing results of this study difficult. Currently, all *Sos* mutants are being introgressed in to the W22-ACR mutant background and have strong respective phenotypes. This genetic material will be used to perform *Sos1/Sos2/Sos3* complementation testing, and genetic analysis.

The work presented in this thesis demonstrates that gaps still exist in our understanding of meristem maintenance throughout development and taking a comprehensive approach to studying them can help to paint a more specific picture of how individual genes function throughout development.

WORKS CITED

Bommert, P., Je, B. il, Goldshmidt, A., & Jackson, D. (2013). The maize Gα gene COMPACT PLANT2 functions in CLAVATA signalling to control shoot meristem size. *Nature*, *502*(7472), 555–558. https://doi.org/10.1038/nature12583

Bommert, P., Lunde, C., Nardmann, J., Vollbrecht, E., Running, M., Jackson, D., Hake, S., & Werr, W. (2005). Thick tassel dwarf1 encodes a putative maize ortholog of the Arabidopsis CLAVATA1 leucine-rich repeat receptor-like kinase. *Development*, *132*(6), 1235–1245. https://doi.org/10.1242/dev.01671

Chen, Z., Li, W., Gaines, C., Buck, A., Galli, M., & Gallavotti, A. (2021). Structural variation at the maize WUSCHEL1 locus alters stem cell organization in inflorescences. *Nature Communications*, *12*(1), 1–12. https://doi.org/10.1038/s41467-021-22699-8

Du, Y., Lunde, C., Li, Y., Jackson, D., Hake, S., & Zhang, Z. (2021). Gene duplication at the Fascicled ear1 locus controls the fate of inflorescence meristem cells in maize. *Proceedings of the National Academy of Sciences of the United States of America*, *118*(7). https://doi.org/10.1073/pnas.2019218118

Gallavotti, A., Zhao, Q., Kyozuka, J., Meeley, R. B., Ritter, M. K., Doebley, J. F., Pè, M. E., & Schmidt, R. J. (2004). The role of barren stalk1 in the architecture of maize. *Nature*, *432*(7017), 630–635. https://doi.org/10.1038/nature03148

Johnson, E. (2017). *Evolution and development of the paired spikelet trait in maize and other grasses (Poaceae)*.

Juarez, M. T., Kui, J. S., Thomas, J., Heller, B. A., & Timmermans, M. C. P. (2004). microRNA-mediated repression of rolled leaf1 specifies maize leaf polarity. *Nature*, *428*(6978), 84–88. https://doi.org/10.1038/nature02363

Kim, Y. S., Kim, S. G., Lee, M., Lee, I., Park, H. Y., Pil, J. S., Jung, J. H., Kwon, E. J., Se, W. S., Paek, K. H., & Park, C. M. (2008). HD-ZIP III activity is modulated by competitive inhibitors via a feedback loop in Arabidopsis shoot apical meristem development. *Plant Cell*, *20*(4), 920–933. https://doi.org/10.1105/tpc.107.057448

Lunde, C., Kimberlin, A., Leiboff, S., Koo, A. J., & Hake, S. (2019). Tasselseed5 overexpresses a wound-inducible enzyme, ZmCYP94B1, that affects jasmonate catabolism, sex determination, and plant architecture in maize. *Communications Biology*, *2*(1), 1–11. https://doi.org/10.1038/s42003-019-0354-1

McSteen, P., & Hake, S. (2001). Barren inflorescence2 regulates axillary meristem development in the maize inflorescence. *Development*, *128*(15), 2881–2891. https://doi.org/10.1242/dev.128.15.2881

Muller, H. J. (1932). Further studies on the nature and causes of gene mutations. *Proceedings of the 6th International Congress of Genetics*, 213–255.

Shi, B., Zhang, C., Tian, C., Wang, J., Wang, Q., Xu, T., Xu, Y., Ohno, C., Sablowski, R., Heisler, M. G., Theres, K., Wang, Y., & Jiao, Y. (2016). Two-Step Regulation of a Meristematic Cell Population Acting in Shoot Branching in Arabidopsis. *PLoS Genetics*, *12*(7), e1006168. https://doi.org/10.1371/journal.pgen.1006168

Taguchi-Shiobara, F., Yuan, Z., Hake, S., & Jackson, D. (2001). *The fasciated ear2 gene encodes a leucine-rich repeat receptor-like protein that regulates shoot meristem proliferation in maize*. https://doi.org/10.1101/gad.208501

Wenkel, S., Emery, J., Hou, B. H., Evans, M. M. S., & Barton, M. K. (2007). A feedback regulatory module formed by Little Zipper and HD-ZIPIII genes. *Plant Cell*, *19*(11), 3379–3390. https://doi.org/10.1105/tpc.107.055772

Yao, H., Skirpan, A., Wardell, B., Matthes, M. S., Best, N. B., McCubbin, T., Durbak, A., Smith, T., Malcomber, S., & McSteen, P. (2019). The barren stalk2 Gene Is Required for Axillary Meristem Development in Maize. *Molecular Plant*, *12*(3), 374–389. https://doi.org/10.1016/j.molp.2018.12.024

Zhang, F., May, A., & Irish, V. F. (2017). Type-B ARABIDOPSIS RESPONSE REGULATORs Directly Activate WUSCHEL. In *Trends in Plant Science* (Vol. 22, Issue 10, pp. 815–817). Elsevier Ltd. https://doi.org/10.1016/j.tplants.2017.08.007

APPENDIX A:

Genetic materials and stocks

Katy Guthrie

Various genetic materials were created for this project, although not all were analyzed for my thesis. Below is a list of genetic materials created throughout the course of this project, and their location in the McSteen Lab's seed stocks. Always double check stocks and numbers with the lab's corn cards and harvest lists and verify genotyping and phenotyping with laboratory and field notebooks. Some stocks may no longer be present if the packets were used to plant seed for bulking or analysis in subsequent generations. Please refer to the Excel workbook on the McSteen Lab server for notes related to individual stocks.

Remember: *Sos2* phenotypes look different in Missouri and Hawaii growing conditions. When in doubt, I would recommend taking a few seasons to remake the respective cross in the W22-ACR or MO17 genetic backgrounds. When dealing with introgressions into the W22-ACR background, remember to choose the purple kernels over the yellow ones as the A, C, and R genes give the purple pigmentation.

Maize mutant introgressions into W22-acr (yellow)

In general, all maize mutants were genotyped before selfing each season. When possible, single mutants were outcrossed to W22-acr to continue introgression and to be used as testers in subsequent seasons. The resulting seed was not always planted out and therefore is not present in the corn cards, however harvest lists from the most recent field seasons should be mined if a desired tester is not found in the list below.

	Genetic Material	Most Recent Planting	Years Planted	F1
Tester Introgressions (W22-acr, yellow)	kn1-r1	HI17: 289-290	HI17, MO16, HI16: B/C-3	Before 2015
	kn1-l4	HI17: 295-296	HI17, MO16, HI16: B/C-3	Before 2015
	ra1	MO18: 2282-2284	MO18, HI18, MO16: B/C-3	Before 2015
	ra2	MO20: 2383/84	MO20, MO18, HI18, HI17, MO16: B/C>3	Before 2015
	fea2	MO19:2510	MO19, MO18, HI18, MO17, MO16: B/C>3	Before 2015
	bd1/Pn1	HI17:219/220	HI17: B/C-1	MO16: 2555/56
	fea4-ref	MO18:2280/81	MO18, HI18, MO17, HI18, MO18: B/C-3	HI17: 666/237
	td1	MO19: 2506	MO19, MO18, HI18, MO17: B/C>3	HI17: 237
	Bif4	HI18: 369-370	HI18, MO17	HI17: 314
	Bif3	Not subquently grown	HI18 (F1)	HI18:371-372
	spi	MO20:2381/82	MO19, MO17	HI17: 238
	ra3	MO18: 2287	HI18, MO17	HI17: 308
	Bif3	Not subquently grown	HI18 (F1)	HI18: 371-372
	Bif1	MO17: 3273	MO17: B/C-1	HI17: 684
	bif2	Not subquently grown	MO17 (F1)	MO17: 3274
	crn	HI19: 617-618	HI19: B/C-1	MO18:383-384
	Hsf	MO18: 3376/77	MO18: B/C-1	HI18: 386
	aphl1	Not subquently grown	MO17: 3275 (F1)	MO17: 3275
	Abph2	HI17: 225-228	HI17: B/C-1	MO16: 2552

Maize mutant introgressions into W22-ACR (purple)

W22-ACR seed was obtained from the Vollbrecht Lab and first planted in the HI2019 field season (rows 599-600). To keep W22-ACR tester seed healthy, I would recommend sibing between rows/families instead of selfing when bulking. Always check that the packets have purple seed when using anything introgressed to W22-ACR.

	Genetic Material	Most Recent Planting	Years Planted	F1
Tester Introgressions (W22-ACR, purple)	Sos1	MO20: 4173-4176 (backcrossed)	HI20: @, MO20: B/C-1	MO19: 2558
	Sos2	MO20: 4177/78, 2655-2668 (backcrossed)	MO20, HI20: B/C-2	MO19: 2561, 2529
	Sos3	MO20: 2432/33 (backcrossed)	MO20: B/C-1	MO19: 2561
	fea2	MO20: 2377/78 (backcrossed)	MO20: B/C-1	MO19: 2560
	td1	MO20: 4179/80 (backcrossed)	MO20: B/C-1	MO19: 2307
	ct2	MO20: 2375/76 (backcrossed)	MO20: B/C-1	MO19: 2503
	spi	MO20: 2381/82 (backcrossed)	M020: B/C-1	MO19: 2543
	ra2	MO20: 2383/84 (backcrossed)	MO20: B/C-1	MO19: 2560
	cr4	MO20: 2417-2431 (backcrossed)	MO20, HI20, MO19, HI19, MO18: B/C > 3	HI18: 375-379
	fea3	MO20: 2379/80 (backcrossed)	MO20: B/C-1	MO19: 2527

Sos2 inbred introgressions

Sos2 inbred introgressions were performed to identify naturally occurring genetic modifiers of *Sos2* (enhancers/suppressors). In addition, this helped to identify genetic backgrounds in which the *Sos2* phenotype is stable. Moving forward, I would recommend using the *Sos2;*MO17 introgression to assess heterozygous and homozygous phenotypes as this genetic background has good germination and seems to segregate in a Medellin fashion in Missouri growing conditions.

	Genetic Material	Most Recent Planting	Years Planted	F1
Sos2 Introgressions	Sos2, MO45	MO20: 2361 (outcross/@)	MO20: B/C-1	MO19: 4043-46
	Sos2, PHG47	MO20: 2362 (outcross/@)	MO20: B/C-1	MO19: 4043-46
	Sos2, B97	MO20: 2363 (outcross/@)	MO20: B/C-1	MO19: 4043-46
	Sos2, A659	MO20: 2364 (outcross/@)	MO20: B/C-1	MO19: 4043-46
	Sos2; OH43	MO19: 6704-6707 (outcross/@)	HI17, MO17, MO19: B/C-2-3	MO16: 2574
	Sos2; A632	MO19: 6796-6698 (outcross/@)	HI17, MO17, MO19: B/C-2-3	MO16: 2568
	Sos2; A619	MO19: 6688-6691 (outcross/@)	HI17, MO17, MO19: B/C-2-3	MO16: 2570/71
	Sos2, MO17	MO19: 6700-6702 (outcross/@)	HI17, MO17, MO19: B/C-2-3	MO16: 2573
	Sos2; B73	PM19: 6684-6687 (outcross/@)	HI17, MO17, MO19: B/C-2-3	MO16: 2572
	Sos2, A188	MO19: 6580-6600 (@)	PM05, PM09: B/C > 3	PM04: 728

Sos2 double mutant genetic material

As the W22-ACR genetic seed stock was not introduced to the lab until 2019, a majority of the *Sos2* double mutants were introgressed into the W22-acr (yellow) seed stock. I believe that double mutant F1 crosses were attempted for *Sos2;ba1*, *Sos2;ba2*, and *Sos2;ba*CL*, however, these lines were never subsequently replanted. To check if seed set for *Sos2;ba1* and *Sos2;ba2,* refer to the harvest lists and respective seed stock boxes for the MO16 and MO17 seasons. For *Sos2;ba*CL,* refer to the harvest lists and respective seed stocks for MO18, in both the *Sos2* tester and *ba*CL*;Mo17 introgression sections.

When planting out these stocks in Missouri, I would recommend treating the seed for mold before planting, if time allows. There is a significant increase in germination when this is done. If grown in Hawaii, I would recommend asking for an additional mold spray a week to two weeks after pollinations to combat ear mold and aid in seed set.

	Genetic Material	Most Recent Planting	Years Planted	F1
Sos2 Double Mutants, W22-acr (Yellow)	Sos2; bd1	HI19: 555-558 (outcross/@)	HI19, MO18, HI18, MO17: B/C -3	HI17: 220
	Sos2; Bif1	MO18: 2215-2217 (outcross/@)	MO18, HI18, MO17: B/C-3	HI17: 675/678
	Sos2; bif2	MO20:2393-2396 (@)	MO20, HI20, MO19, MO18, HI18, MO17: B/C-5	HI17:679
	Sos2; crn	HI20: 385/338 (@)	MO18, HI19, MO19: B/C-3	HI18: 383/384
	Sos2; ct2	MO20: 4195/96 (@)	MO20, HI20, MO19, HI19: B/C-3	MO18: 2268/69
	Sos2; fea2	HI20: 334/379 (@)	Grown every season: B/C-5	MO16: 2527/ HI18: 359/360
	Sos2; fea3	MO20: 2407/08 (@)	MO20: B/C-1	MO19: 2530
	Sos2; fea4-ref	HI18: 120-131 (outcross/@)	HI18: B/C-1	MO17: 3307/08
	Sos2; kn1-l4	HI17: 291-294 (outcross/@)	HI17: B/C-1	PM16: 2535
	Sos2; kn1-r1	HI17: 285-289 (outcross/@)	HI17: B/C-1	PM16: 2534
	Sos2; ra1	MO19: 2531-2533 (@)	HI17,MO18,MO19: B/C>5	MO16:2529/30
	Sos2; ra2	MO19: 2534-2537 (@)	HI17,MO18,MO19: B/C>5	PM16:2531/32
	Sos2; ra3	MO17: 3237 (outcross/@)	MO17, B/C-1	HI17:669
	Sos2; spi	MO20: 2397-2400 (@)	MO20, HI20, MO19, MO18, HI18, MO17: B/C-5	HI17: 657/660
	Sos2; td1	MO20: 4193/94 (@)	MO20, HI20, MO19, HI19, MO18, HI18, MO17: B/C-5	HI17:656/ 645-646
	Sos2; tls1	MO20: 2405/06 (@)	MO20, MO19, MO18, HI18, MO17: B/C-5	HI17: 638
	Sos2; vt2	MO20:2401-2404 (@)	MO20, HI20, MO19, HI19, MO20, HI20: B/C>3	MO18: 2211

The *Sos2* double mutants that were used for analysis in Chapter 2 began intorgression from the W22-acr to W22-ACR genetic backgrounds in MO2019. This was done in case reviewers asked for consistency in genetic background between *Sos2* sequenced and *Sos2* double mutant material. I have found increased germination and stronger phenotypes in these lines, although additional backcrossing needs to occur to fully introgress these mutants. Note: *cr4* has

multiple alleles ordered both from the Maize Stock Center and received from Phillip Benfey. Some of these alleles were received already introgressed into the W22-ACR background in HI2018. Cross-reference the corn cards for information on the specific alleles.

	Genetic Material	Most Recent Planting	Years Planted	F1
Sos2 DM, W22 ACR (purple)	Sos2; cr4	HI20: 340-341 (@)	MO19, MO20, HI20: B/C>3	HI18: 376-378
	Sos2; las1	MO20: 4185/86 (outcross)	HI20, MO20: B/C-2	MO19: 2557/56
	Sos2; fea2	MO20: 4183/84 (outcross)	MO20: B/C-1	HI20: 337, 390
	Sos2; td1	MO20: 4179/80 (outcross)	MO20: B/C-1	HI20: 428
	Sos2; ct2	MO20: 4181/82 (outcross)	MO20: B/C-1	HI20: 333

Sos2 transgenic material

Starting after 2018, plants were identified as transgenic through BASTA treatment after the leaf transition from juvenile to adult. Be sure to check tassels for phenotype while detasseling to denote which plants have the *Sos2* phenotype for crossing.

	Genetic Material	Most Recent Planting	Years Planted	F1
Sos2 Transgenic Material	Sos2;cycD2B-YFP	MO16: 2843-2846	MO16: B/C-1	MO15: 2690-2692
	Sos2;Histone-YFP	MO19: 2682-2686	MO19, MO18, MO17, MO16: B/C-4	MO15:2694-2695
	Sos2;YFP::Ra1	MO16: 2870-2872	MO16: B/C-1	MO15: 2635
	Sos2;pWUS:NLS-RFP	MO19: 2687-2689	MO19, MO18, MO16: B/C-3	MO15: 2701, 2703
	Sos2;pWUS:NLS-RFP (new)	MO20: 2075-2076	MO20: B/C-1	GH20 (Janlo)
	Sos2;TCS v2-tdTomato	MO20: 2071-2072	MO19, MO18, MO17, MO16: B/C-4	MO15: 2712, 2713
	Sos2;mDII venus	MO19: 2673	MO19, MO17: B/C-2	MO16:
	Sos2;DII venus	MO19: 2672	MO19, MO17: B/C-2	MO16:
	Sos2;mDII venus (new)	MO20:2065-2066	MO20, MO19, MO17: B/C-3	MO16: 2885
	Sos2;DII venus (new)	MO20: 2063-2064	MO20, MO19, MO17: B/C-3	MO16: 2888
	Sos2;PIN1a-YFP	MO20:2069-2070	MO19, MO18, MO17: B/C-3	MO16: 2873-2875
	Sos2;DR5-RFP	MO19: 2674-2675	MO19, MO17: B/C-2	MO16: 2876-2877
	Sos2;PIN1a-YFP;DR5-RFP	MO20:2067-2068	MO20, MO19: B/C-2	MO17: 3755, 3759
	Sos2;RR7	MO20: 2077-2078	MO20: B/C-1	GH20 (Janlo)
	Sos2;Wox5b	MO20: 2073-2074	MO20: B/C-1	GH20 (Janlo)
	Sos2;BES1	MO20: 2079	MO20: B/C-1	MO20: 2089, GH20 (Janlo)
	Sos2;PIP2	MO20: 2080	MO20: B/C-1	GH20 (Janlo)
	Sos2;ABA-R17	-	MO20 (F1)	MO20: 2090
	Sos2;expe1	-	MO20 (F1)	MO20:2091
	Sos2;GA-R1b	-	MO20 (F1)	MO20: 2092

Other project material

This appendix does not include *Sos3* double mutant or transgenic material generation, or *Sos1*;*crn* double mutant generation. This material was primarily generated by me with the support of three undergraduate researchers: Austin Morgan, Jackson Marsch, and Connor Nordwald. In general, the double mutants created for *Sos2* were also created for *Sos3* in the same seasons, so the years documented above would be a good place to start to find *Sos3* double mutant and introgressed seed.

Additional projects that are either related to the *Sos2* project, or were funded, in part, by my USDA-NIFA grant, are listed below. The three EMS M2 selfed alleles discovered in MO20 are currently being grown in the MO21 field season. The material for the *Sos2* dosage study was subsequently grown in the Sears Greenhouse in the, where roots were collected for FISH analysis between January and February of 2019. The results of this study yielded no significant results (see my folder on the McSteen Lab Server), although it might be worth repeating after the identity of the *Sos2* mutation is uncovered.

	Project	Most Recent Planting	Years Planted	Initated
Other Projects	Progressve Chlorosis (EMS)	MO21:1396-1407	MO20: B/C-1 (2654), MO19 (M2@)	MO18
	Short Fuzzy Panicle (EMS)	MO21: 1408-1417	MO20: B/C-1 (2606), MO19 (M2@)	MO18
	CPD (EMS)	MO21: 1418-1420	MO20: B/C-1 (3021), MO19 (M2@)	MO18
	Sos Round Robin	MO17: 2328-2343 (Phenotyped/@)	HI17 (@), MO17 (@)	MO16: 2538-2542, MO17: 3278-3284
	Sos2 Enhancer/ Supressor Screen	PM19: 6789-6796	PM19: B/C-1	MO18
	Sos2 MUK	MO20: 2434-2454	MO19: 2589-2592	PM04:776
	Sos2 Modifer (from OG stock)	MO20: 2369-71 (Phenotyped/@)	MO20: B/C-1	MO19:2527
	Sos2 Dosage Analysis	Not subquently grown	MO18	MO18: 22556-2259

VITA

Katherine (Katy) Guthrie was born and raised outside St. Louis, Missouri. Katy uses she/her pronouns. Before attending the University of Missouri – Columbia, she attended Northwest Missouri State University where she received her Bachelor of Science in Biological Sciences with an Emphasis in Botany and a Minor in Deaf Studies in 2015. During this time, Katy worked as a peer supplemental instructor Botany and teaching assistant for Botany lab, as well as a tutor for various courses in the Department of Natural Sciences.

Katy started at the University of Missouri – Columbia in 2015, focusing her research on maize development. She received her PhD in Biological Sciences in the Summer 2021. During this time, Katy completed additional course work and a teaching internship towards a graduate minor in College Science Teaching. In addition, Katy also worked for two years on the HHMI-funded THRIVE project, housed in the Department of Higher Education and Natural Sciences, focused on increasing retention of historically excluded students in STEM fields. In addition, Katy was a teaching assistant for Botany Lab and Genetic Recitation, and an instructor of record for Genetic Diseases (an online course for non-majors). She was awarded the Sandra K. Abell Science Education Award in 2019. Katy expects three first-author publications from her PhD research, and authorship on at least two more.

Currently, Katy is working as an Active Learning Initiative (ALI) Post-Doctoral education specialist for the Integrative School of Plant Sciences (SIPS) at Cornell University in Ithaca, New York.